

What has solid-state NMR ever done for us?

Structure and dynamics from organic crystals to nano-composite materials

Jeremy Titman
School of Chemistry, University of Nottingham, UK

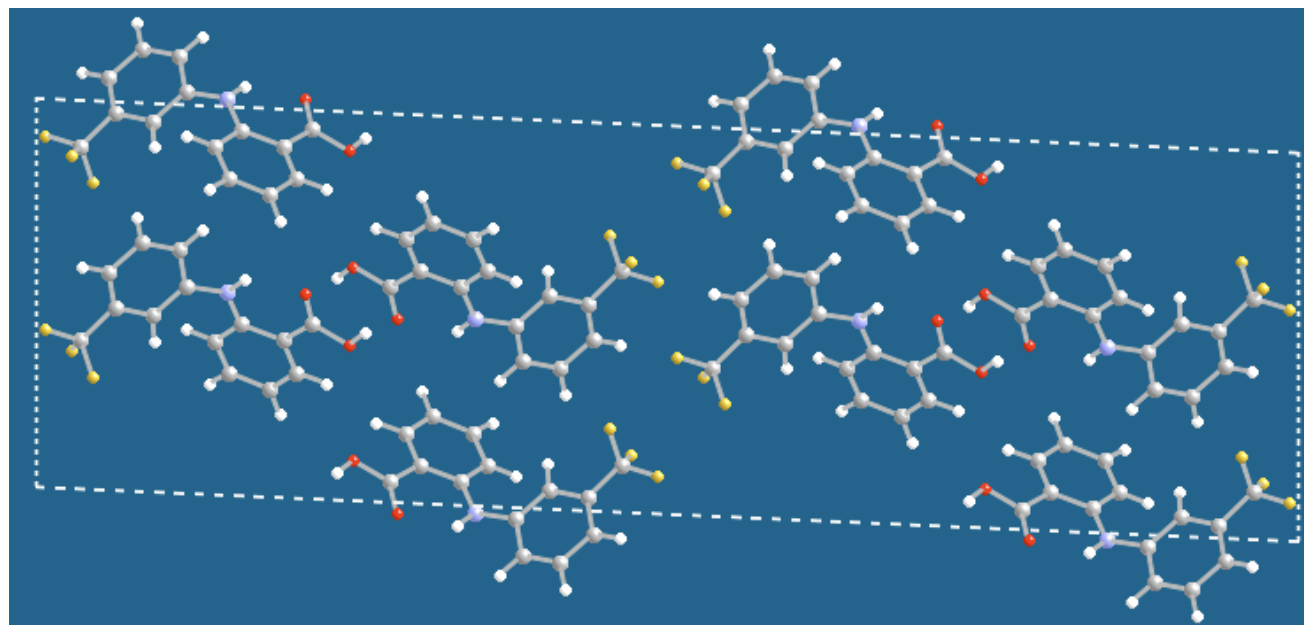
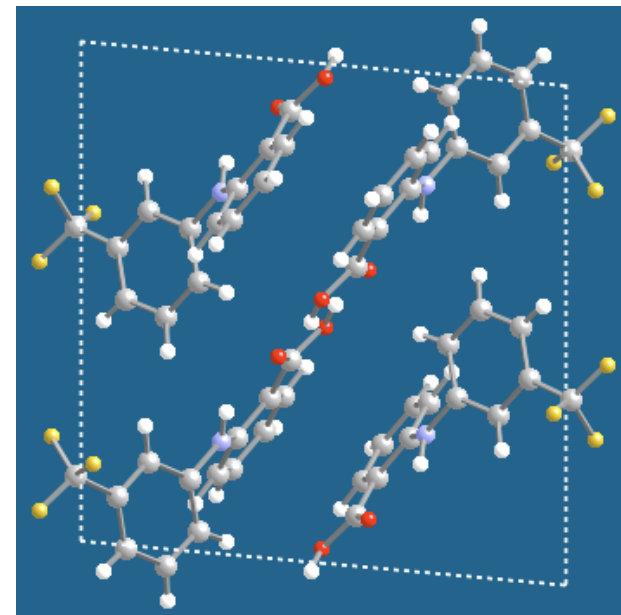


“but apart from better sanitation and medicine and education and irrigation and public health and roads and a freshwater system and baths and public order... what have the Romans ever done for us?”

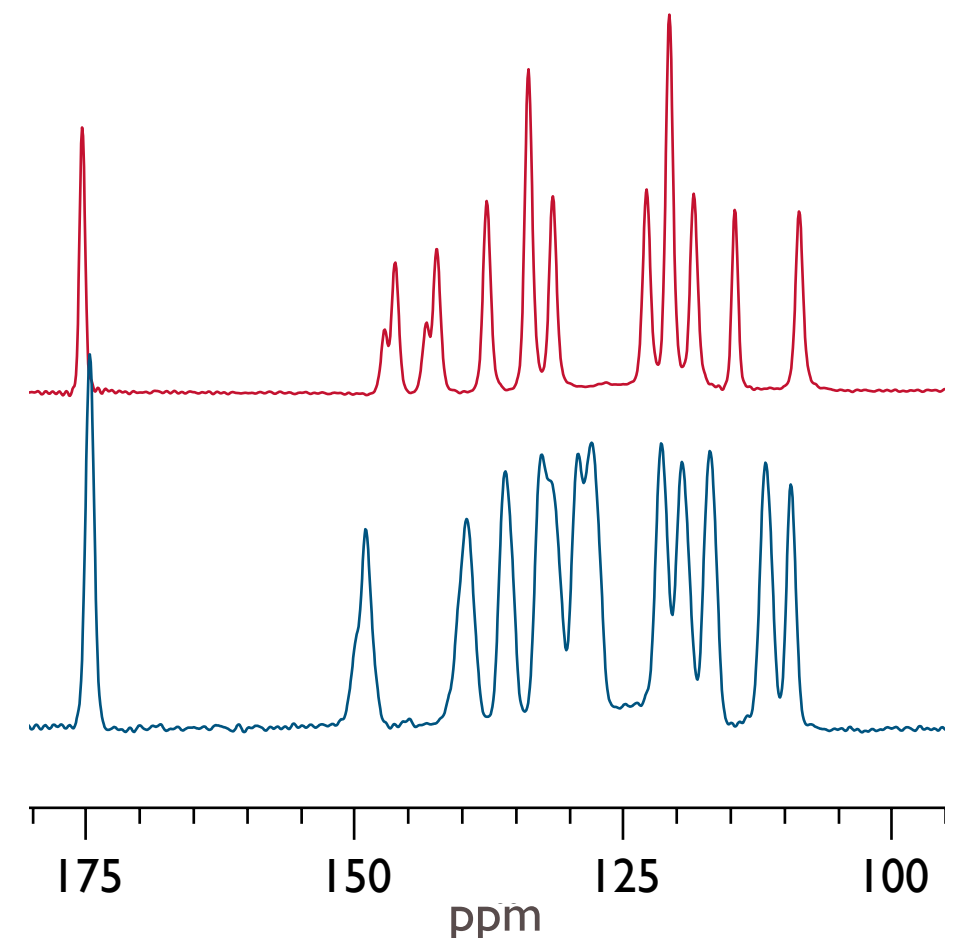
“What has solid-state NMR ever done for us?”

Flufenamic acid

Form I:
monoclinic P21/c



Carbon-13 NMR spectra



Form III:
monoclinic C2/c

Structure: proteins; peptides; carbohydrates; **pharmaceutical molecules;** synthetic polymers; zeolites; conformational details like interatomic distances and dihedral angles

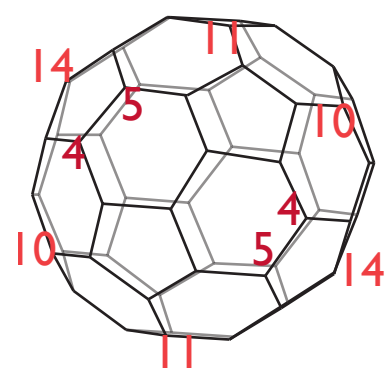
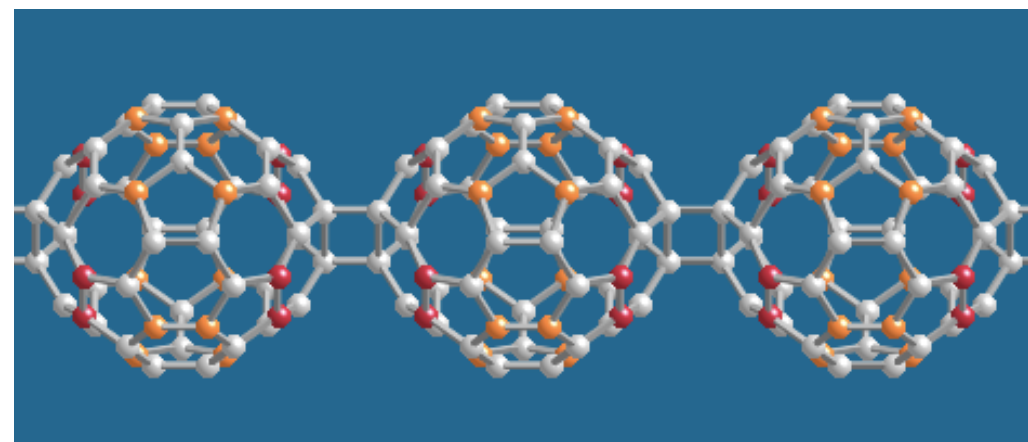
“What has solid-state NMR ever done for us?”

Disordered solids: molecular structure; orientational order; polymers; glasses; liquid crystals ...
where diffraction techniques are less useful.

Caesium fulleride

DFT Calculations

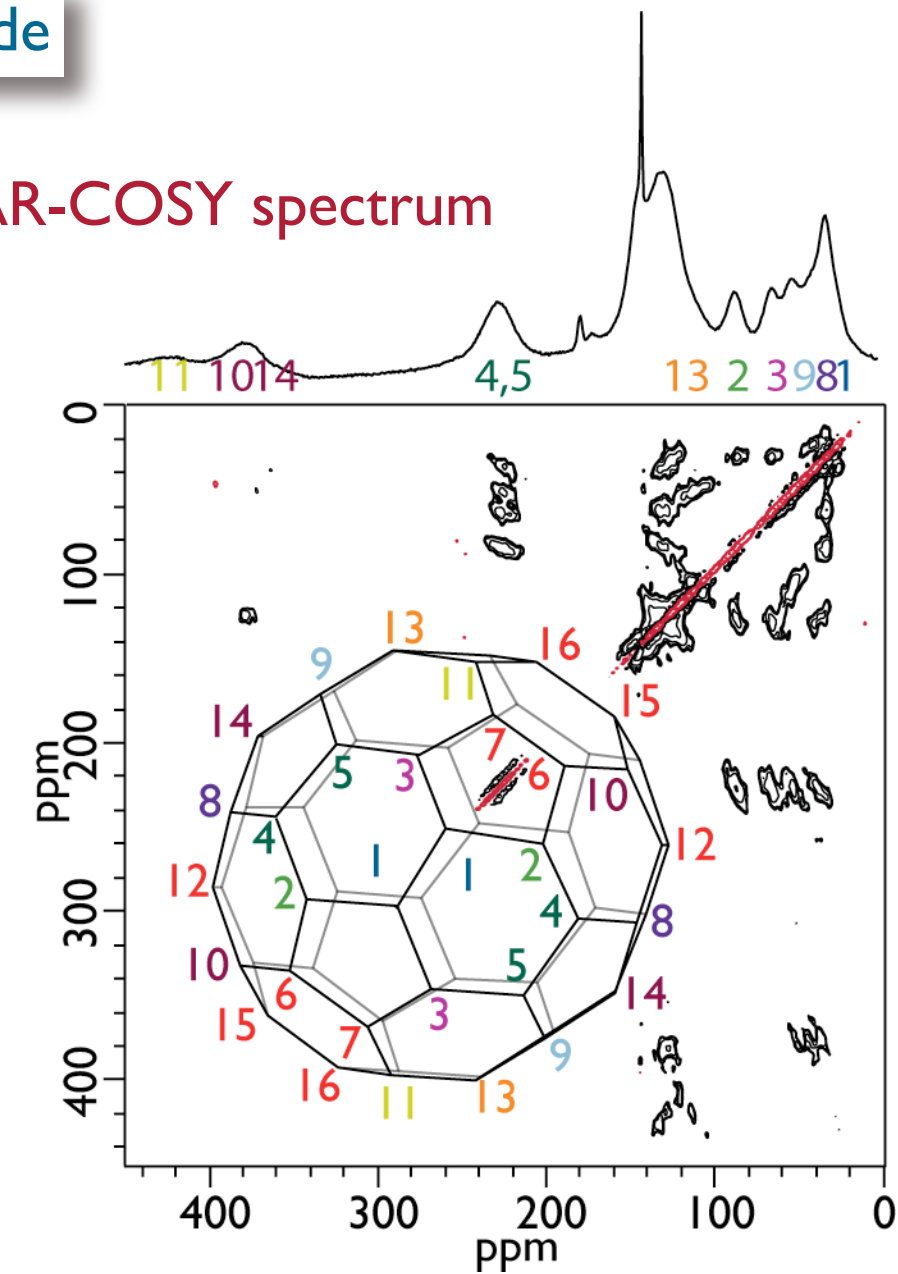
GAUSSIAN98, CsC₆₀ trimer



Hyperfine couplings / MHz

- (4,5) 2.2
- (14,10,11) 6.8

SAR-COSY spectrum

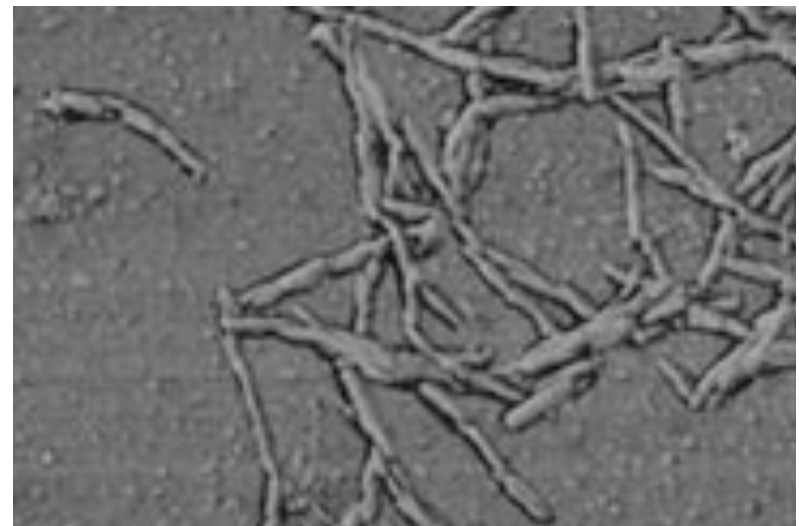


T. M. de Swiet, J. L. Yarger, T. Wagberg, J. Hone, B. J. Gross, M. Tomaselli, J. J. Titman, A. Zettl and M. Mehring, *Phys. Rev. Lett.*, **84**, 717 (2000)

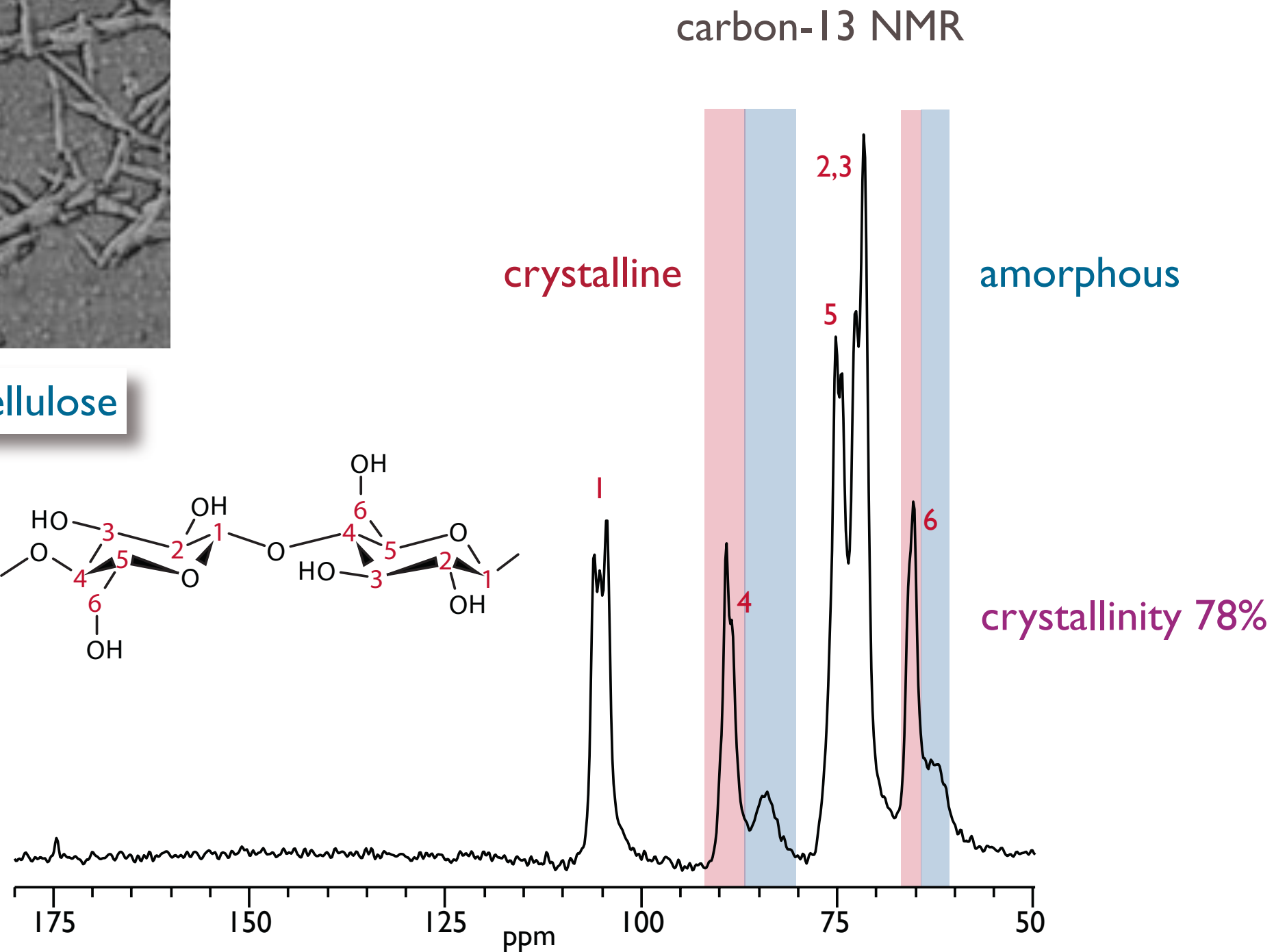
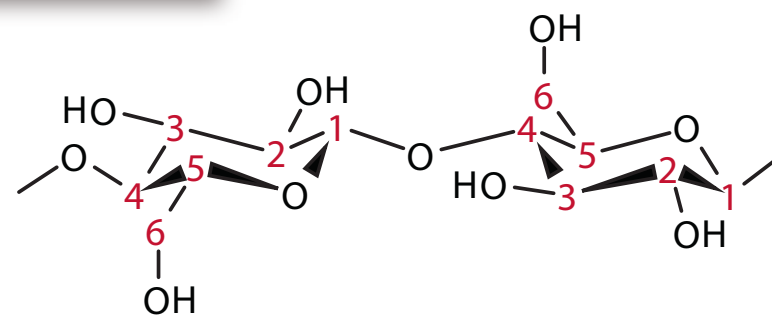
G. Grasso, T. M. De Swiet and J. J. Titman, *J. Phys. Chem. B*, **106**, 8676 (2002)

D. Lee, J. Struppe, D. W. Elliott, L. J. Mueller and J. J. Titman, *Phys. Chem. Chem. Phys.*, **11**, 3547 (2009)

“What has solid-state NMR ever done for us?”



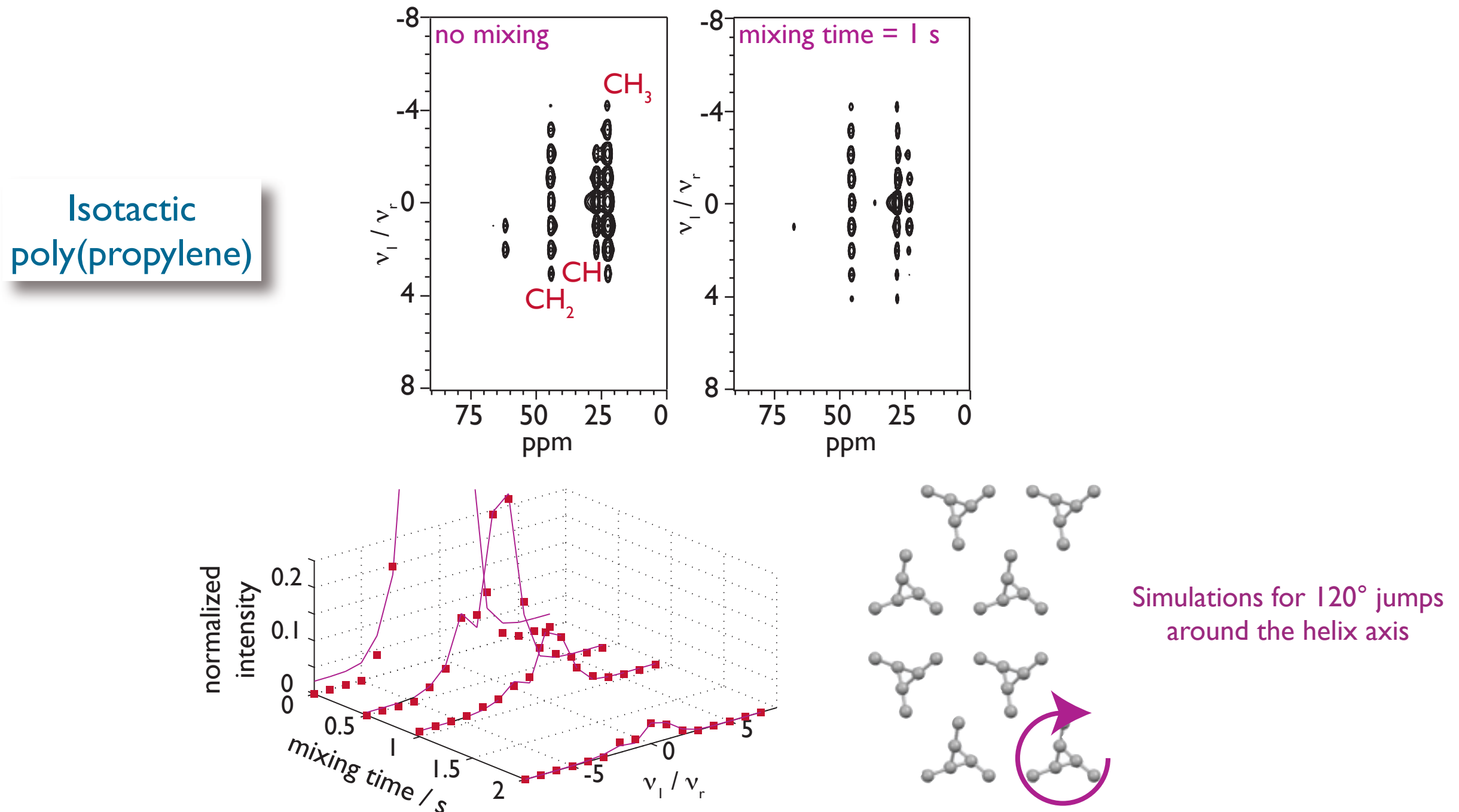
Nano-crystalline cellulose



Heterogeneity: amorphous and crystalline domains; phase separation; domain sizes; interfaces; polymer blends; block copolymers; nano-composites; supramolecular systems

“What has solid-state NMR ever done for us?”

Dynamics: plastic crystals, polymers, superionic conductors ... molecular **rotations** and diffusion; range of correlation times from s to ps; model-free.



Nuclear spin Hamiltonian

$$H = -\sum_j \gamma_j I_{jz} B_0 - \sum_j \gamma_j \frac{B_{rf}}{2} \left[I_{jx} \cos(\omega_{rf} t + \varphi) + I_{jy} \sin(\omega_{rf} t + \varphi) \right] +$$

$$\sum_j \gamma_j I_j \sigma_j B_0 + 2\pi \sum_{j < k} I_j J_{jk} I_k + \sum_{j < k} I_j D_{jk} I_k + \sum_j I_j Q_j I_j + \sum_j I_j A_j S$$

shift scalar coupling dipolar coupling quadrupolar interaction hyperfine interaction

External terms: static magnetic field B_0 and radio-frequency field B_{rf}

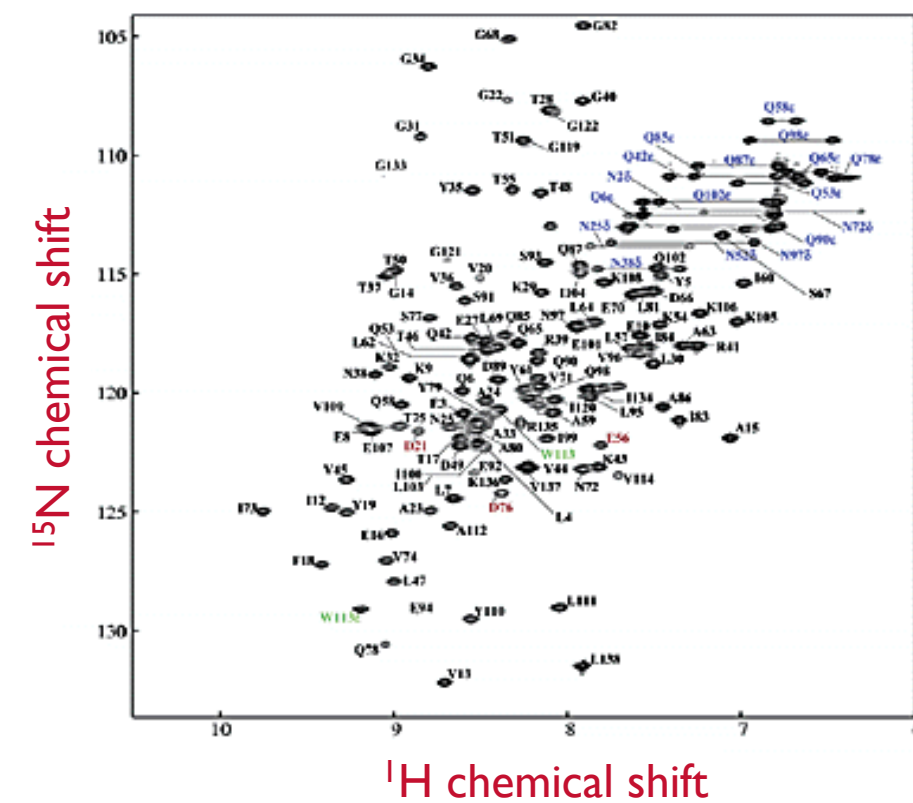
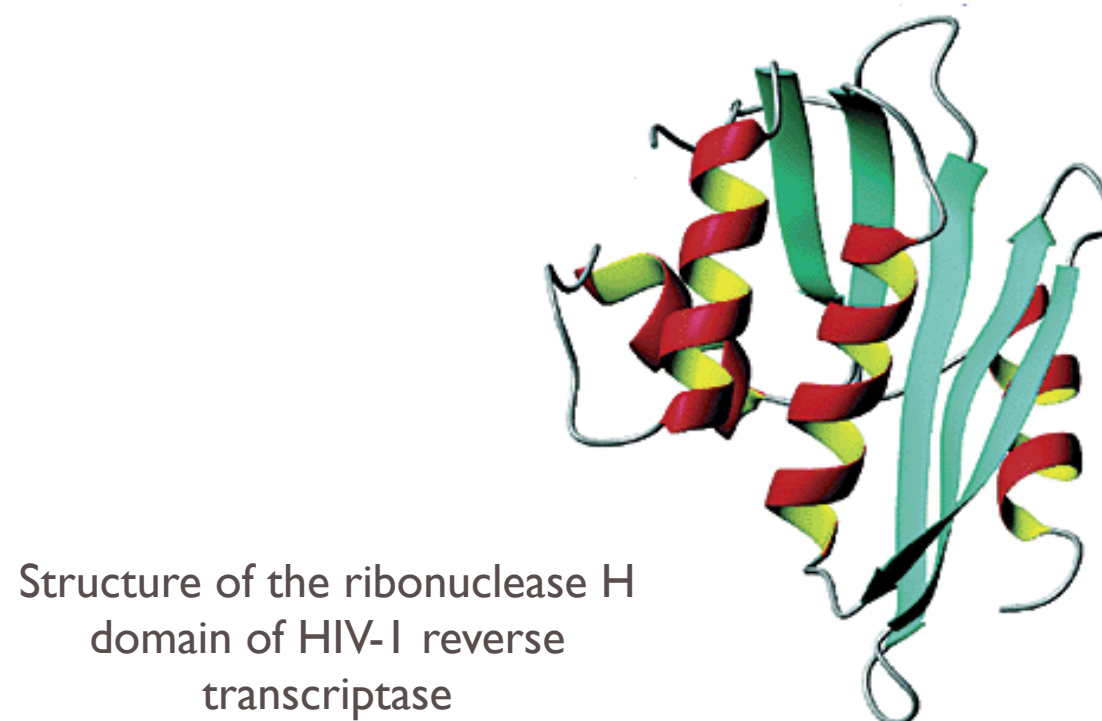
Internal terms: interactions with the surroundings which contain information about the system

Solution-state NMR: chemical environment

$$H = -\sum_j \gamma_j I_{jz} B_0 - \sum_j \gamma_j \frac{B_{rf}}{2} \left[I_{jx} \cos(\omega_{rf} t + \varphi) + I_{jy} \sin(\omega_{rf} t + \varphi) \right] +$$

$\sum_j \gamma_j I_j \sigma_j \mathbf{B}_0$ shift $+ 2\pi \sum_{j < k} \mathbf{I}_j \mathbf{J}_{jk} \mathbf{I}_k$ scalar coupling $+ \sum_{j < k} \mathbf{I}_j \mathbf{D}_{jk} \mathbf{I}_k + \sum_j \mathbf{I}_j \mathbf{Q}_{jj} + \sum_j \mathbf{I}_j \mathbf{A}_j \mathbf{s}$

Solution-state NMR: the NMR frequency is sensitive to environment via shift interaction



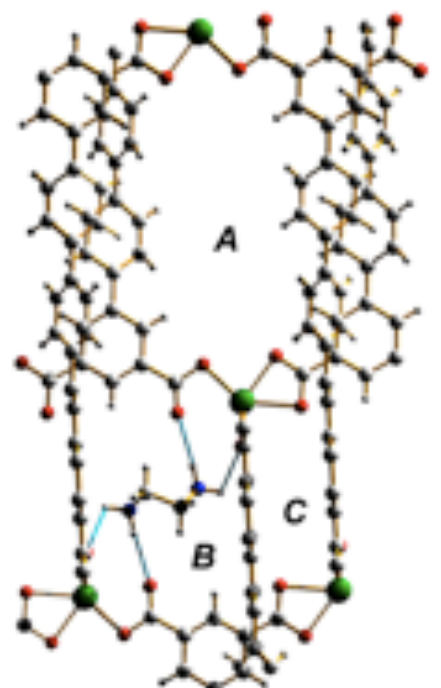
Solid-state NMR: chemical environment

$$H = -\sum_j \gamma_j I_{jz} B_0 - \sum_j \gamma_j \frac{B_{rf}}{2} \left[I_{jx} \cos(\omega_{rf} t + \varphi) + I_{jy} \sin(\omega_{rf} t + \varphi) \right] +$$

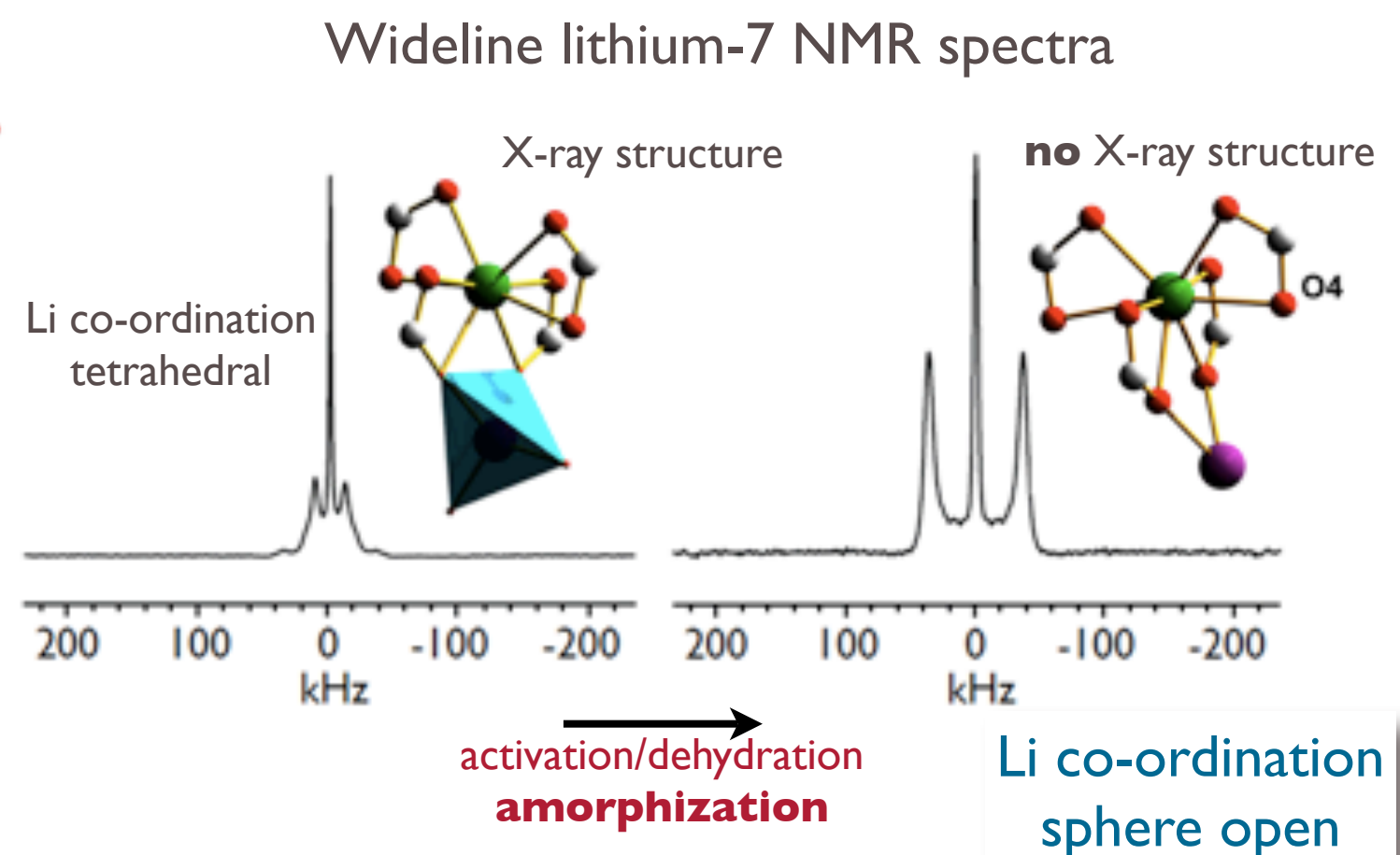
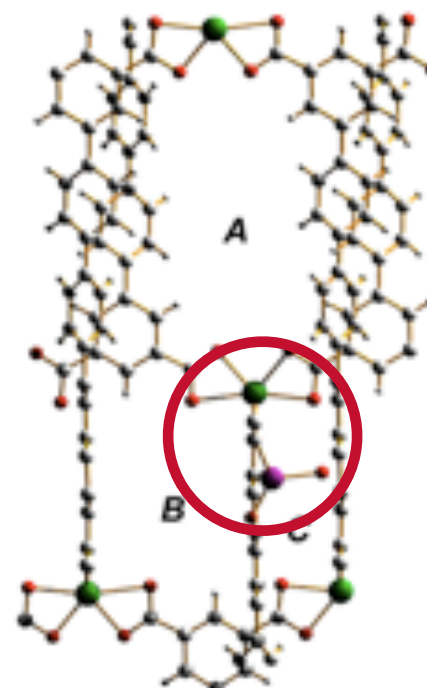
\$\sum_j \gamma_j I_j \sigma_j B_0\$ shift
 \$\sum_{j < k} I_j J_{jk} I_k\$ scalar coupling
 \$\sum_{j < k} I_j D_{jk} I_k\$ dipolar coupling
 \$\sum_j I_j Q_{jj}\$ quadrupolar interaction
 \$\sum_j I_j A_j S\$ hyperfine interaction

shift
 scalar coupling
 dipolar coupling
 quadrupolar interaction
 hyperfine interaction

Solid-state NMR: sensitive to environment via shift, dipolar and quadrupolar interactions



Li^+ ion exchange

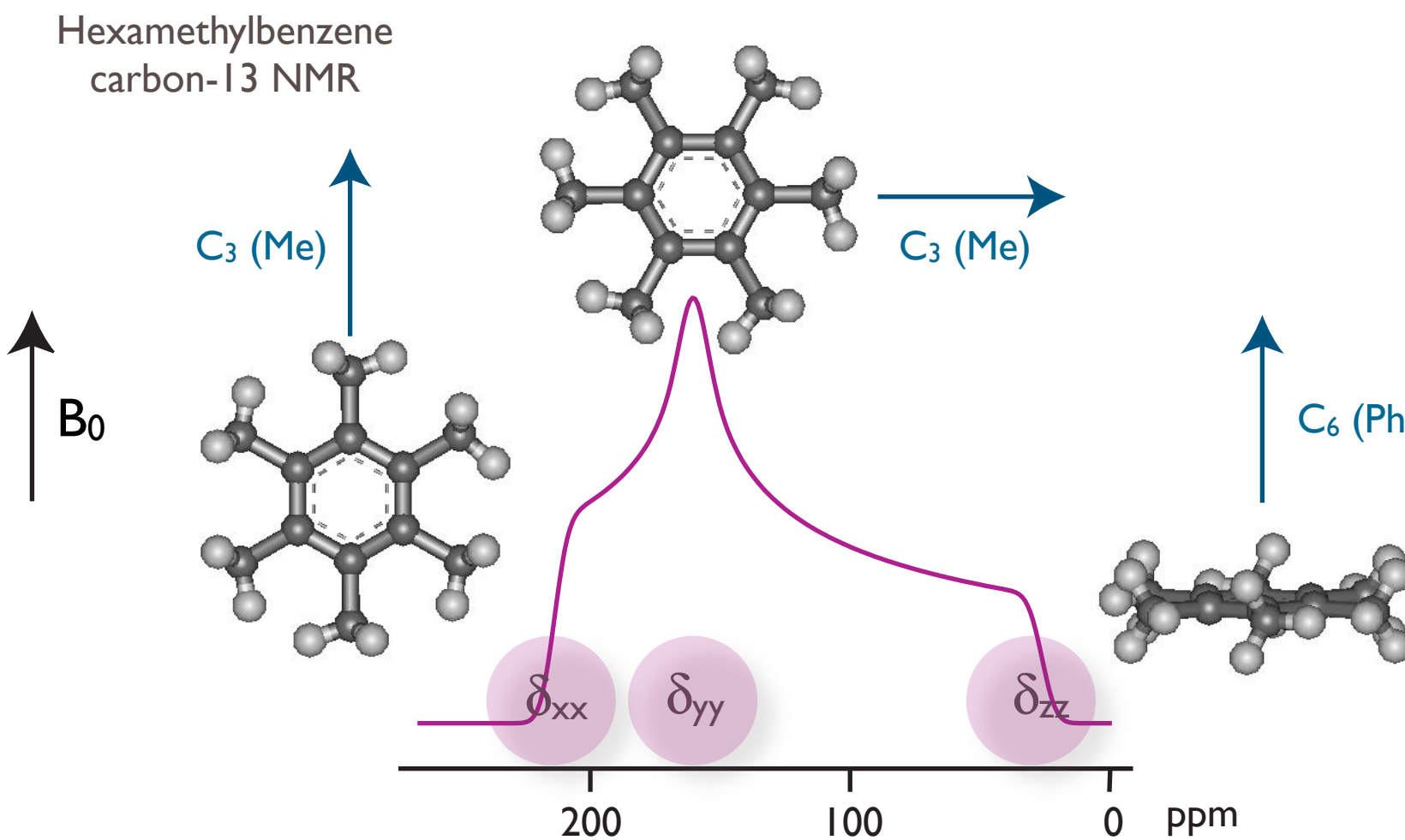


Solid-state NMR: anisotropic interactions

$$H = -\sum_j \gamma_j I_{jz} B_0 - \sum_j \gamma_j \frac{B_{rf}}{2} [I_{jx} \cos(\omega_{rf} t + \varphi) + I_{jy} \sin(\omega_{rf} t + \varphi)] +$$

\$\sum_j \gamma_j I_j \sigma_j \mathbf{B}_0\$ shift
 \$\sum_{j < k} I_j J_{jk} I_k\$ scalar coupling
 \$\sum_{j < k} I_j D_{jk} I_k\$ dipolar coupling
 \$\sum_j I_j Q_{jj} I_j\$ quadrupolar interaction
 \$\sum_j I_j A_j S\$ hyperfine interaction

Solid-state NMR: the NMR frequency is **also** sensitive to orientation

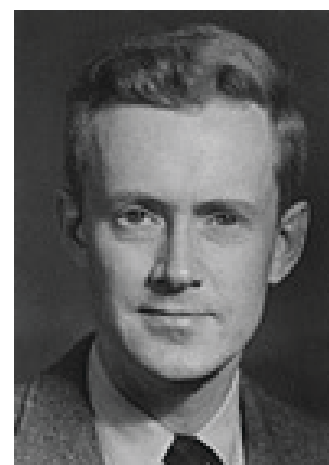


Solid-state NMR

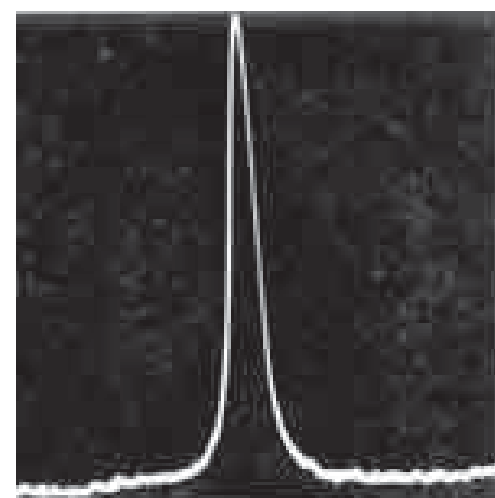
1945



Felix Bloch

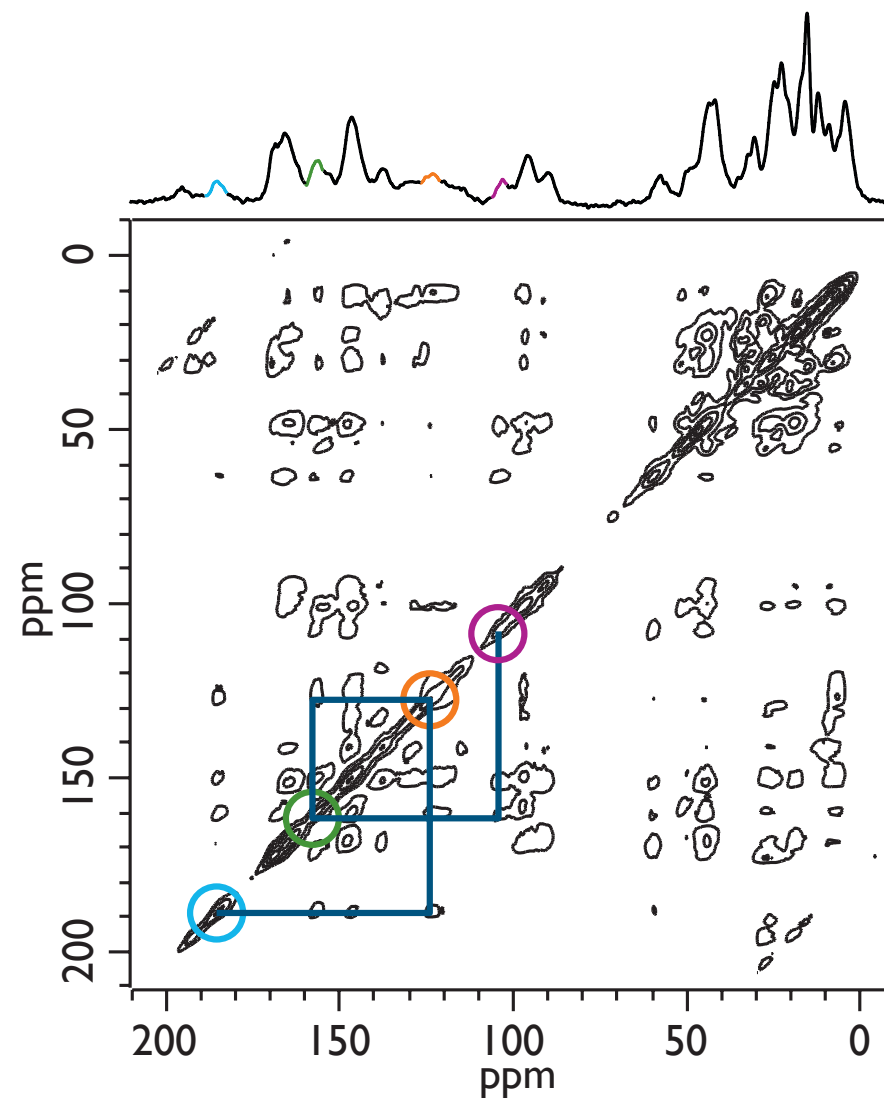


Ed Purcell



Proton NMR
of paraffin wax

Carbon-13 scalar
correlation NMR



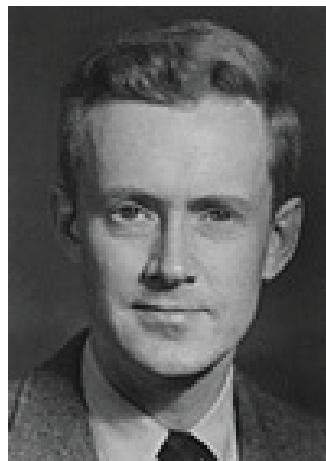
$U-^{13}\text{C}$ -bacteriochlorophyll a

2000

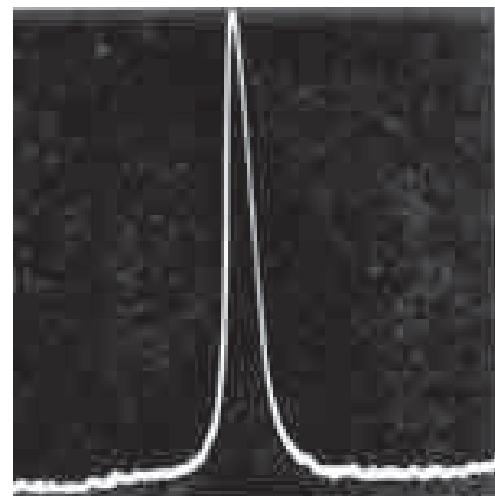
Solid-state NMR



Felix Bloch



Ed Purcell



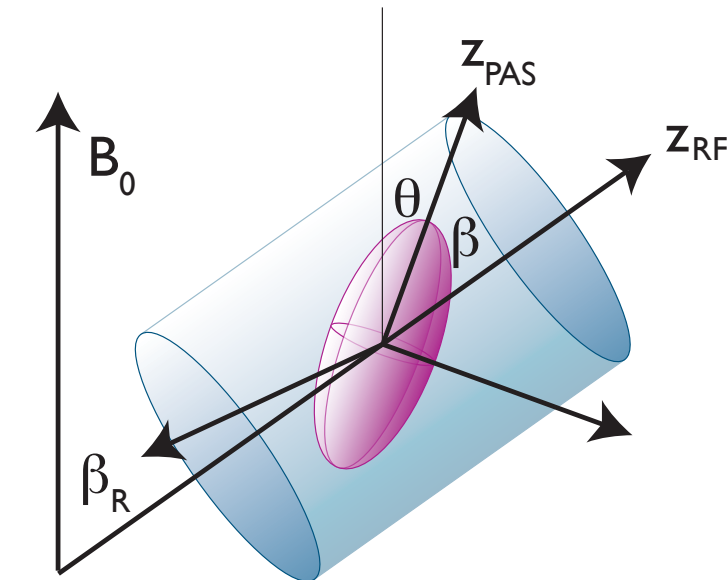
“We were physicists. We knew all the answers. We just
didn’t know what the questions were.”

Magic angle spinning: improving resolution



Raymond Andrew

magic angle: 54.74°
MAS rate: up to 80 kHz



MAS rate

1958

8 kHz



1990

15 kHz

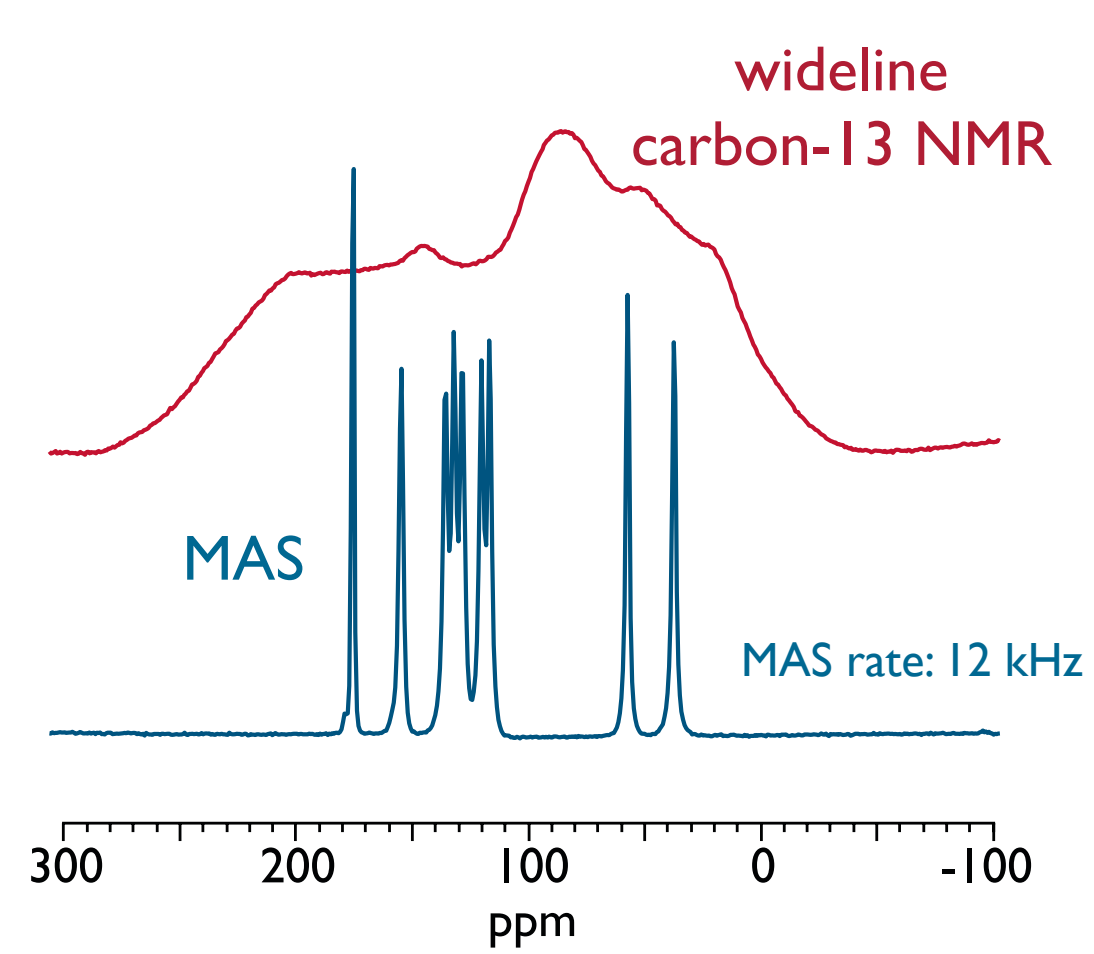


1996

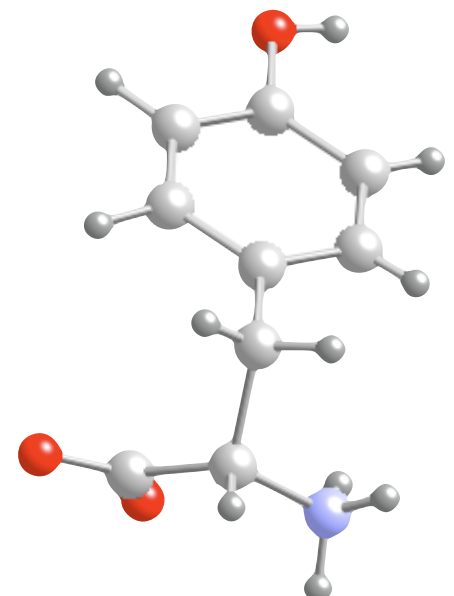
35 kHz

2010

80 kHz



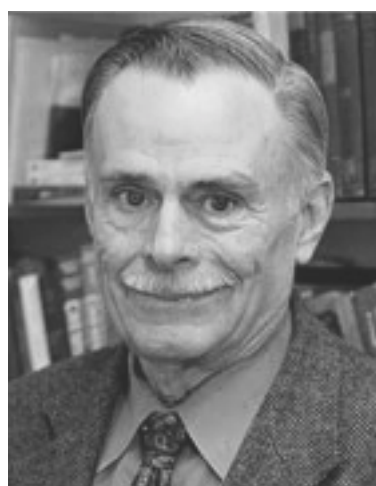
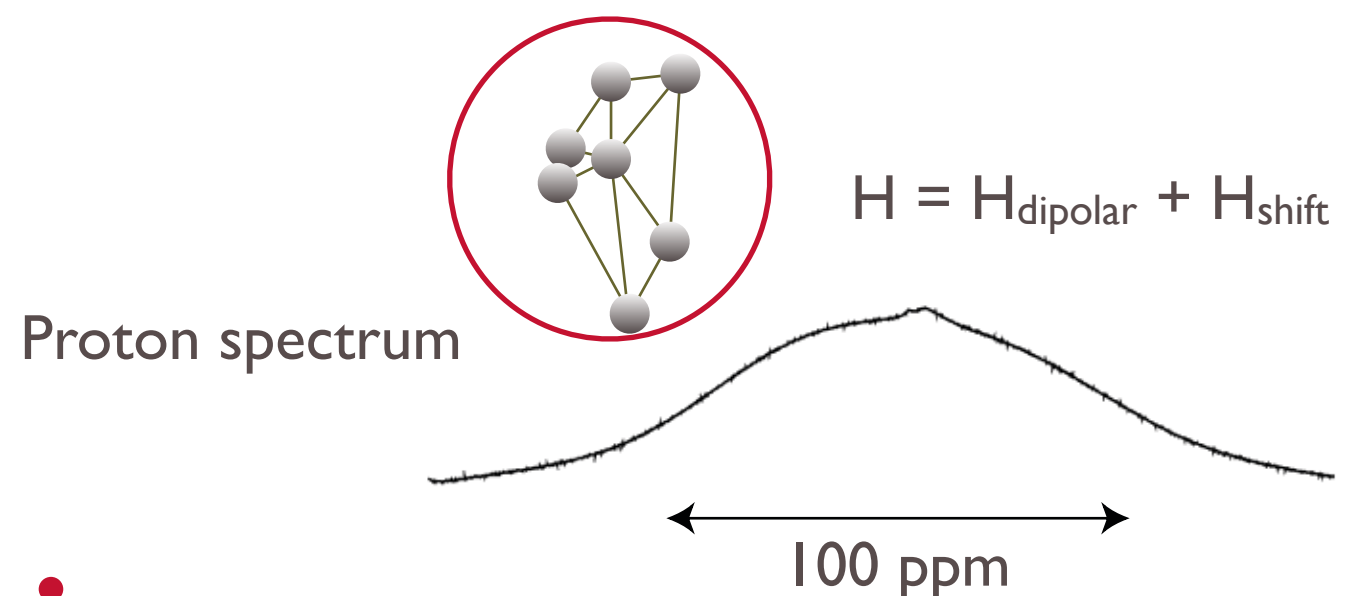
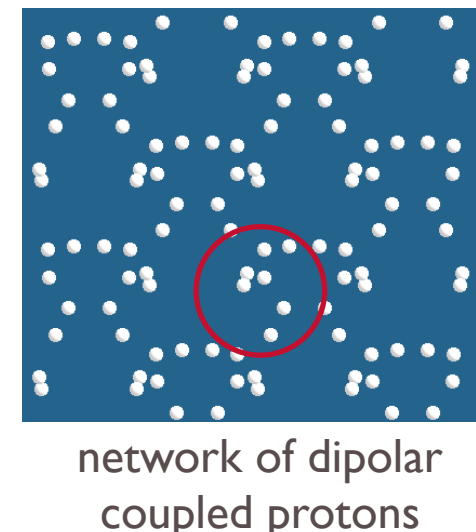
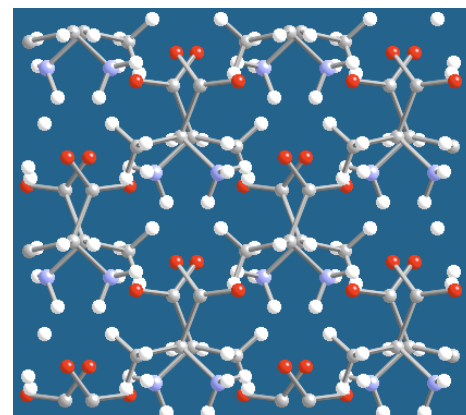
Tyrosine



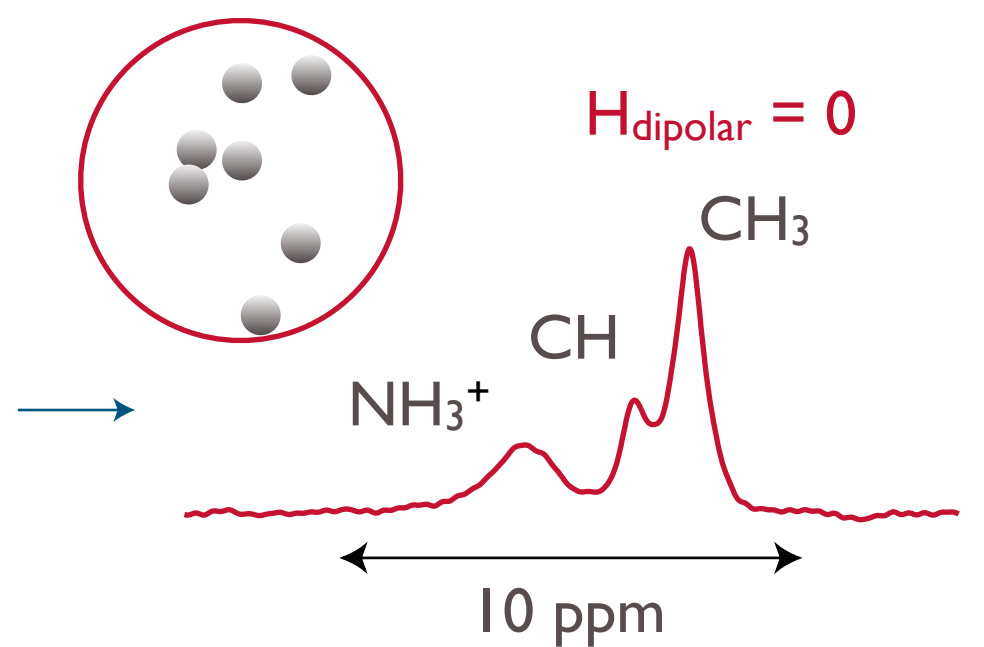
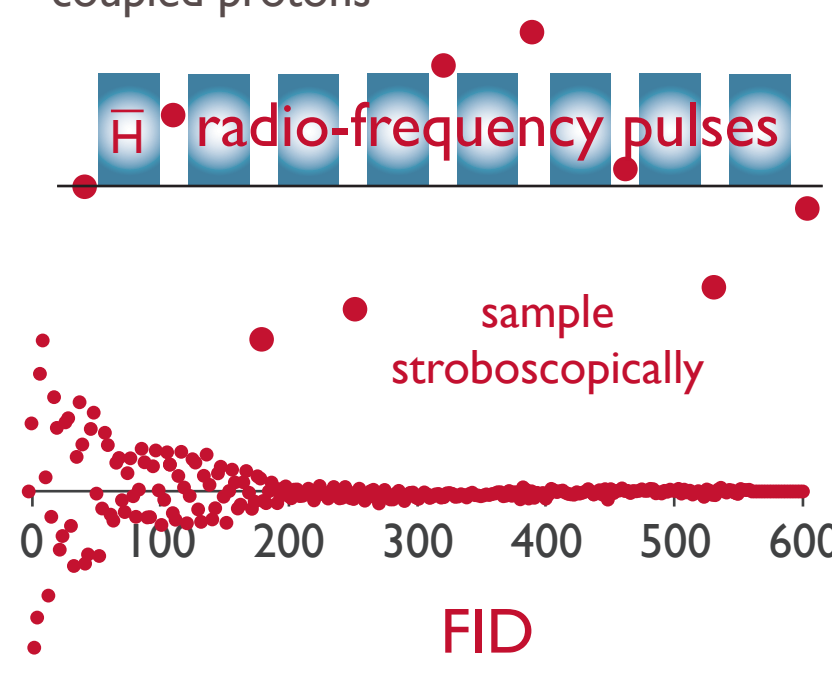
Controlling interactions: average Hamiltonian theory

$$H = -\sum_j \gamma_j I_{jz} B_0 - \sum_j \gamma_j \frac{B_{rf}}{2} \left[I_{jx} \cos(\omega_{rf} t + \varphi) + I_{jy} \sin(\omega_{rf} t + \varphi) \right] + \text{radio-frequency pulses}$$

$$\sum_j \gamma_j I_j \sigma_j B_0 + 2\pi \sum_{j < k} I_j J_{jk} I_k + \sum_{j < k} I_j D_{jk} I_k + \sum_j I_j Q_{jj} + \sum_j I_j A_j S$$

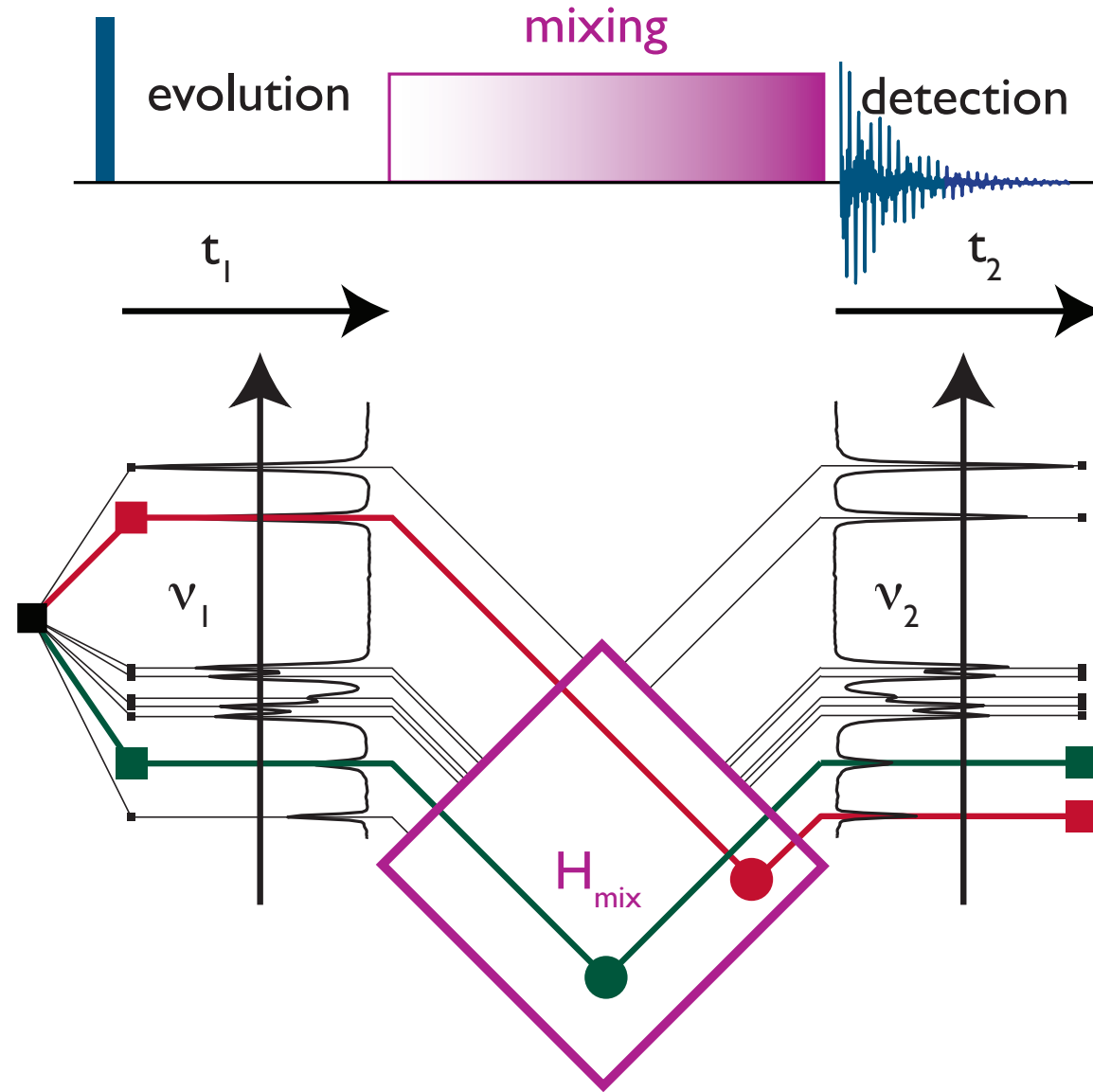


John Waugh

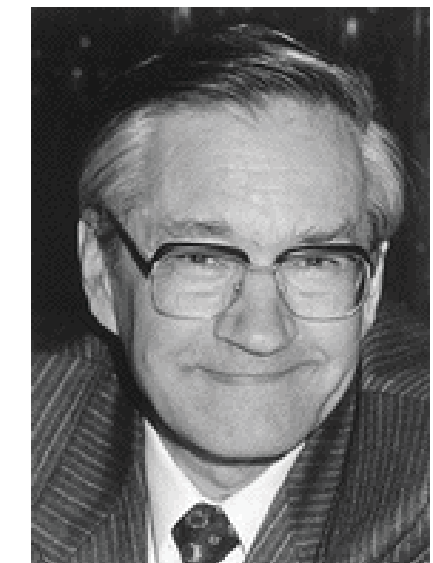
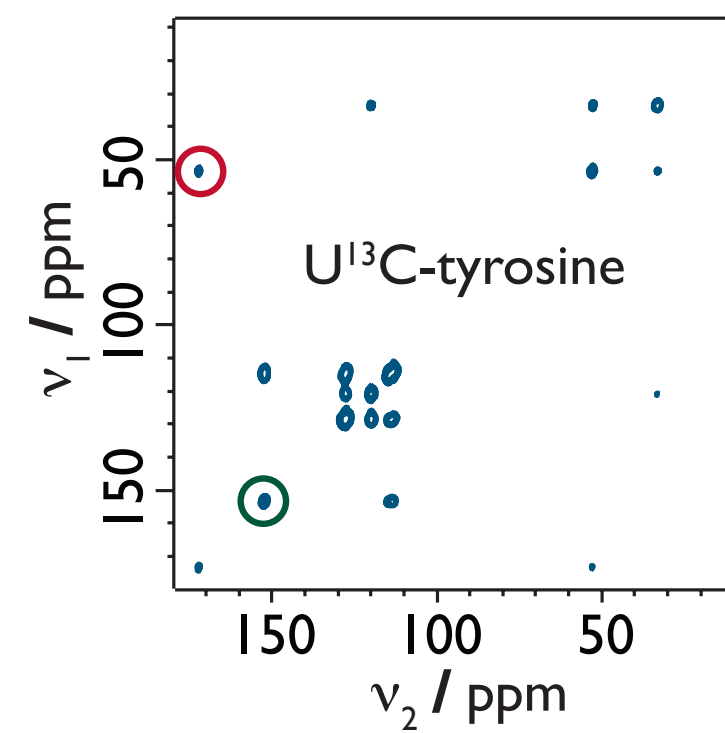


Correlating spins: two-dimensional NMR spectroscopy

preparation



two-dimensional
Fourier transform



Richard Ernst

Solid-state NMR: experiment design

Answers:

Multi-dimensional NMR
Average Hamiltonian theory
Magic angle spinning

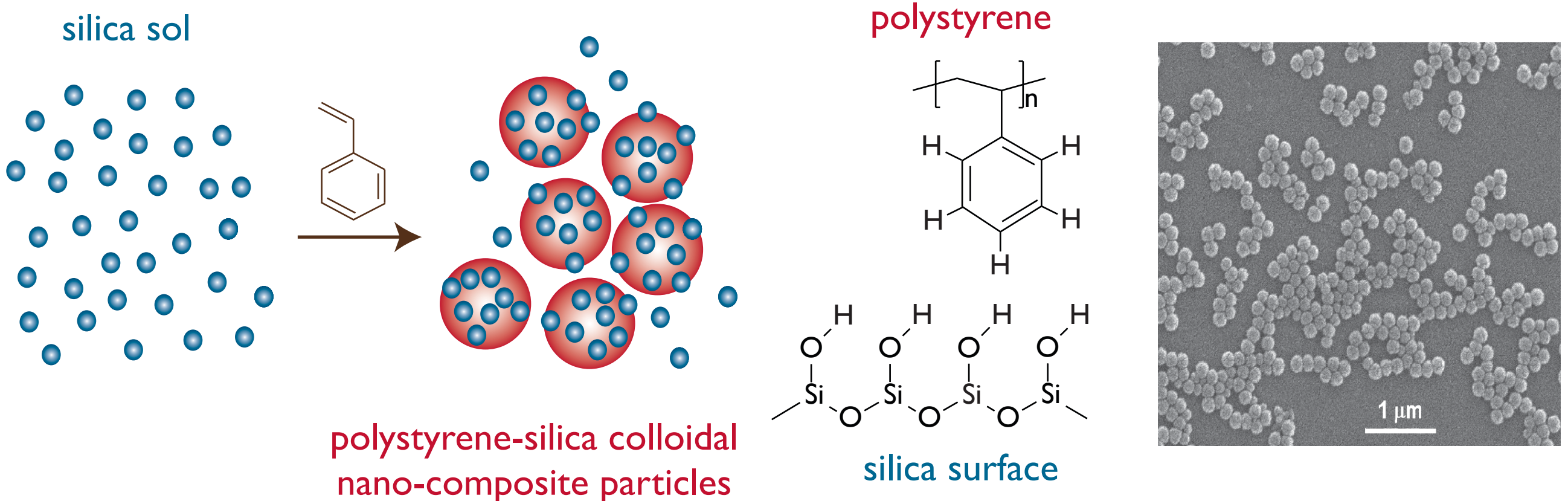


Novel Solid-state
NMR Experiments



Questions

Polystyrene-silica colloidal nano-composites

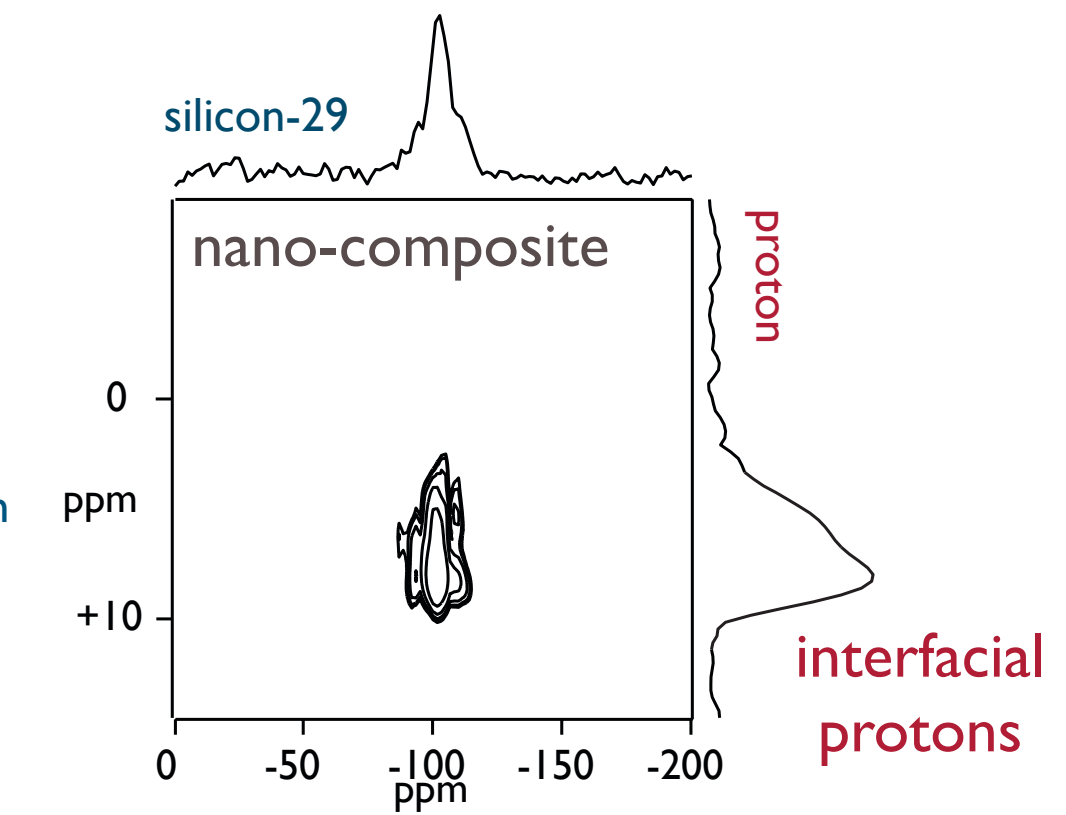
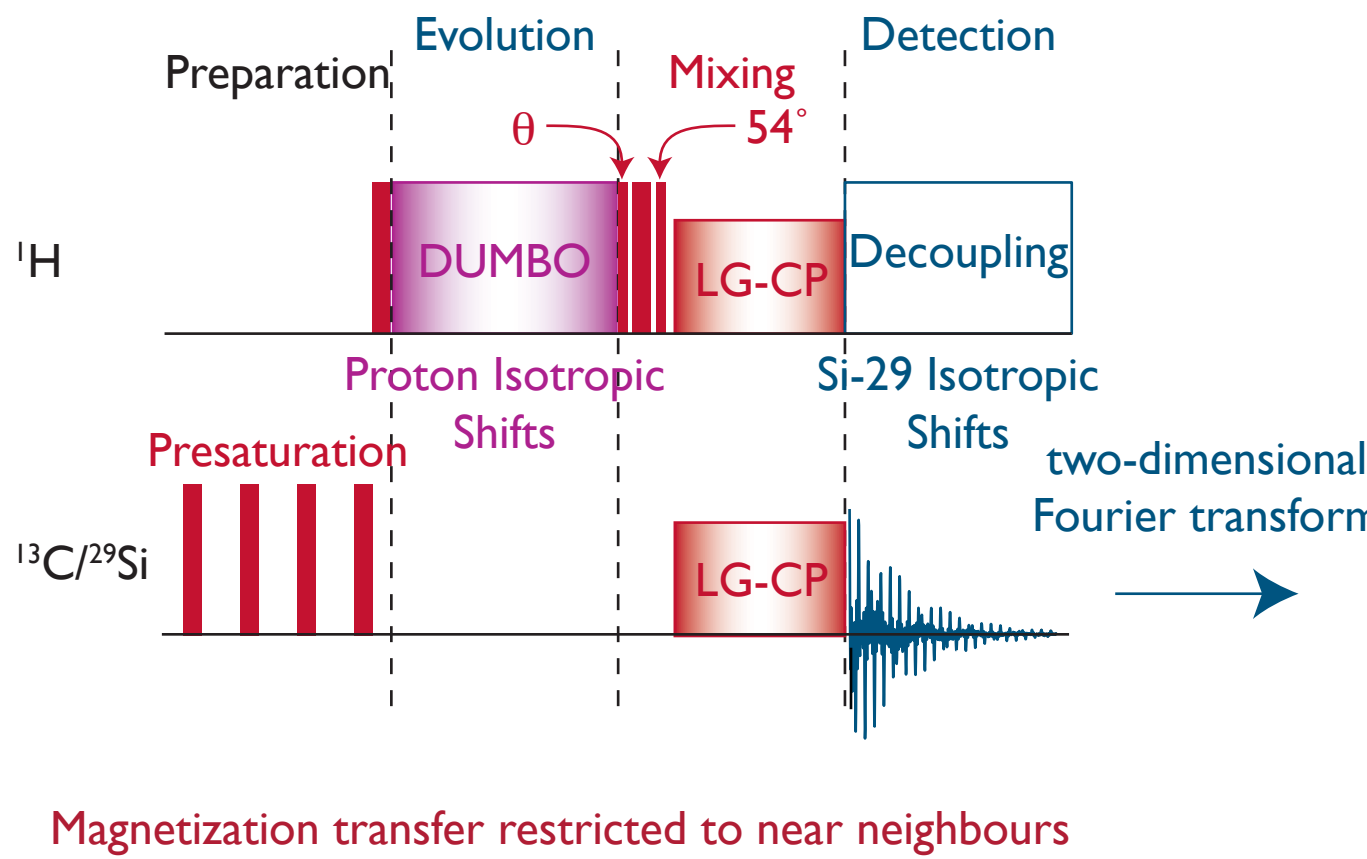
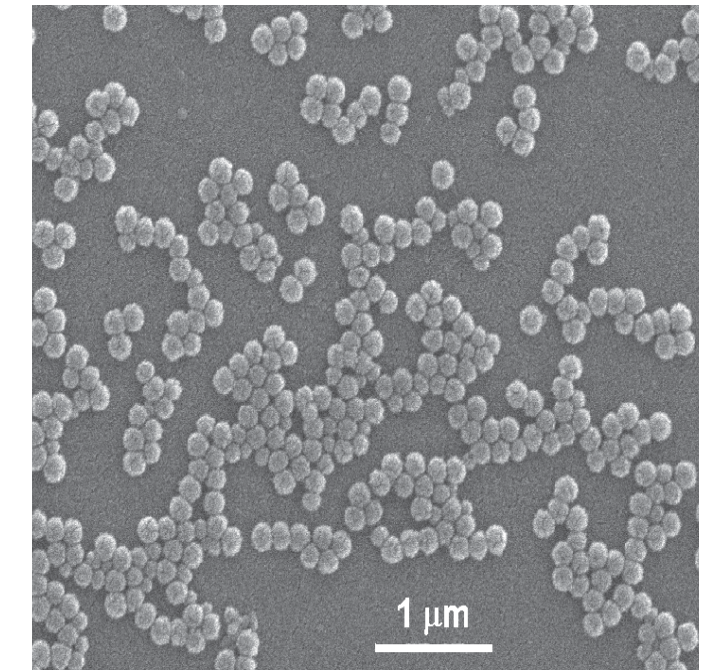
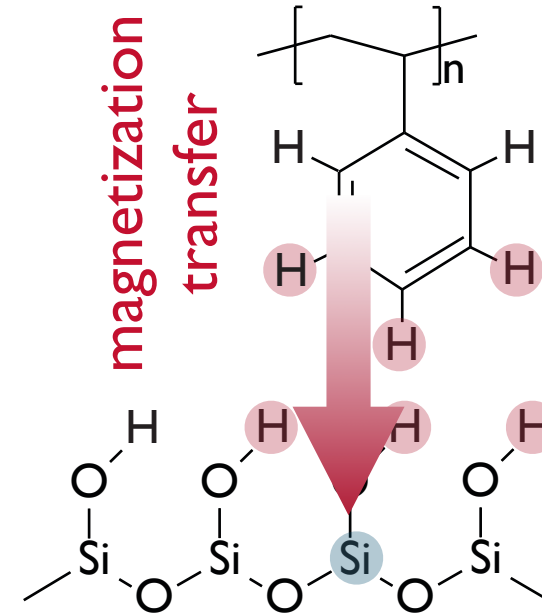
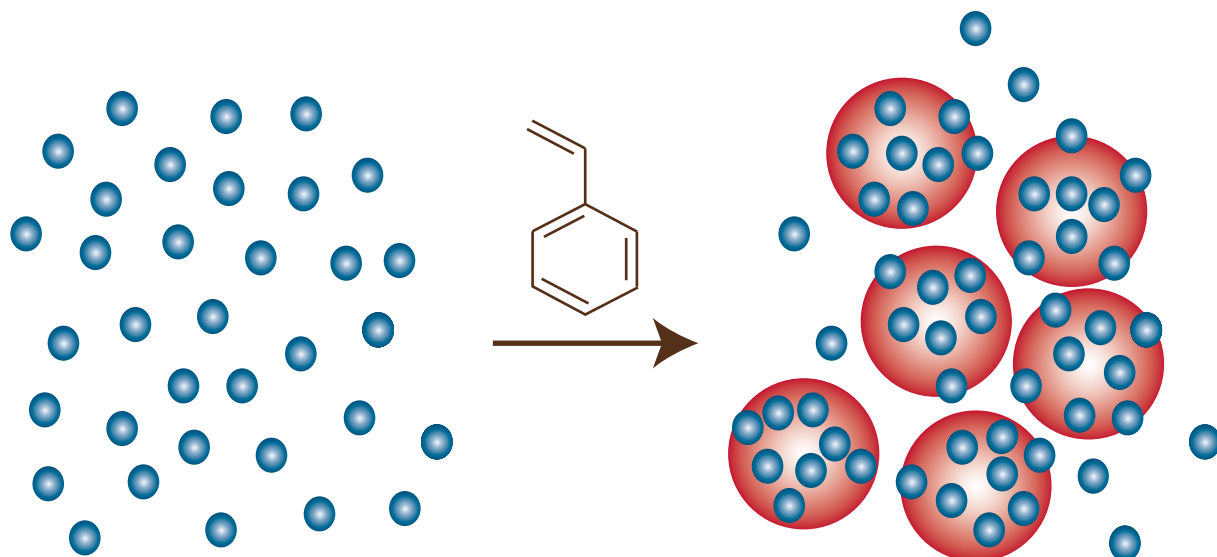


PS-SiO₂ colloidal nano-composites

- * Styrene is emulsion polymerized in the presence of a silica sol to produce nano-composite particles 150 to 300 nm in diameter.
- * Silica adds mechanical strength to the polymer for scratch-resistant coatings.

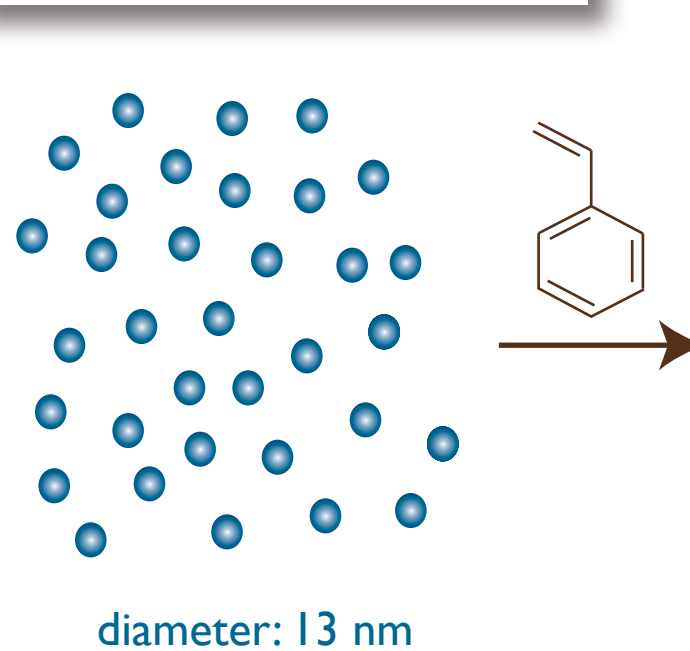
What is the nature of the interaction between the component phases?

Experiment design: NMR of the interface

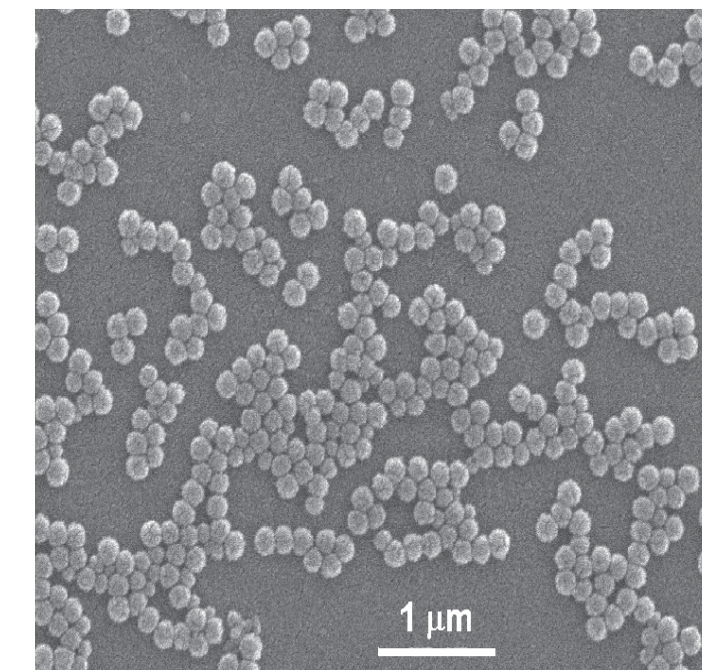
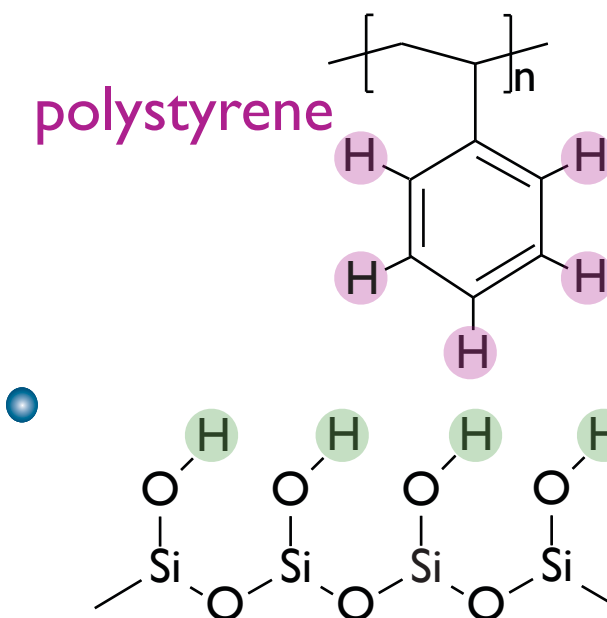


Alcoholic PS-SiO₂ nano-composites

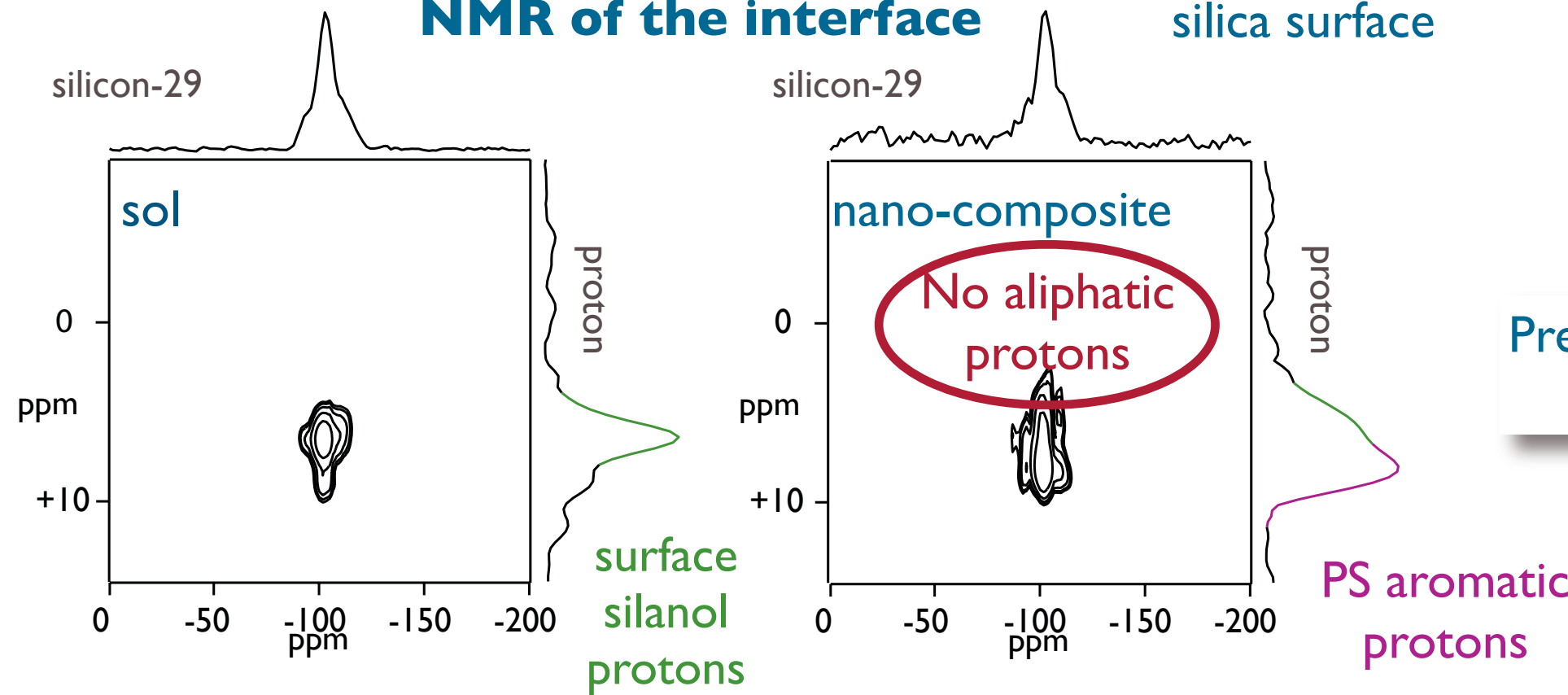
IPA-ST: alcoholic
silica sol



Colloidal nano-composite particles
with a “currant-bun” morphology



NMR of the interface

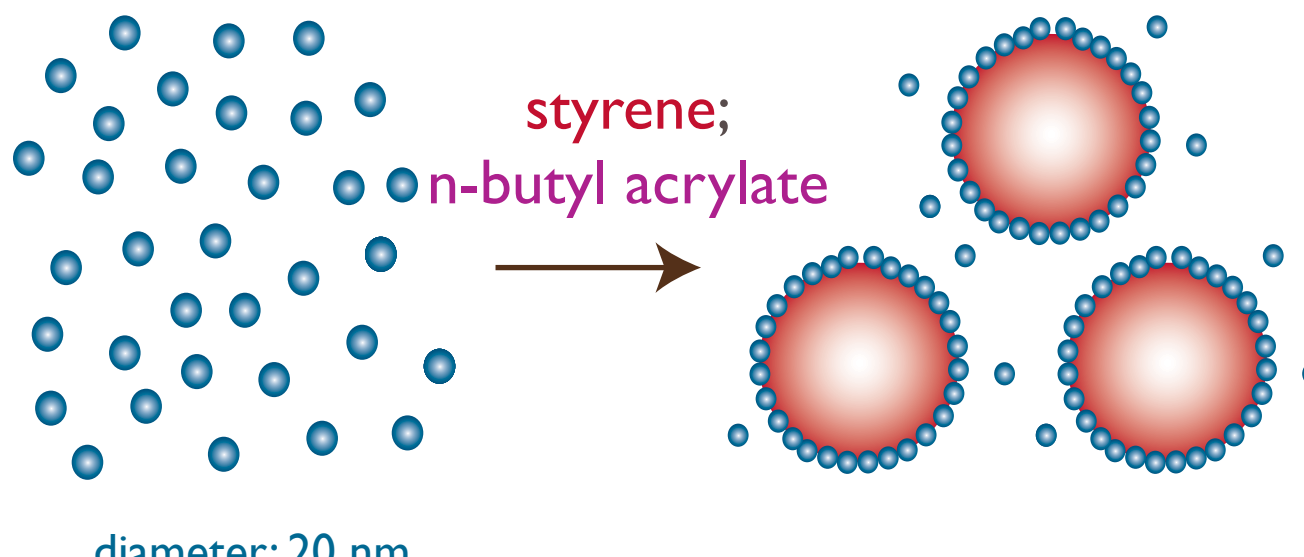


diameter: 180 nm

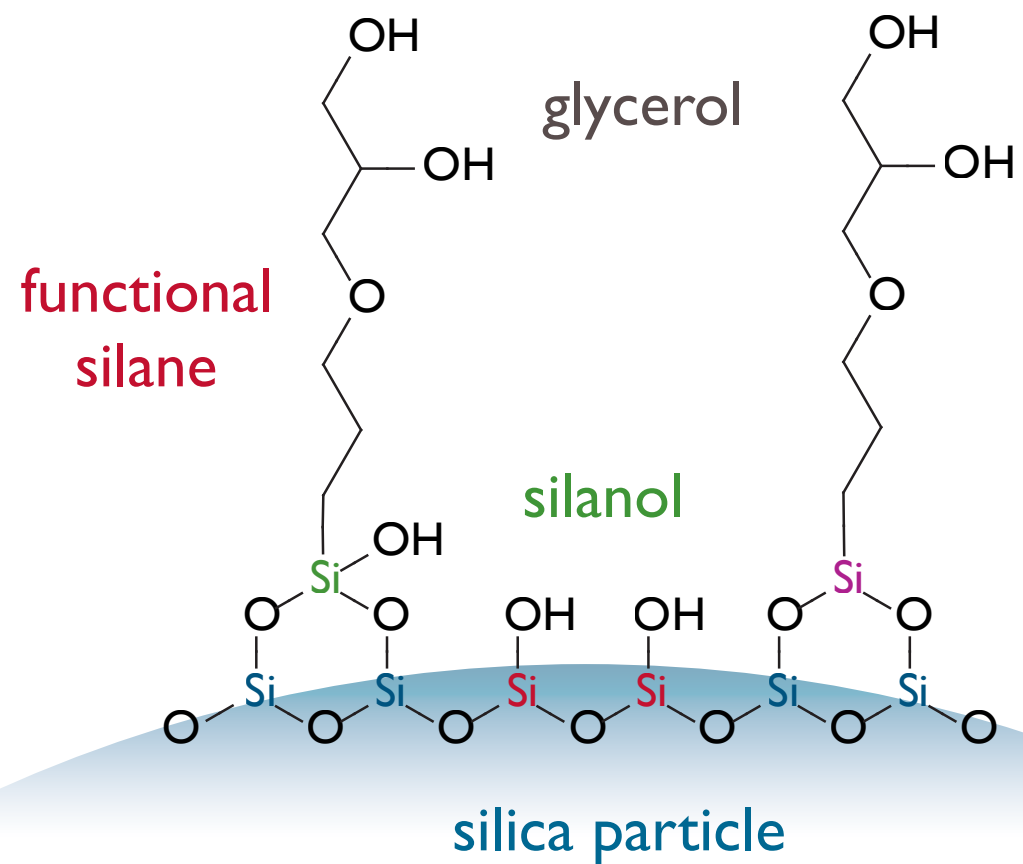
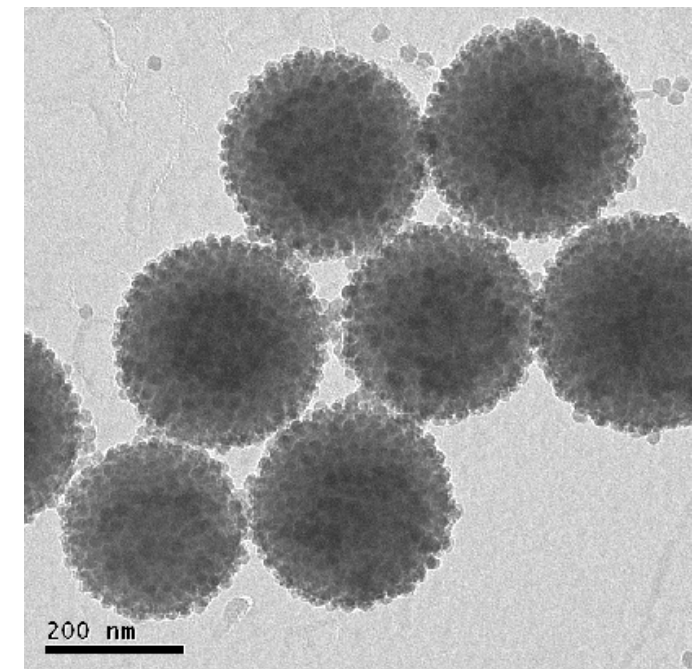
Preferential interaction with
aromatic PS protons

Aqueous PS/P(BuA)-silica nano-composites

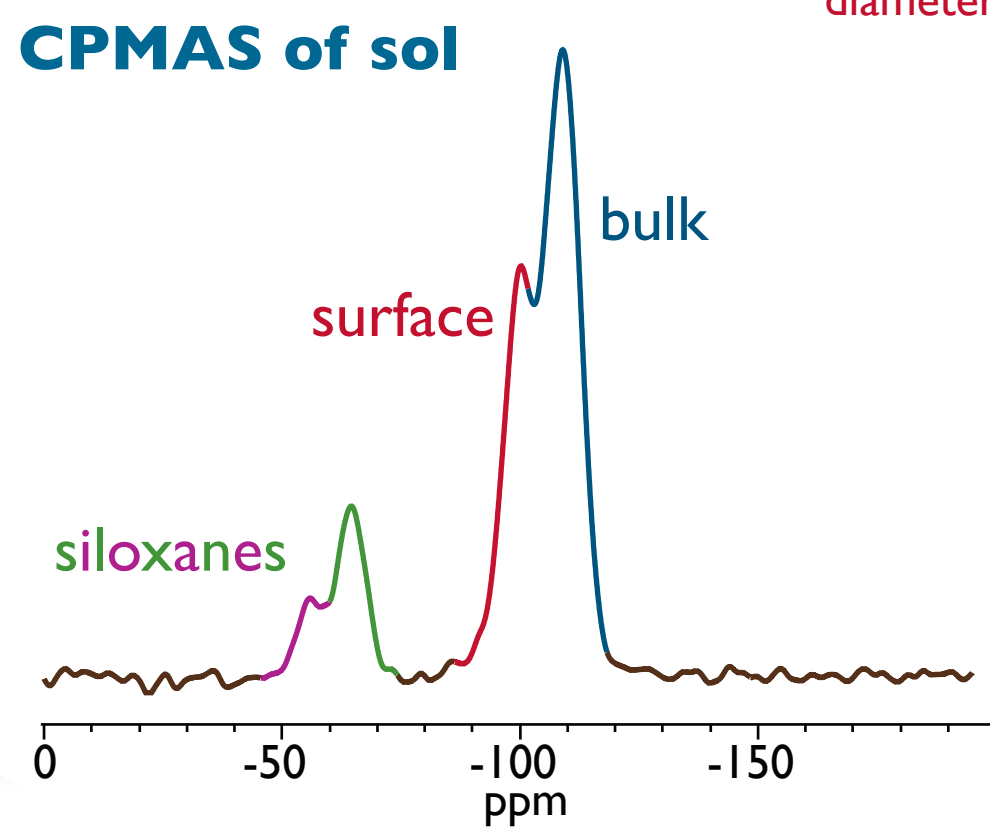
Binzidil CC40: surface functionalized silica sol



Colloidal nano-composite particles with a core-shell morphology

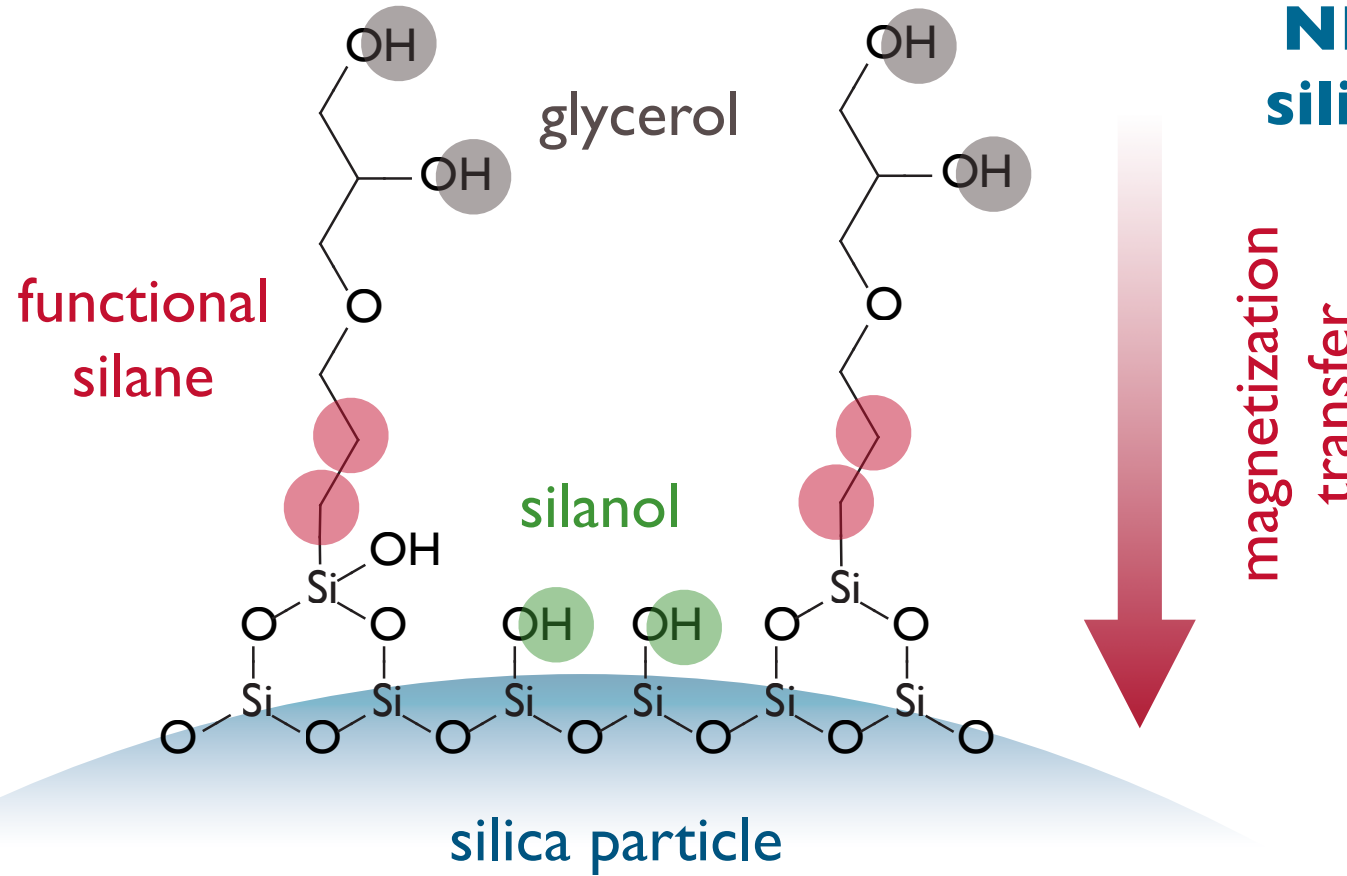
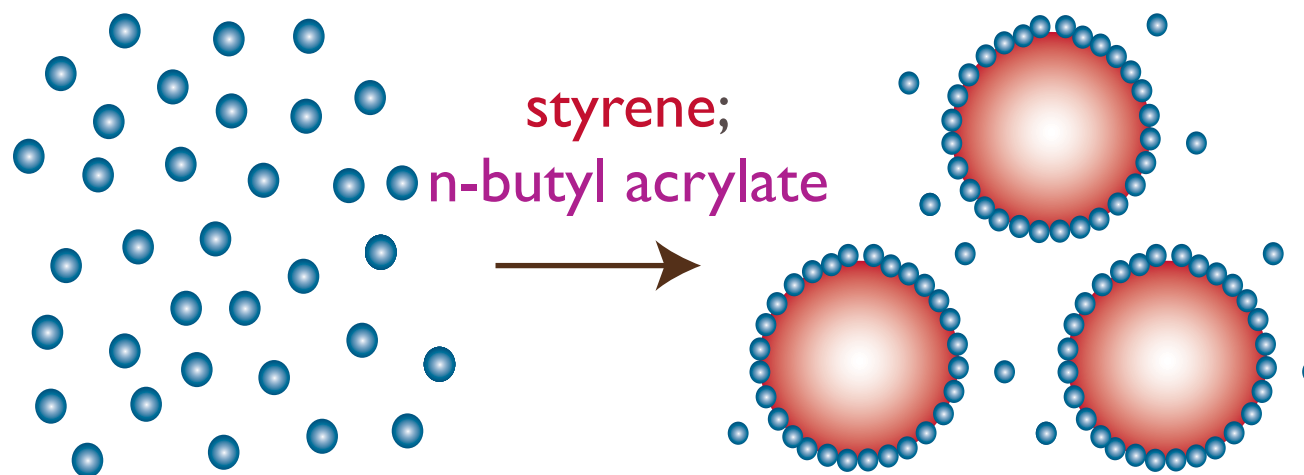


**Silicon-29
CPMAS of sol**

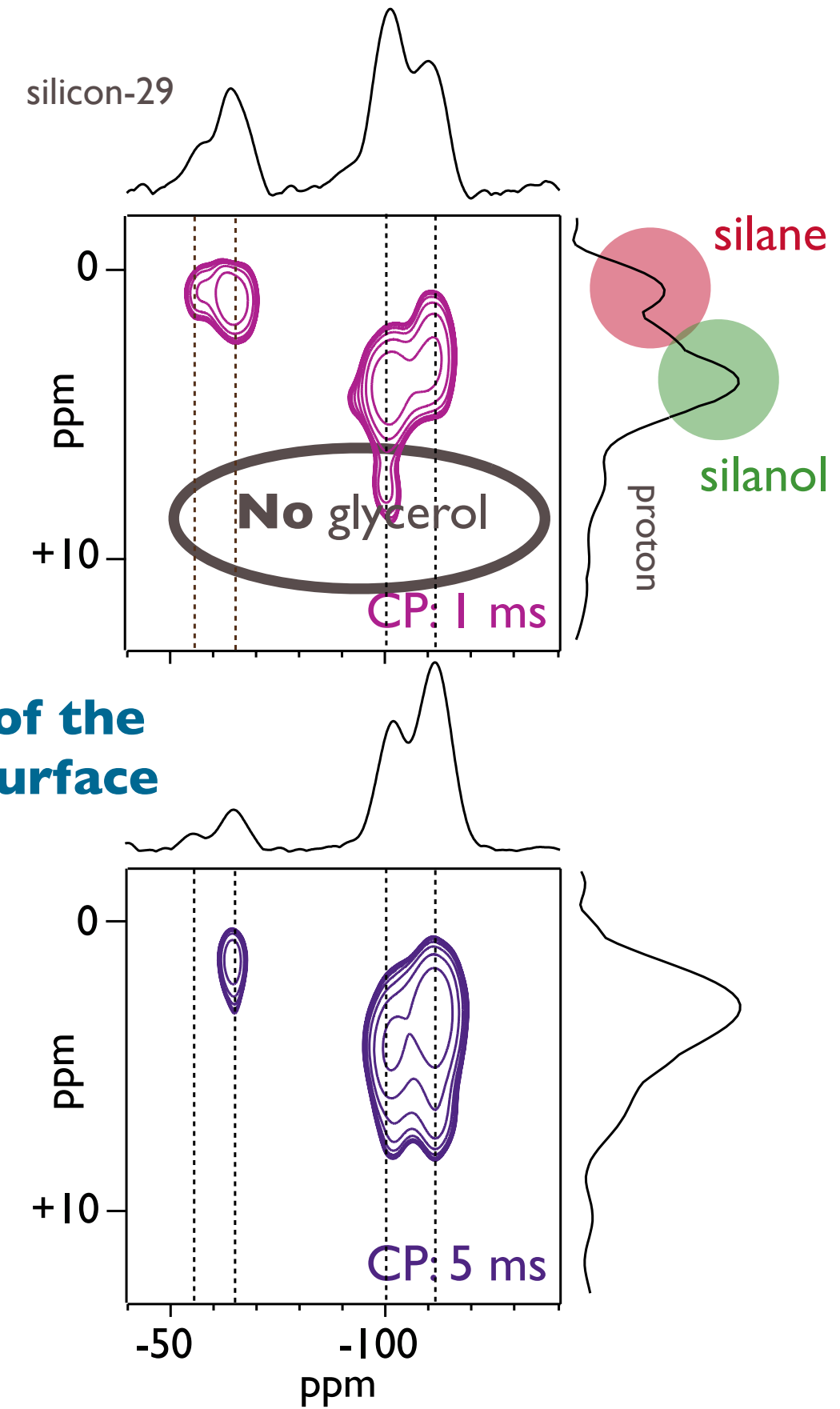


^1H - ^{29}Si NMR: surface of the sol

Binzidil CC40: surface functionalized silica sol

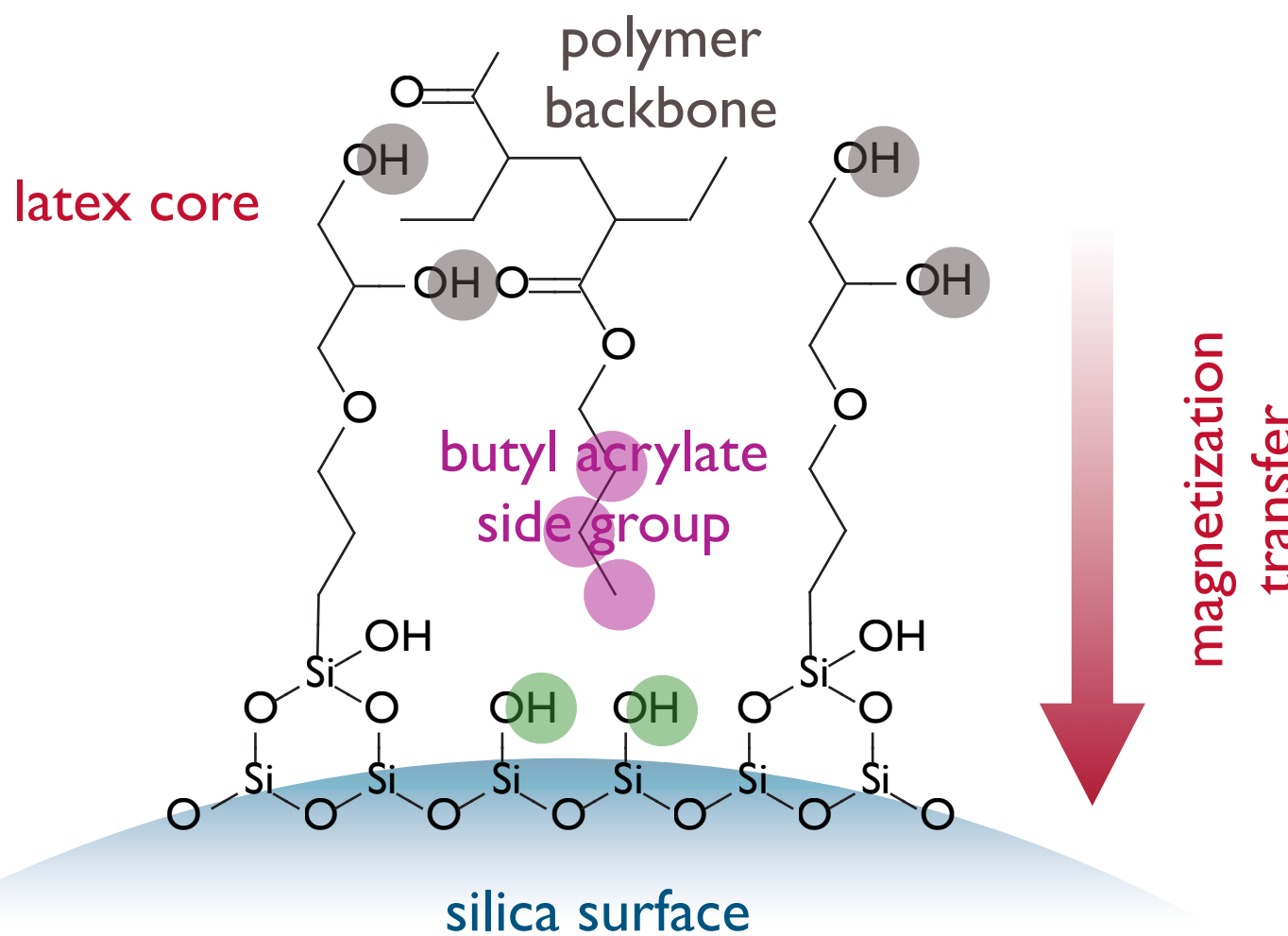
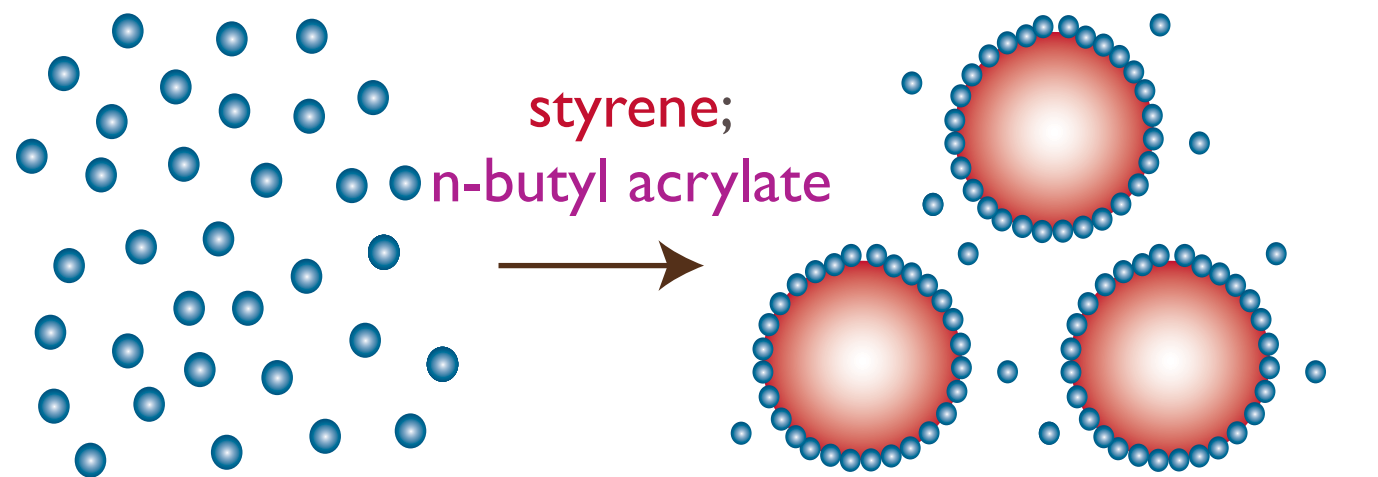


**NMR of the
silica surface**

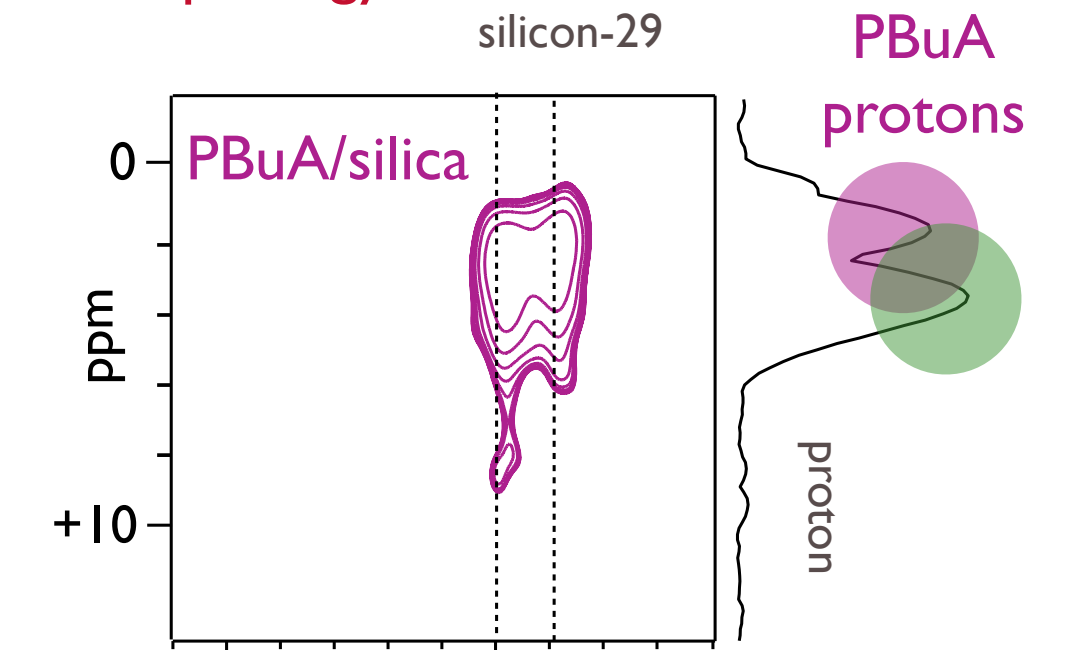


^1H - ^{29}Si NMR: core-shell interface

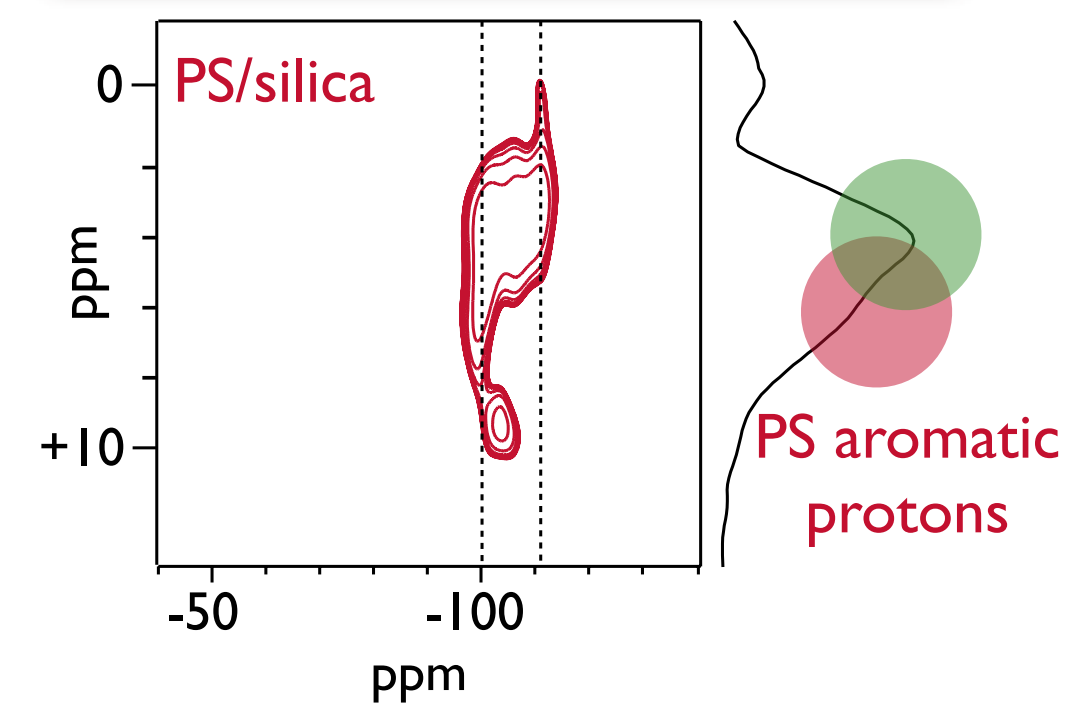
PBuA-silica and PS-silica



Colloidal nano-composite particles
with a core-shell morphology

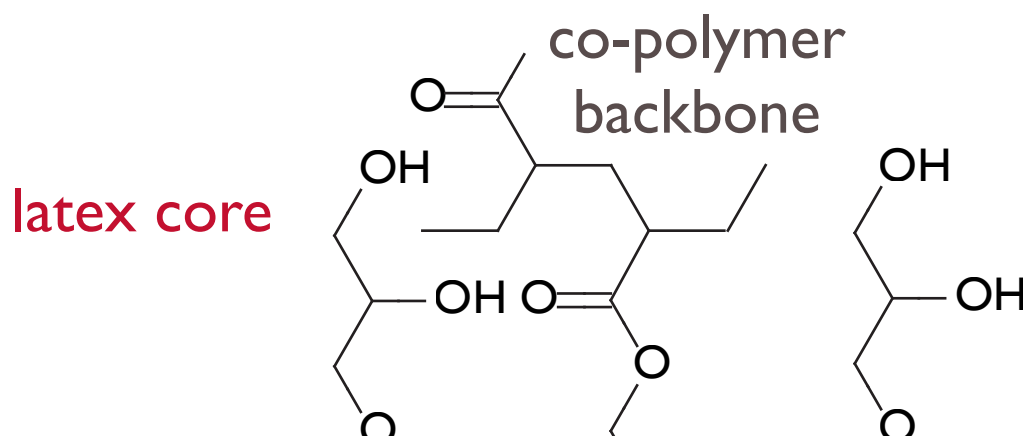
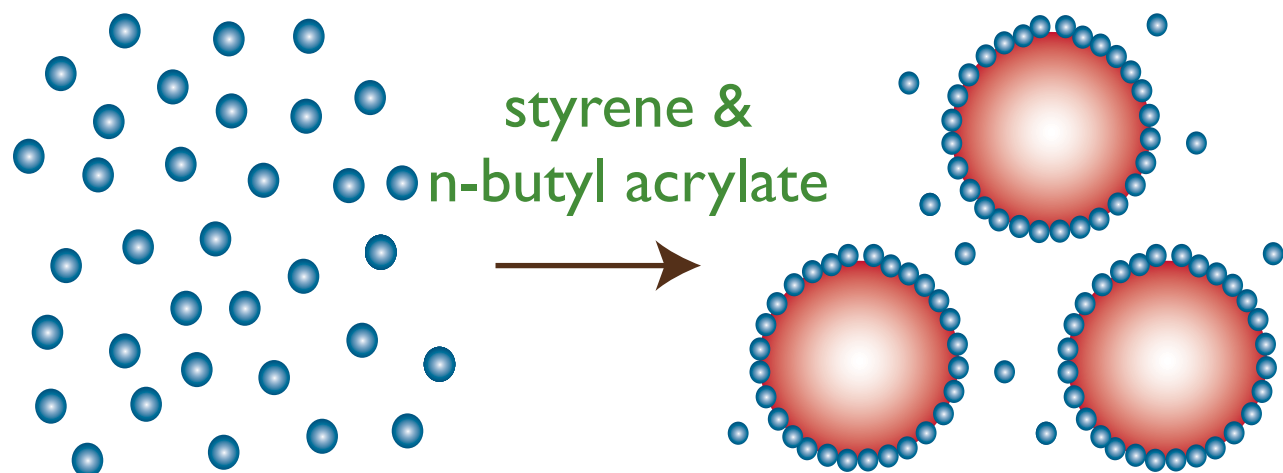


Polymer side chains between the
functionalizing silane groups

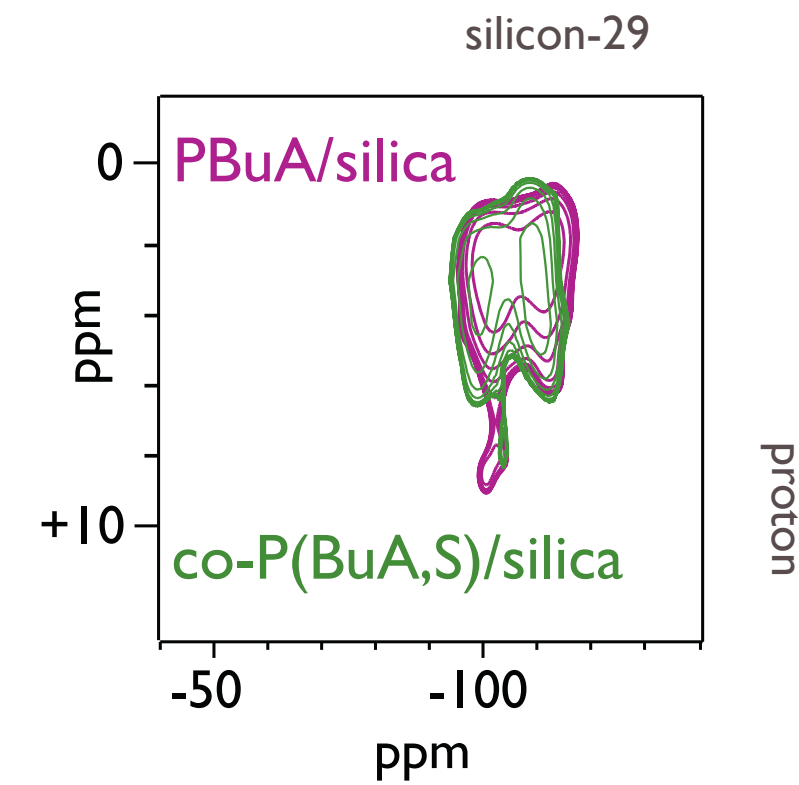
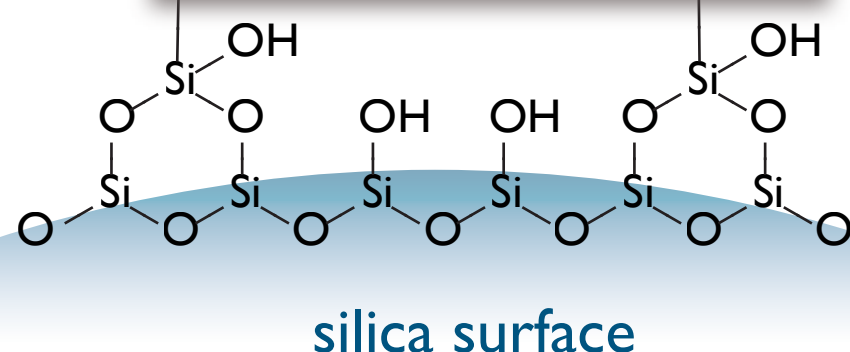


Aqueous co-P(BuA,S)-silica nano-composites

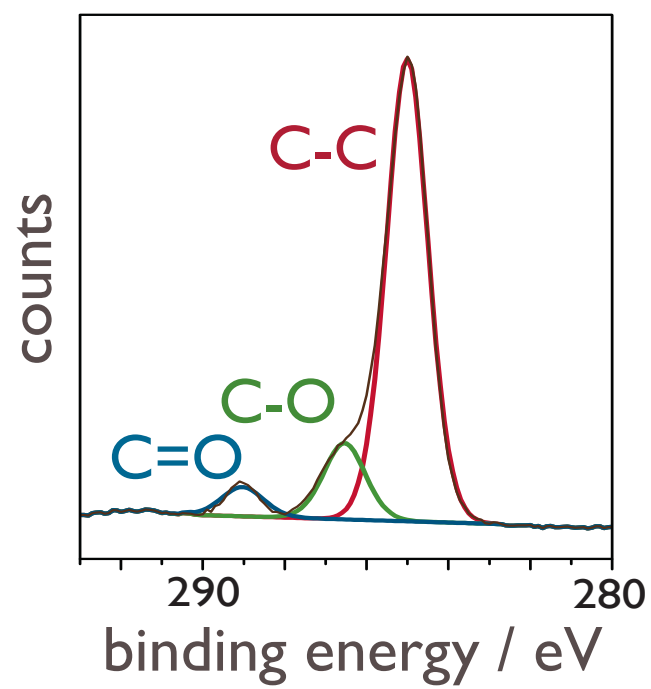
co-P(BuA,S)-silica



preferential interaction
with BuA monomers



XPS measurements also show
C=O in the interface



PS/P(BuA)-silica nano-composites: conclusions

Alcoholic **PS-SiO₂-silica nano-composites**

... adhere via a π interaction between the surface siloxanes and the styrene ring

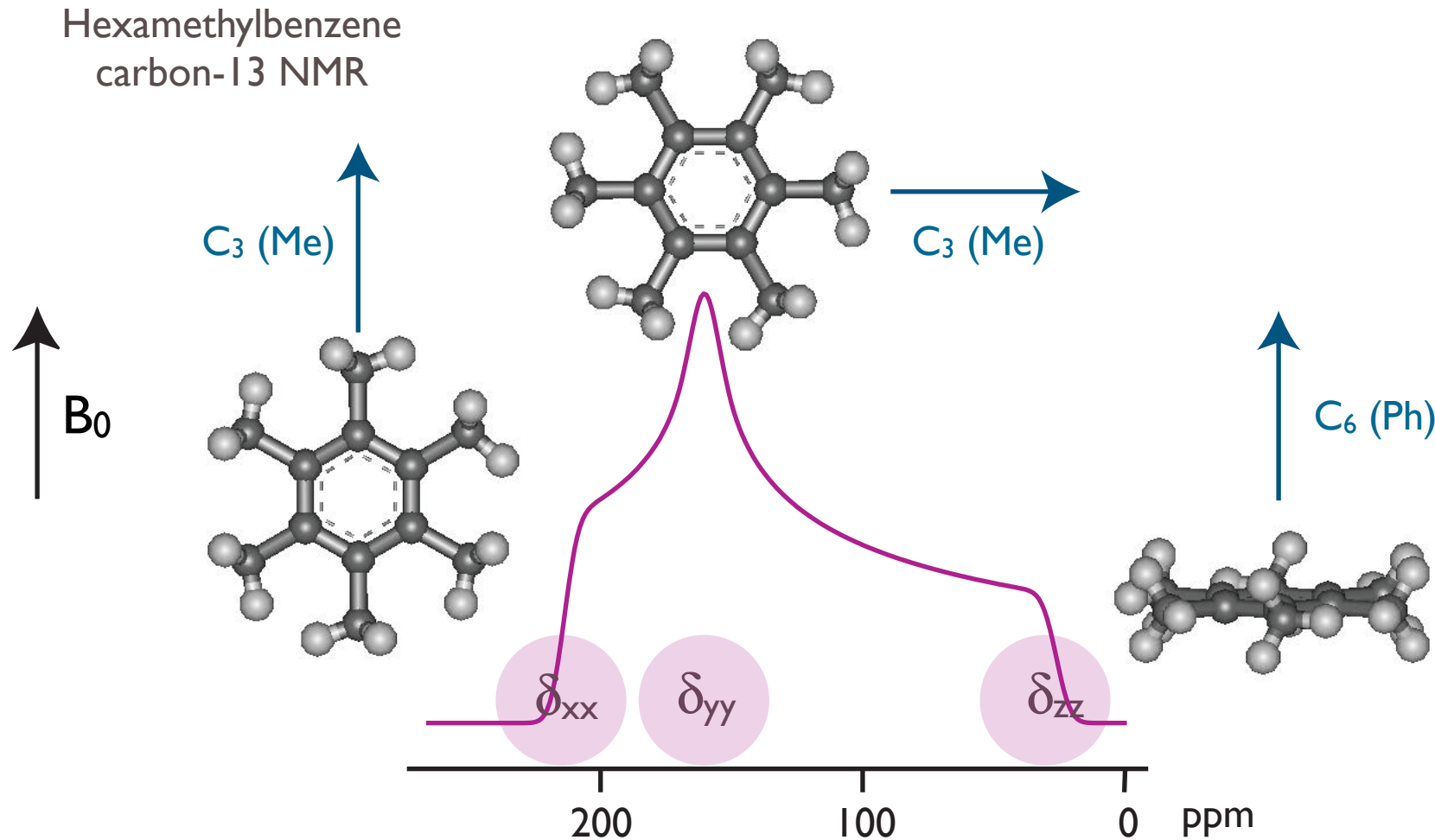
Aqueous **co-P(S,BuA)-silica nano-composites**

... show an unexpected interaction between BuA and silica surface

Carefully designed solid-state NMR experiments can provide information about the interface

Solid-state NMR: anisotropic interactions

Solid-state NMR: the NMR frequency is **also** sensitive to orientation



$$\text{Isotropic: } \delta_{\text{iso}} = (\delta_{xx} + \delta_{yy} + \delta_{zz})/3$$

$$\text{Anisotropy: } \zeta = \delta_{zz} - \delta_{\text{iso}}$$

$$\text{Asymmetry: } \eta = (\delta_{yy} - \delta_{xx})/\zeta$$

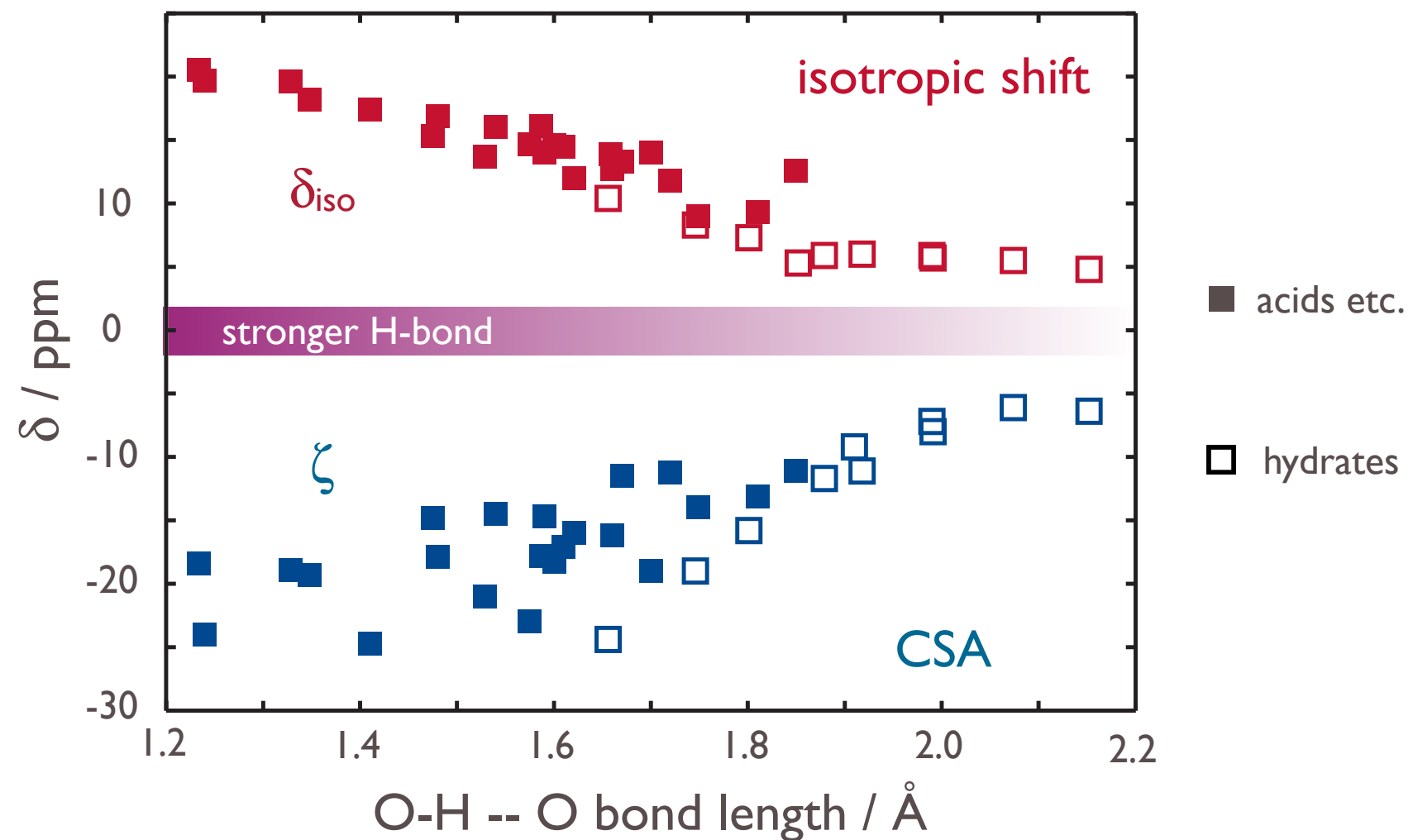
Why measure anisotropic interactions?

- ★ Larger information content cf. isotropic average observed with MAS
- ★ Sensitive to motion, orientational order etc.

Proton CSA: H-bond correlation

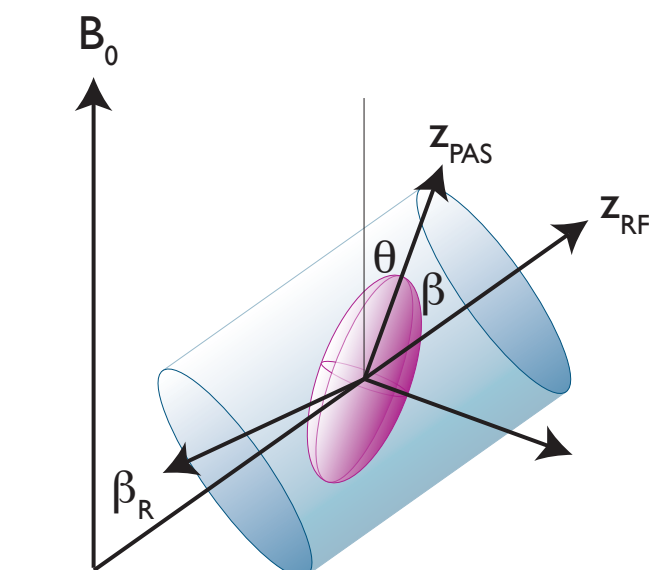
^1H isotropic shift and CSA decrease in magnitude as hydrogen-bond length increases **but ...**

- ★ not a simple linear correlation across the full range of bond lengths
- ★ shift parameters are also influenced by the environment

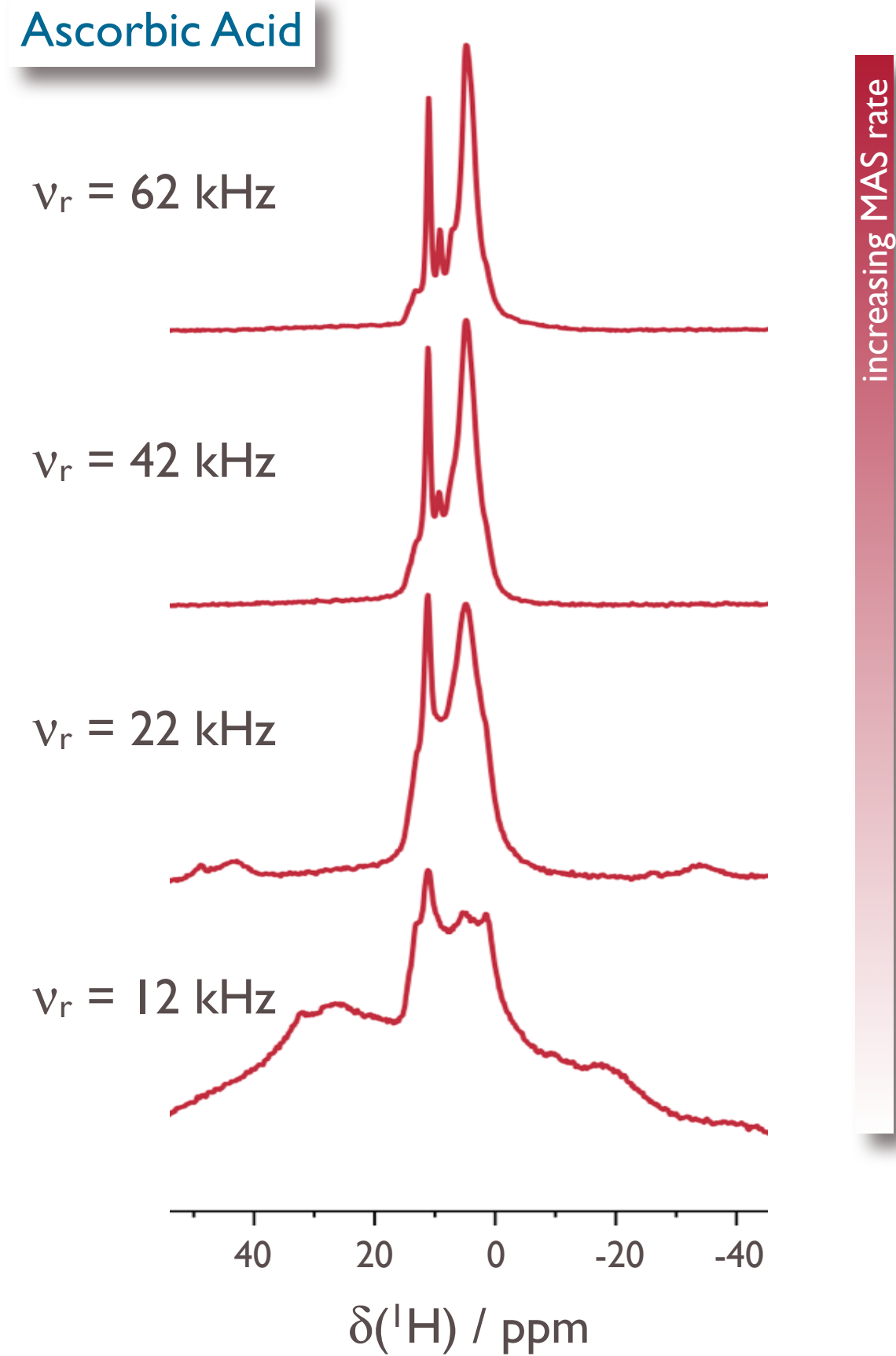


So far measuring proton shift parameters is difficult without single crystals or deuteration

Ultrafast MAS: resolution for protons



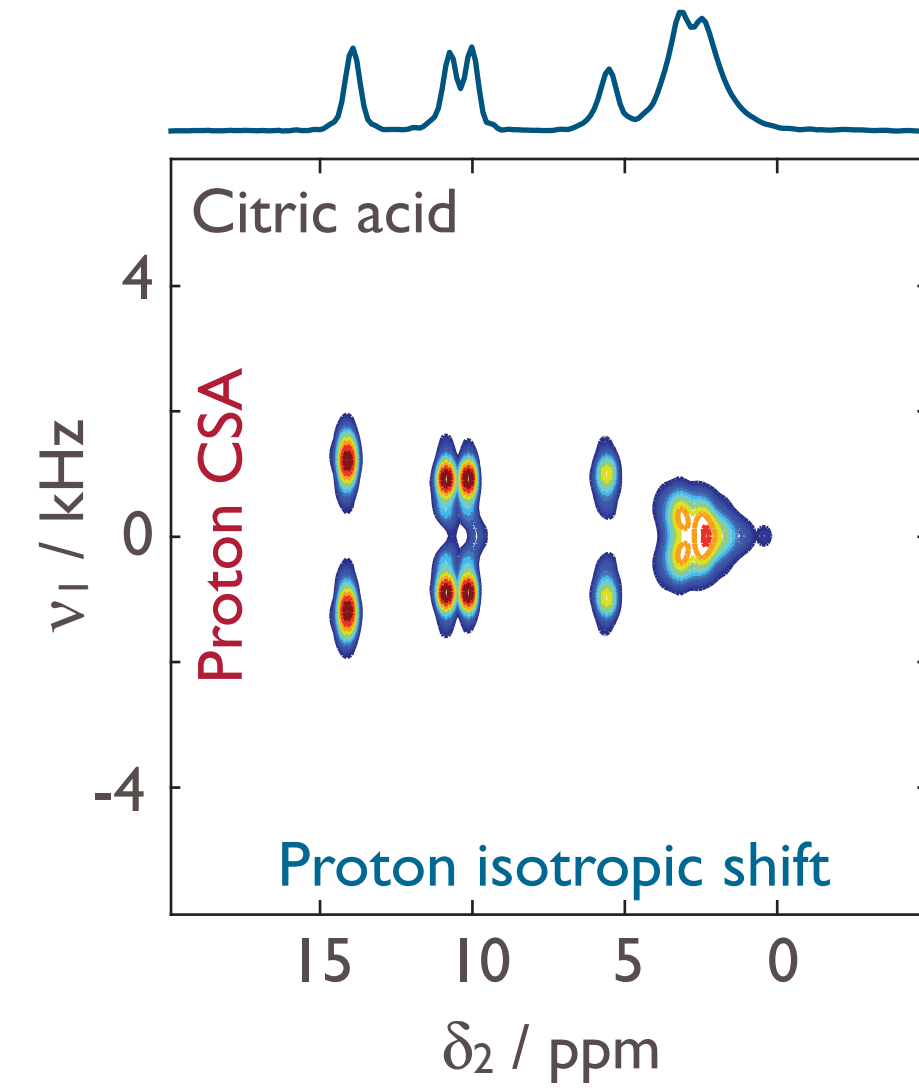
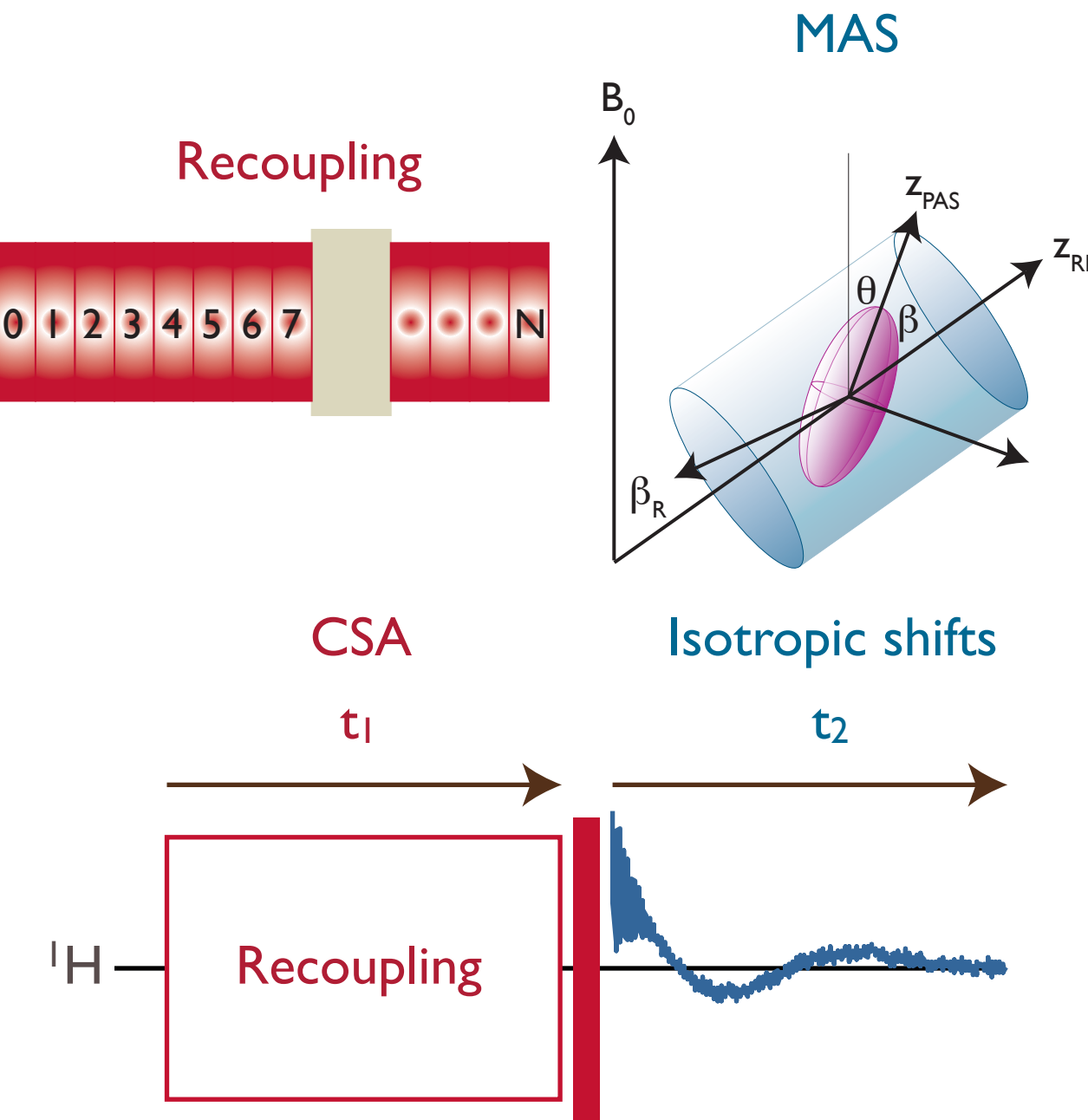
Ultrafast MAS: $v_r > 50 \text{ kHz}$



Proton CSA: measurement

Proton isotropic-anisotropic shift correlation

- ★ fast MAS (> 60 kHz) in t_2 to optimise resolution of proton isotropic shifts
- ★ reintroduce the MAS-averaged CSA in t_1
- ★ cannot gain resolution by utilising carbon-13 chemical shifts in this case

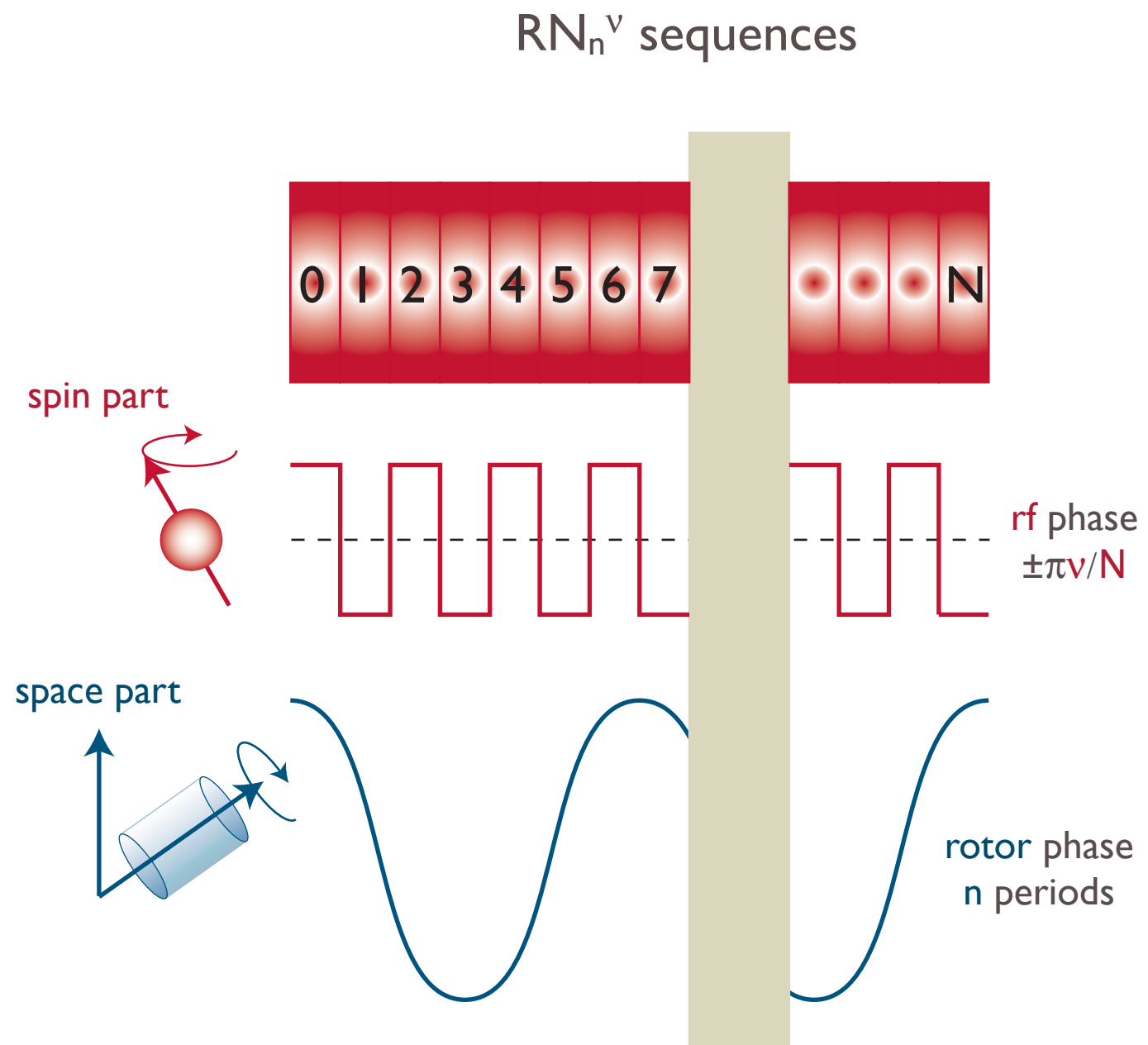


Recoupling sequences: RN_n^ν symmetries

$$H = \sum_{L=0}^2 \sum_{m=-L}^L (-1)^m A_m^L T_{-m}^L$$

spin part space part

interaction	space (L)	spin (Λ)
isotropic shift	0	1
shift anisotropy	2	1
scalar coupling	0	0
homonuclear dipolar coupling	2	2
heteronuclear dipolar coupling	2	1 (each spin)



$$H^{(I)} \propto A_m^L T_\mu^\Lambda \text{ if } \left(nm - v\mu = \frac{N}{2} k_\Lambda \right)$$

where k_Λ is odd if Λ is odd

Recoupling sequences: RI6₃²

RI6₃² sequence

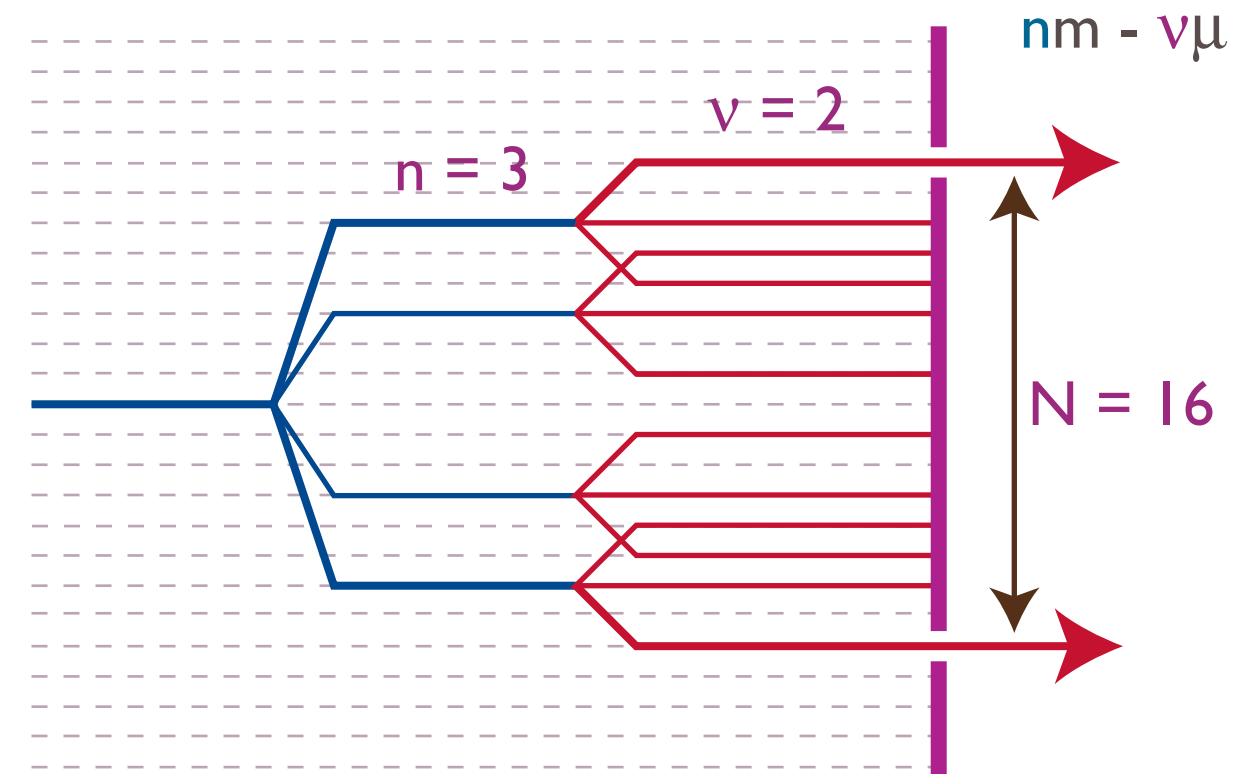
- ★ $\{\pi + 22.5 \pi - 22.5\}^8$
- ★ timed to fit in 3 rotor periods
- ★ rf amplitude 166 kHz
- ★ MAS rate 62.5 kHz

interaction	space (L)	spin (Λ)
isotropic shift	0	1
shift anisotropy	2	1
scalar coupling	0	0
homonuclear dipolar coupling	2	2
heteronuclear dipolar coupling	2	1 (each spin)

Spin-space selection diagram

shift anisotropy

space (m) spin (μ)



Recoupled Hamiltonian

$$H^{(I)} = \omega T_{-I}^I - \omega^* T_I^I$$

where ω depends on the CSA

$$\left(nm - v\mu = \frac{N}{2} k_\Lambda \right)$$

Recoupling sequences: RI6₃²

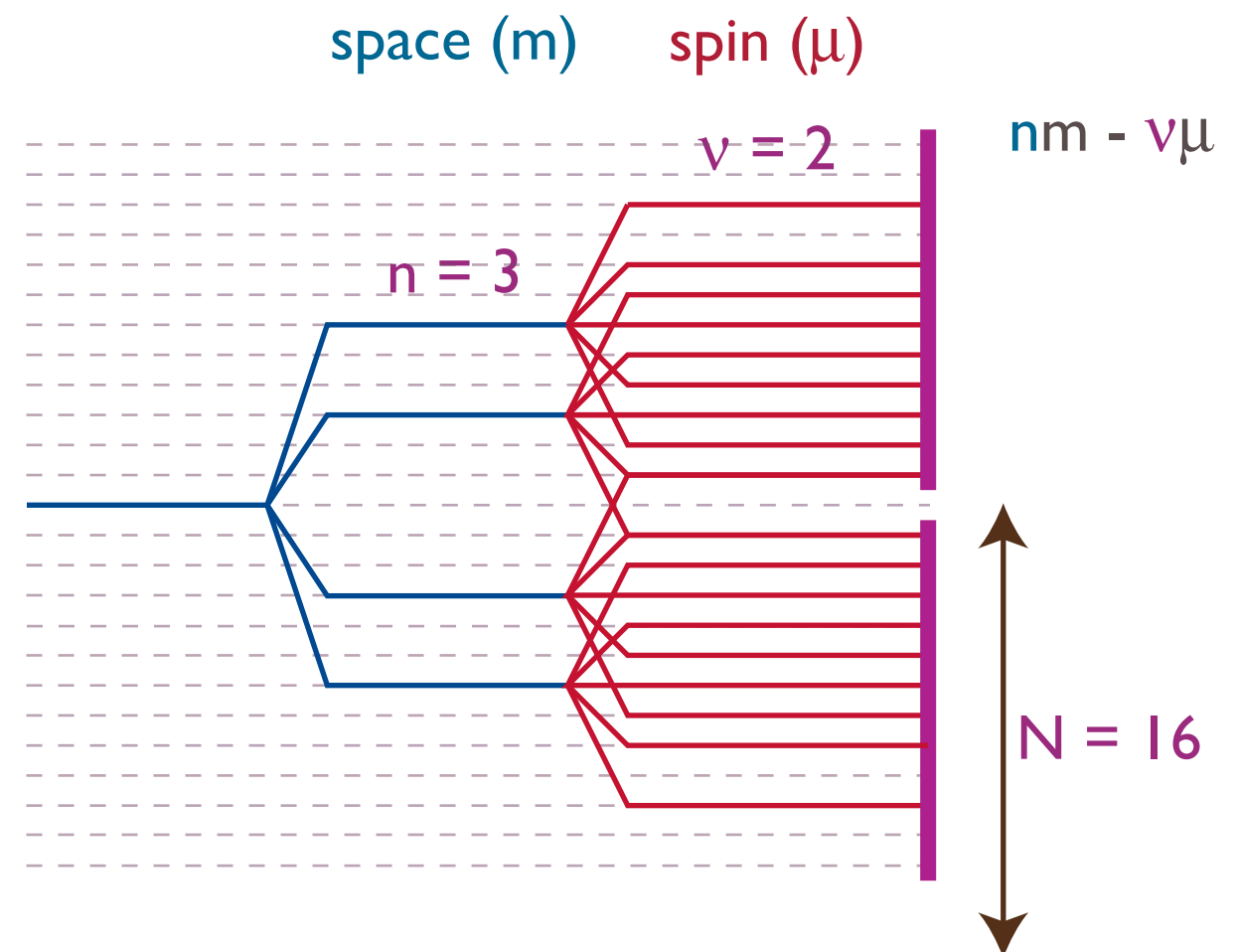
RI6₃² sequence

- ★ $\{\pi + 22.5 \pi - 22.5\}^8$
- ★ timed to fit in 3 rotor periods
- ★ rf amplitude 166 kHz
- ★ MAS rate 62.5 kHz

interaction	space (L)	spin (Λ)
isotropic shift	0	1
shift anisotropy	2	1
scalar coupling	0	0
homonuclear dipolar coupling	2	2
heteronuclear dipolar coupling	2	1 (each spin)

Spin-space selection diagram

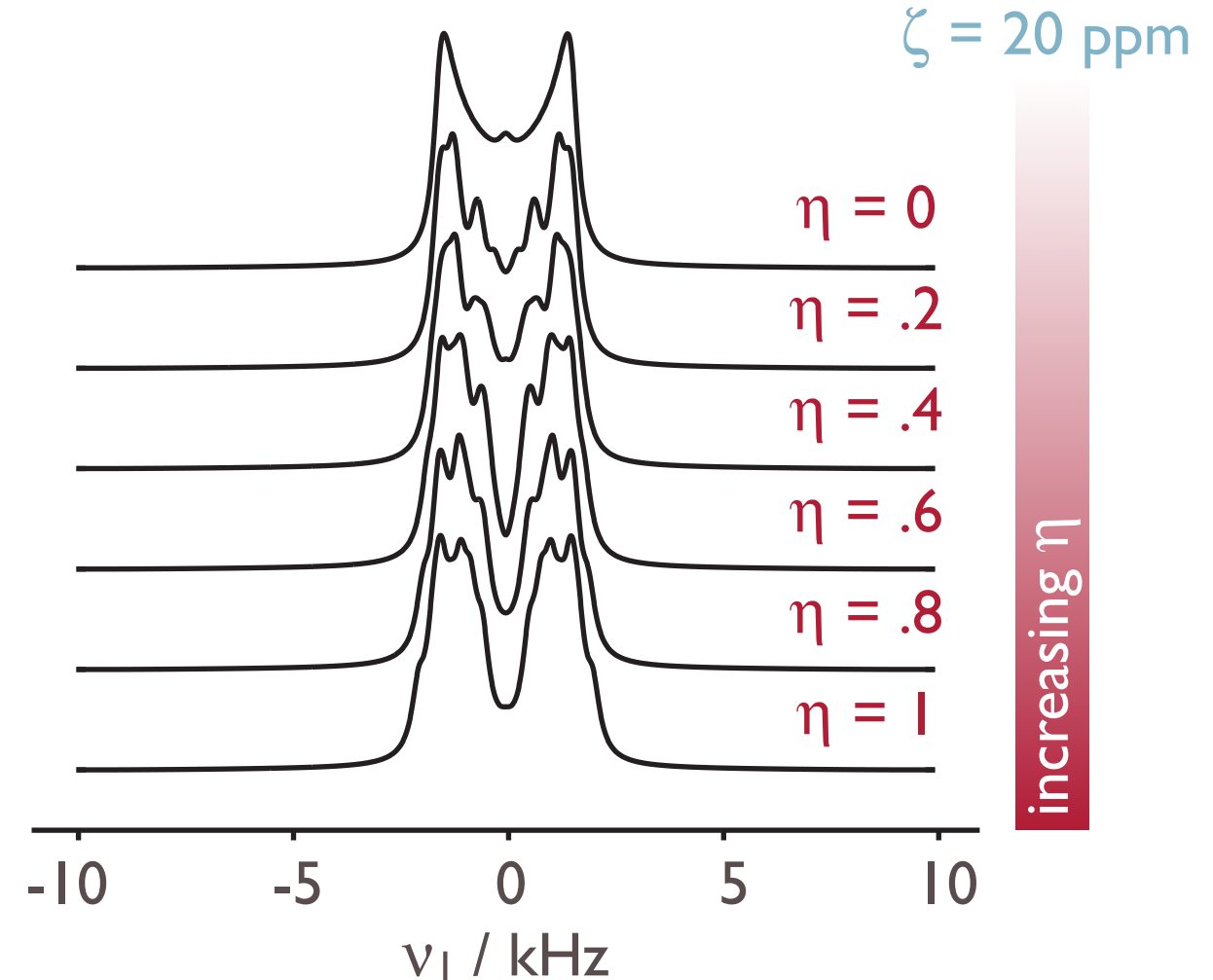
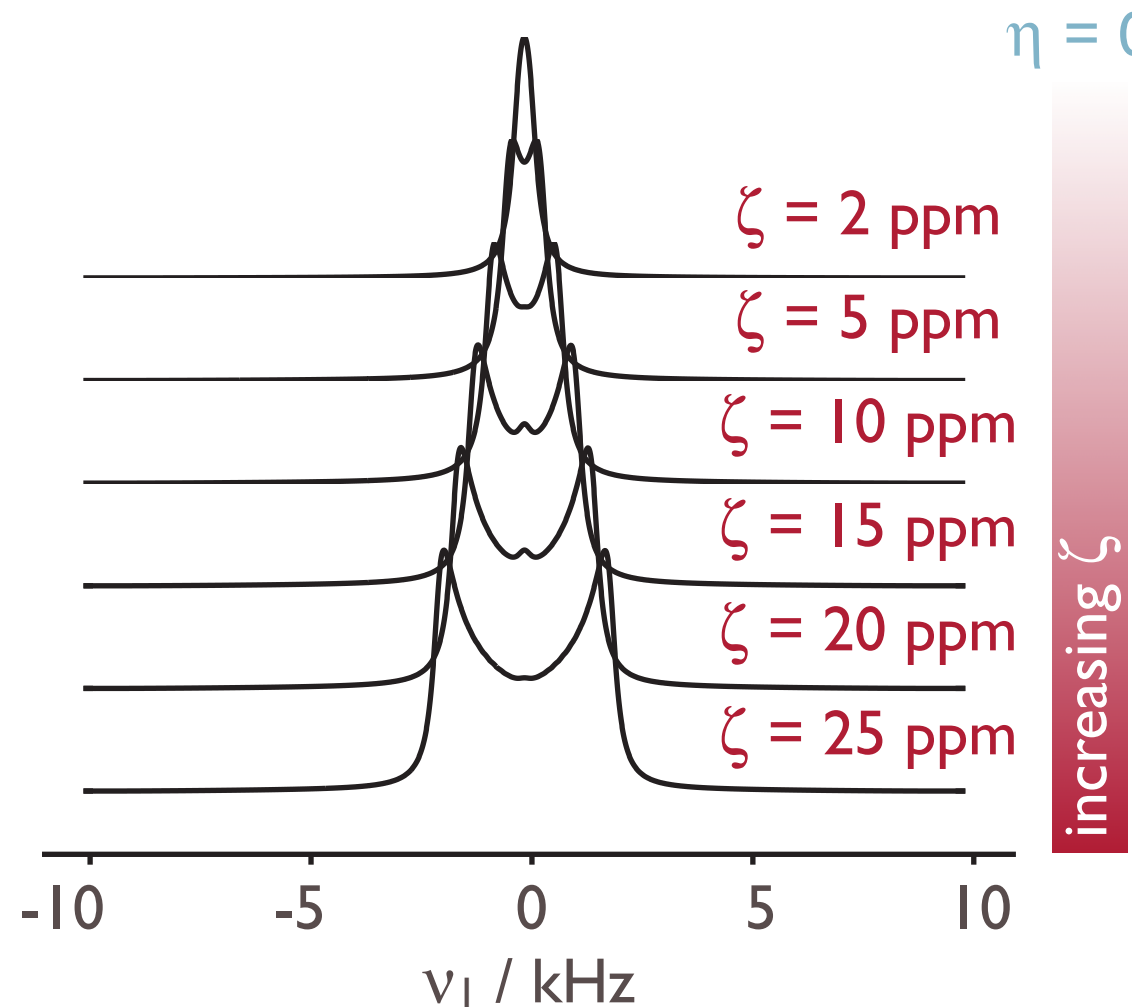
homonuclear dipolar coupling



$$\left(nm - v\mu = \frac{N}{2} k_\Lambda \right)$$

Proton CSA recoupling: sensitivity to shift parameters

Spin physics simulations

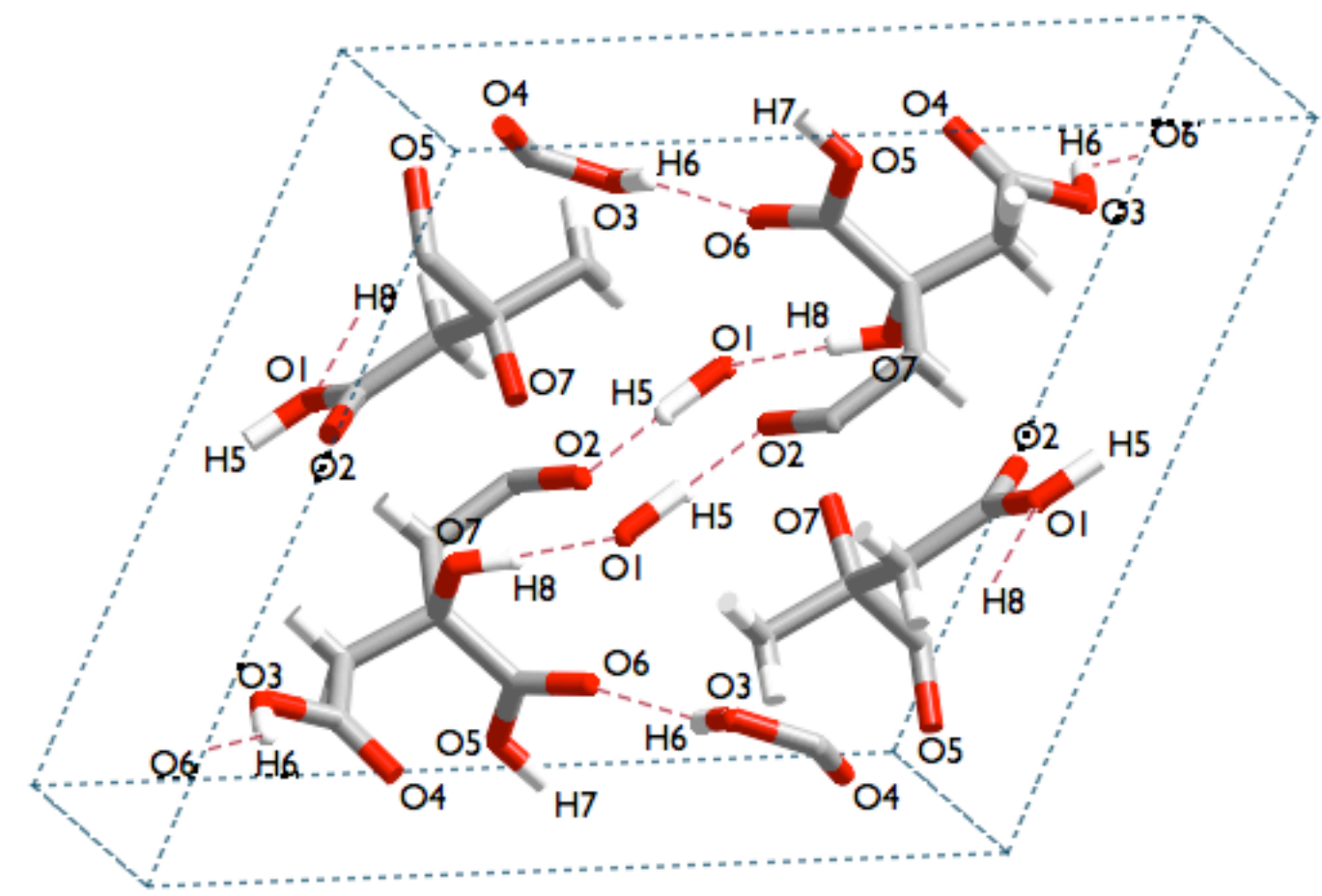
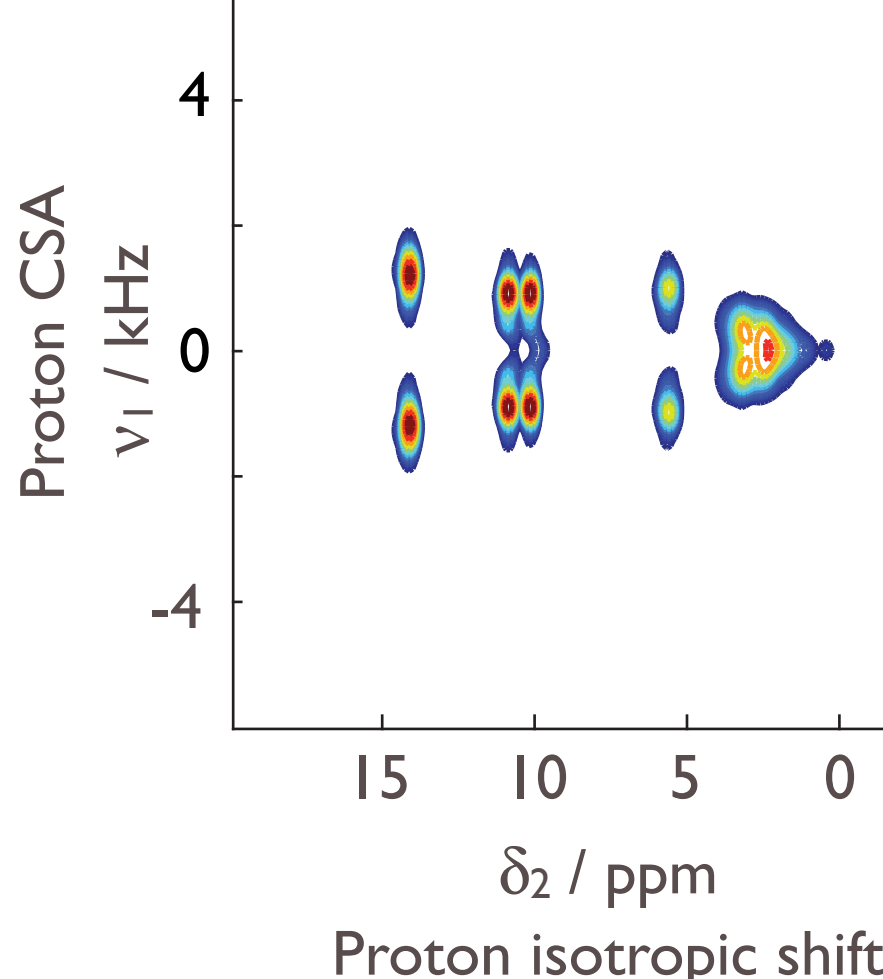


- ★ MAS rate: 62.5 kHz
- ★ Recoupling: R16₃²
- ★ Larmor frequency: 600 MHz

Sensitive to both anisotropy and asymmetry

Proton CSA recoupling: fast MAS

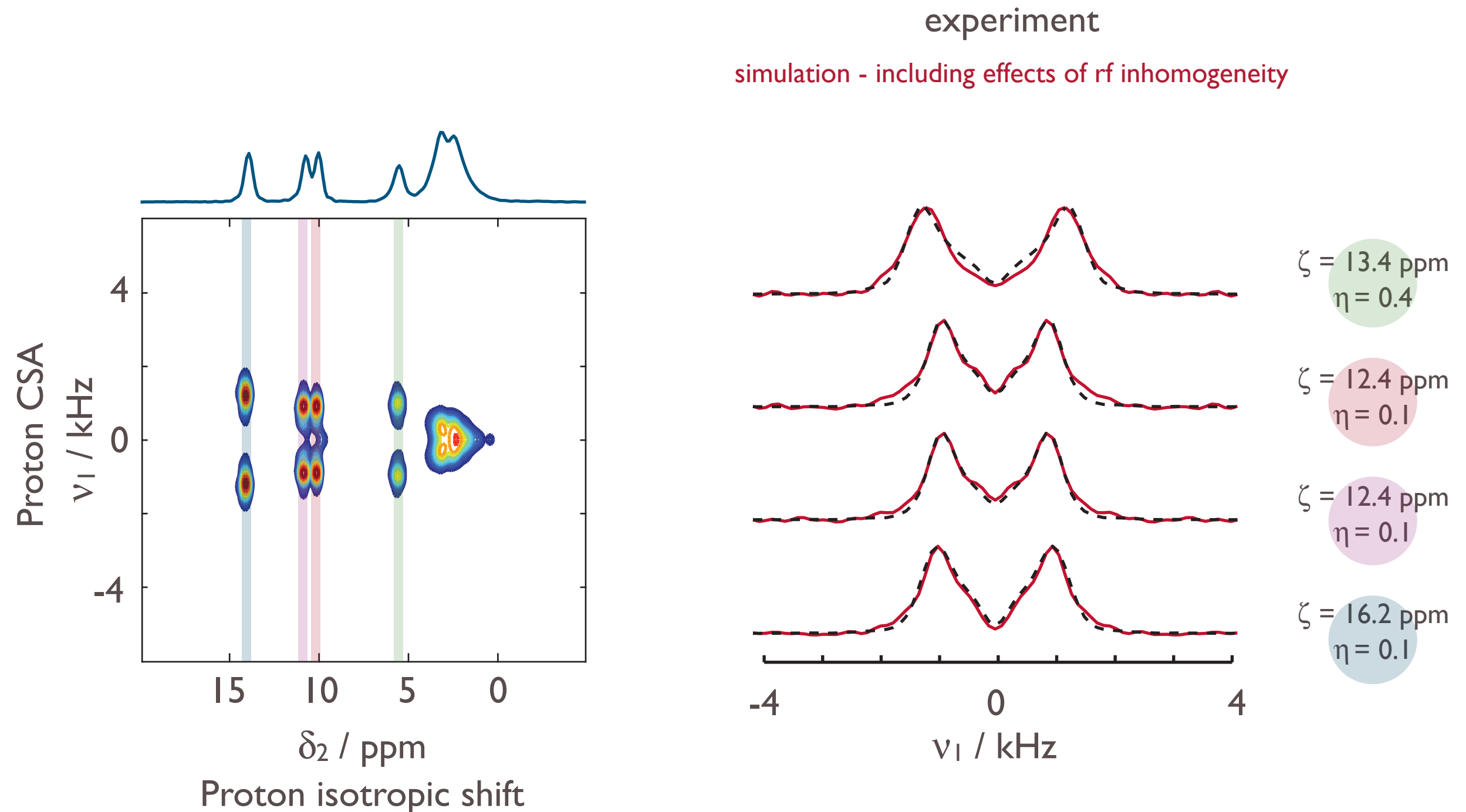
Citric Acid



H-bond	d / Å
$\text{O}1(\text{H}5)\cdots\text{O}2$	1.549
$\text{O}3(\text{H}6)\cdots\text{O}6$	1.906
$\text{O}5(\text{H}7)\cdots\text{O}4$	1.825
$\text{O}7(\text{H}8)\cdots\text{O}1$	2.145

- ★ MAS rate: 62.5 kHz
- ★ Recoupling: R16₃²
- ★ Larmor frequency: 600 MHz

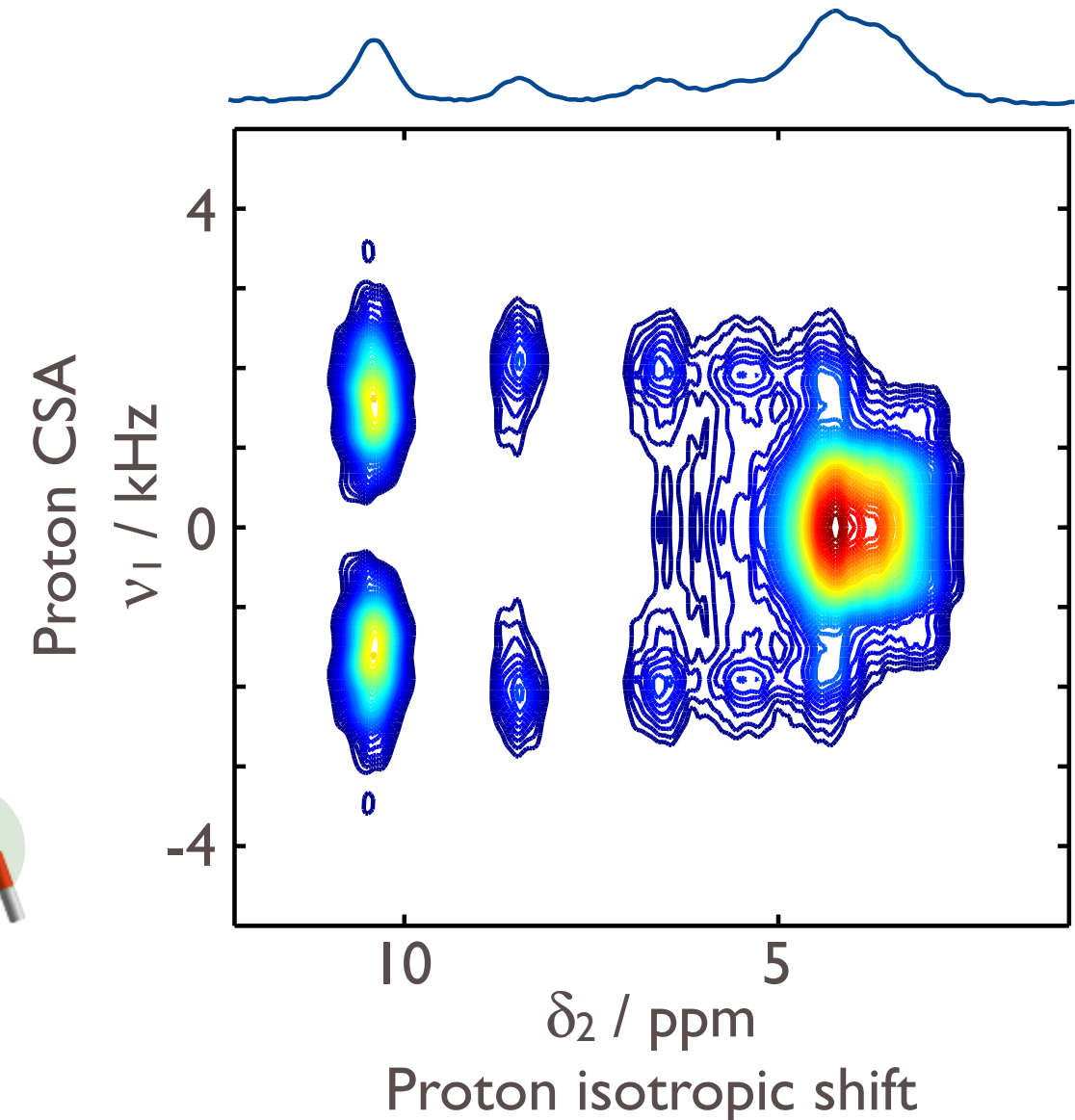
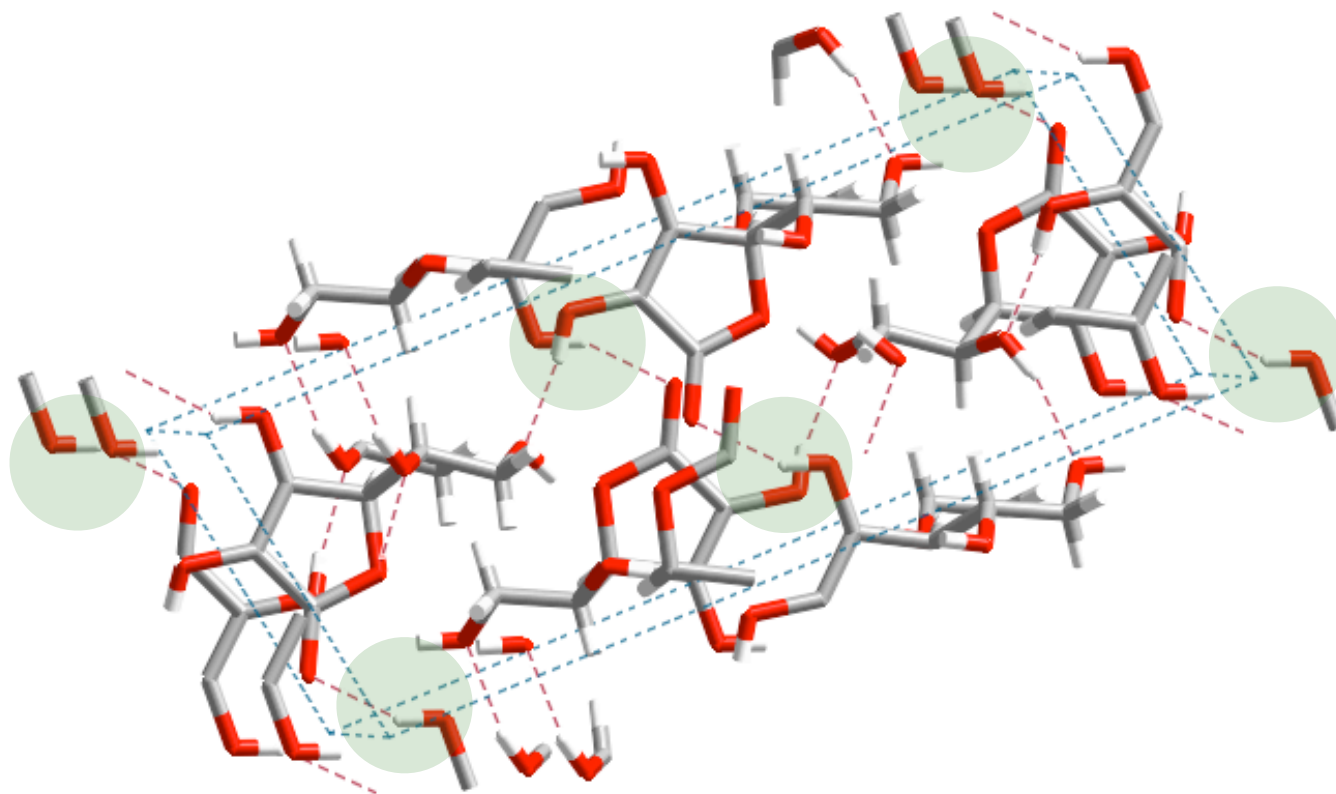
Citric acid: comparison with simulations



Improved resolution: 20 T and 78 kHz

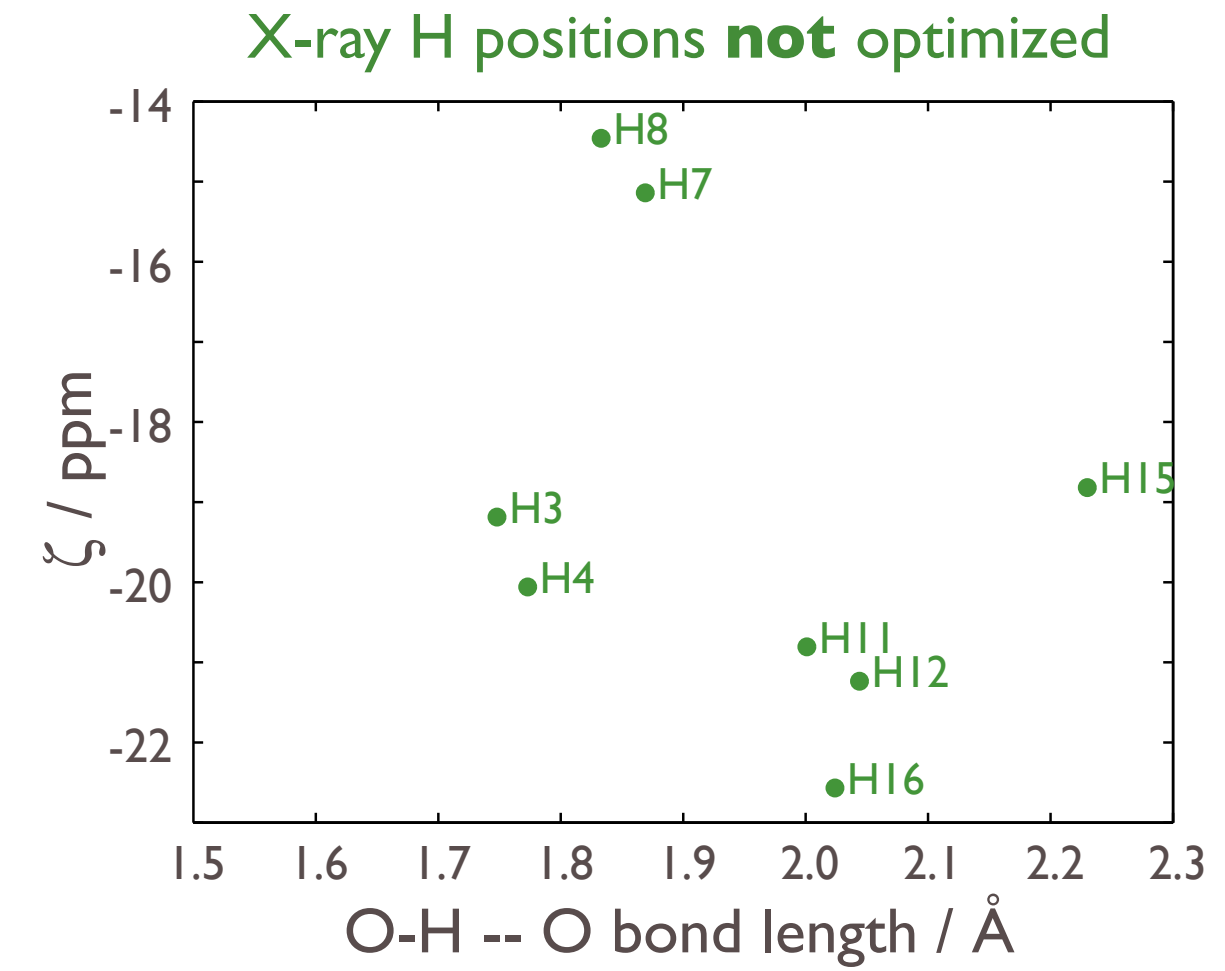
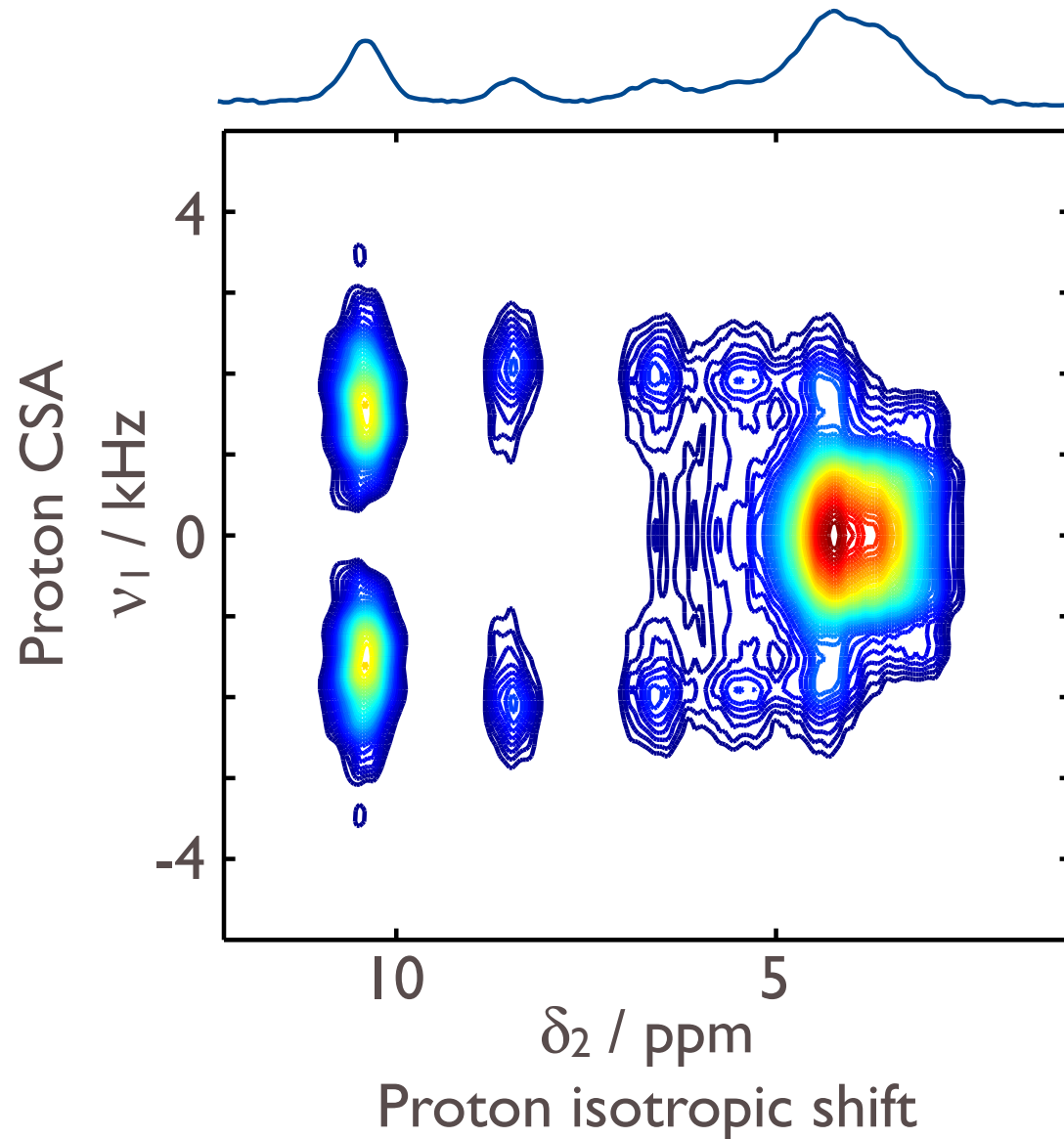
Ascorbic Acid

- ★ 8 hydrogen-bonded sites
- ★ OH--O distances between 1.7 Å and 2.0 Å (according to X-ray structure)
- ★ 2 hydrogen bonds involve sp^2 acceptors



- ★ MAS rate: 78.2 kHz
- ★ Larmor frequency: 850 MHz
- ★ Recoupling: $R16_3^2$

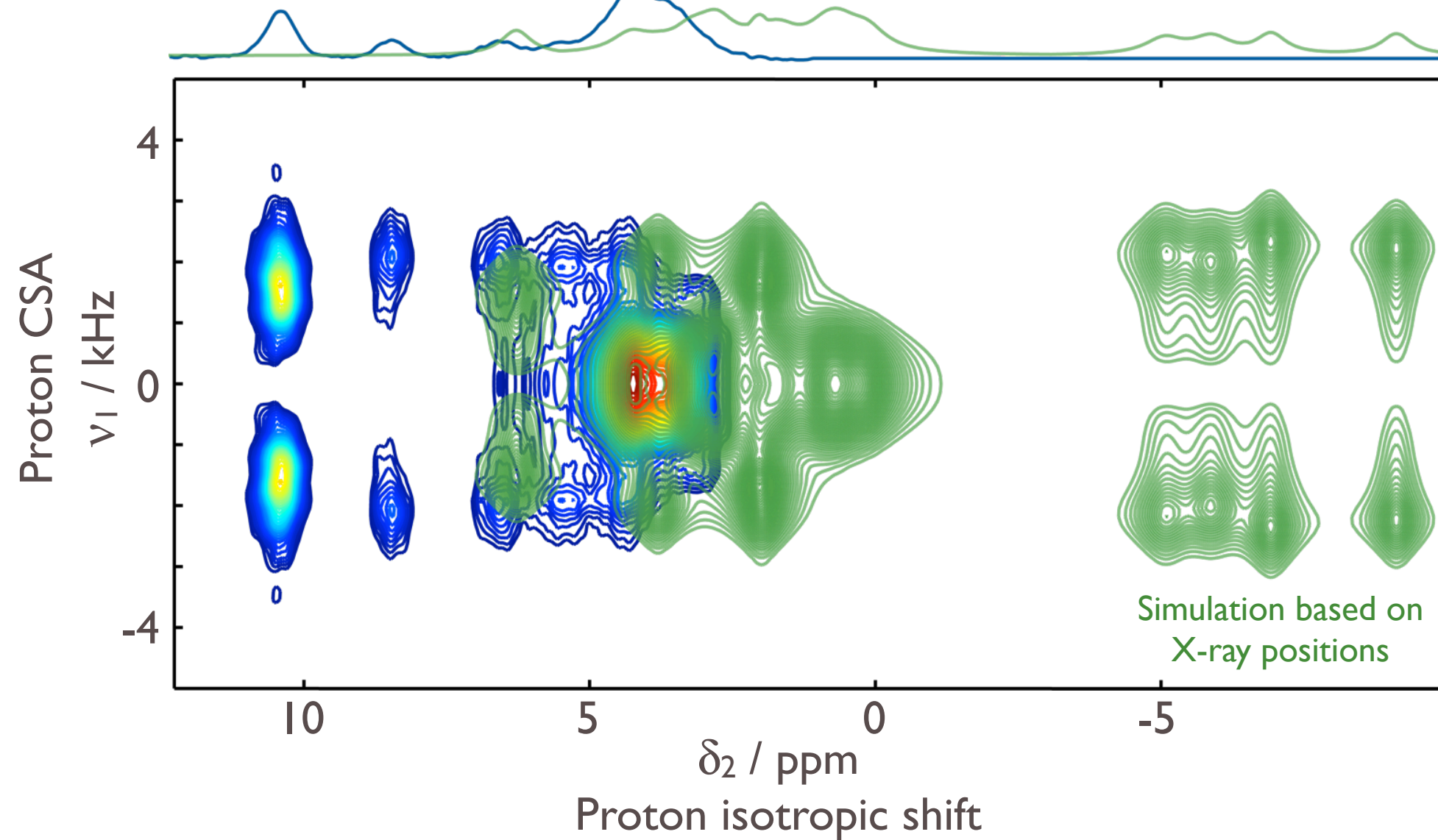
Ascorbic acid: comparison with calculations



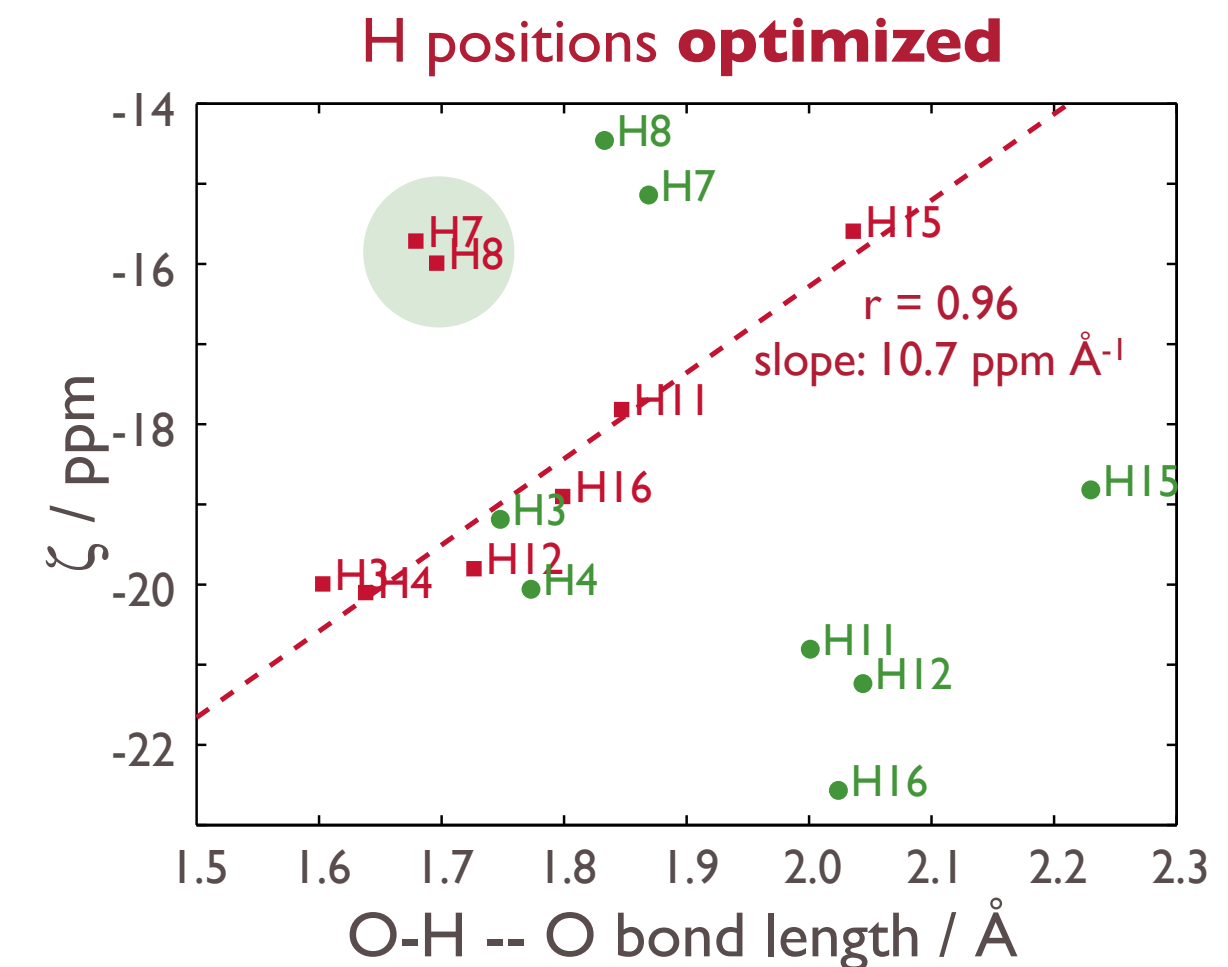
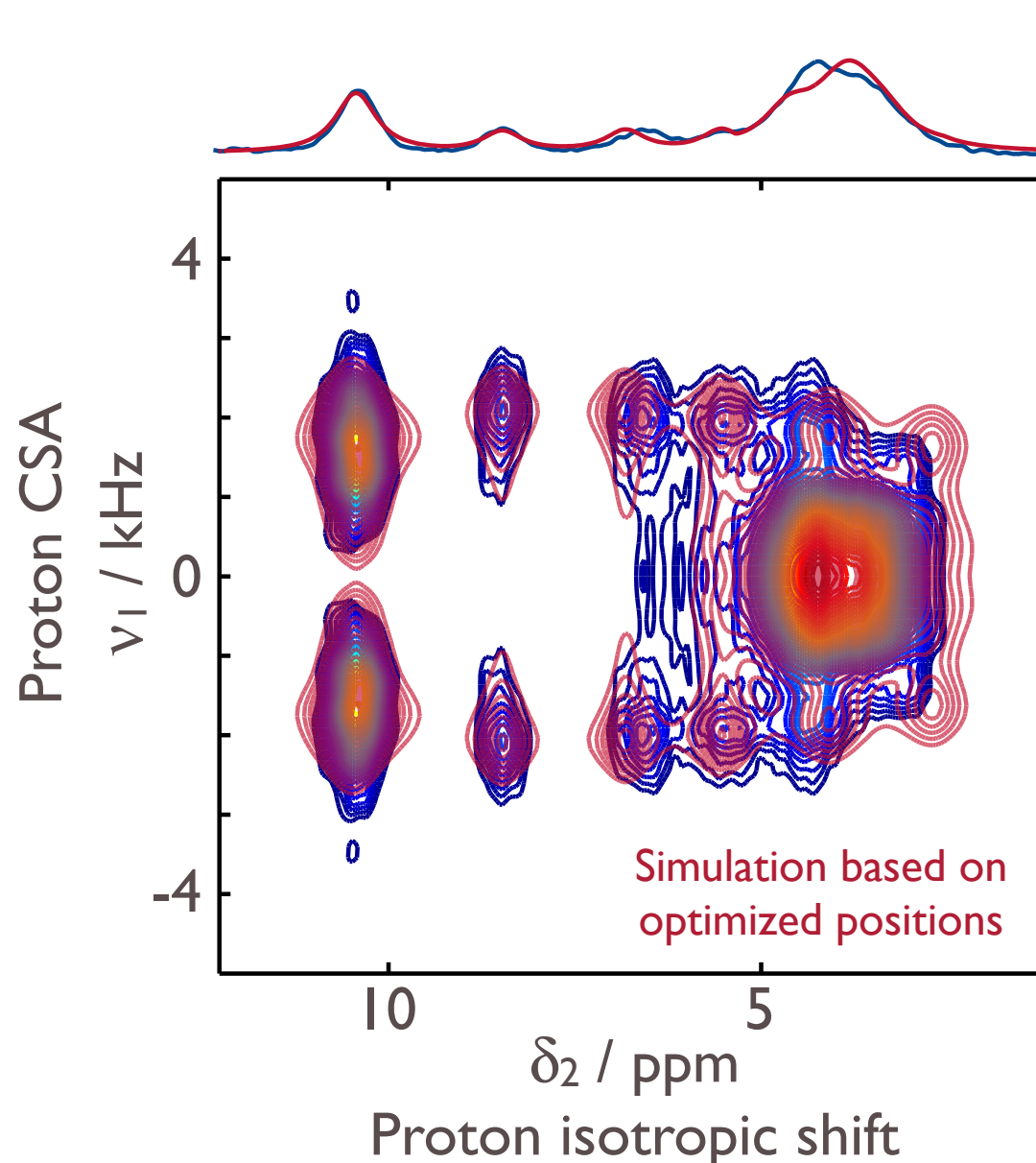
CASTEP DFT code:

- ★ Plane-wave expansion with cutoff energy of 1000 eV.
- ★ Ultra-soft pseudo-potentials to represent the core electrons.
- ★ Gauge including projector augmented wave (GIPAW) approach.
- ★ The Brillouin zone was sampled using a Monkhorst–Pack grid of k-points with a maximum spacing of 0.08 \AA^{-1} .
- ★ PBE approximation to the exchange–correlation interaction.

Ascorbic acid: comparison with calculations



Ascorbic acid: structure refinement



- ★ NMR results suggest significantly shorter hydrogen bonds than X-ray structure (reduced by ~0.2 Å)
- ★ correlation between ζ and hydrogen bond length
- ★ ... excluding hydrogen bonds with sp^2 hybridised acceptor oxygens

Proton CSA: conclusions

CSA recoupling:

... can be used to measure the proton CSA tensor with appropriate R-symmetries at MAS rates as high as 80 kHz for optimal resolution of sites

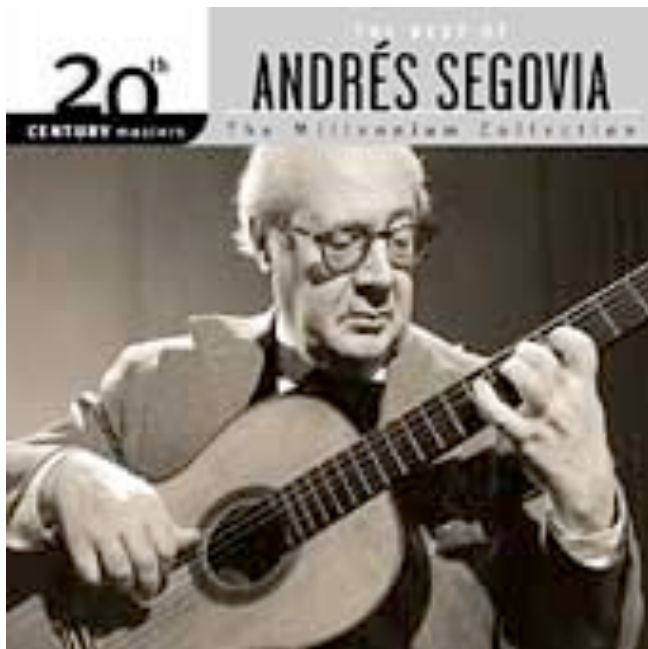
For **organic crystals:**

... significant changes to the hydrogen positions during geometry optimisation of X-ray structure are required to fit with NMR results (for many samples)

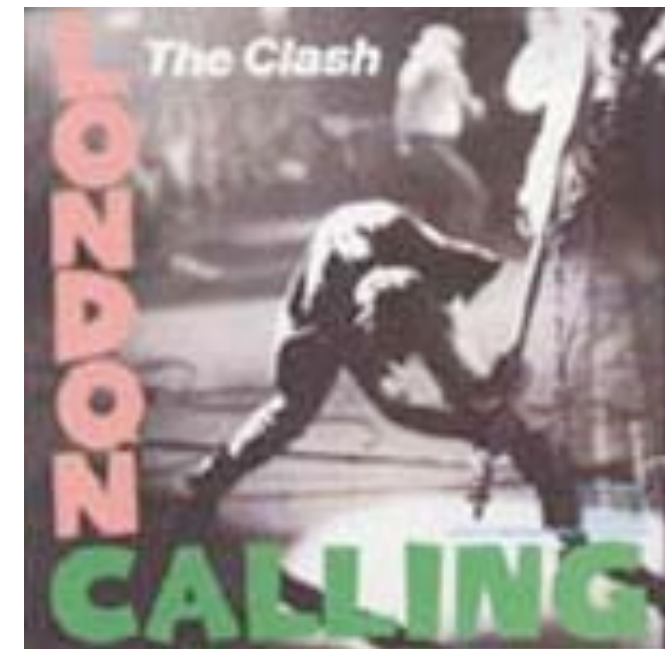
^1H solid-state NMR complements diffraction methods for structure refinement

Experiment design: philosophy

“Classical solids” approach:
Slow (or no) MAS; H = anisotropic



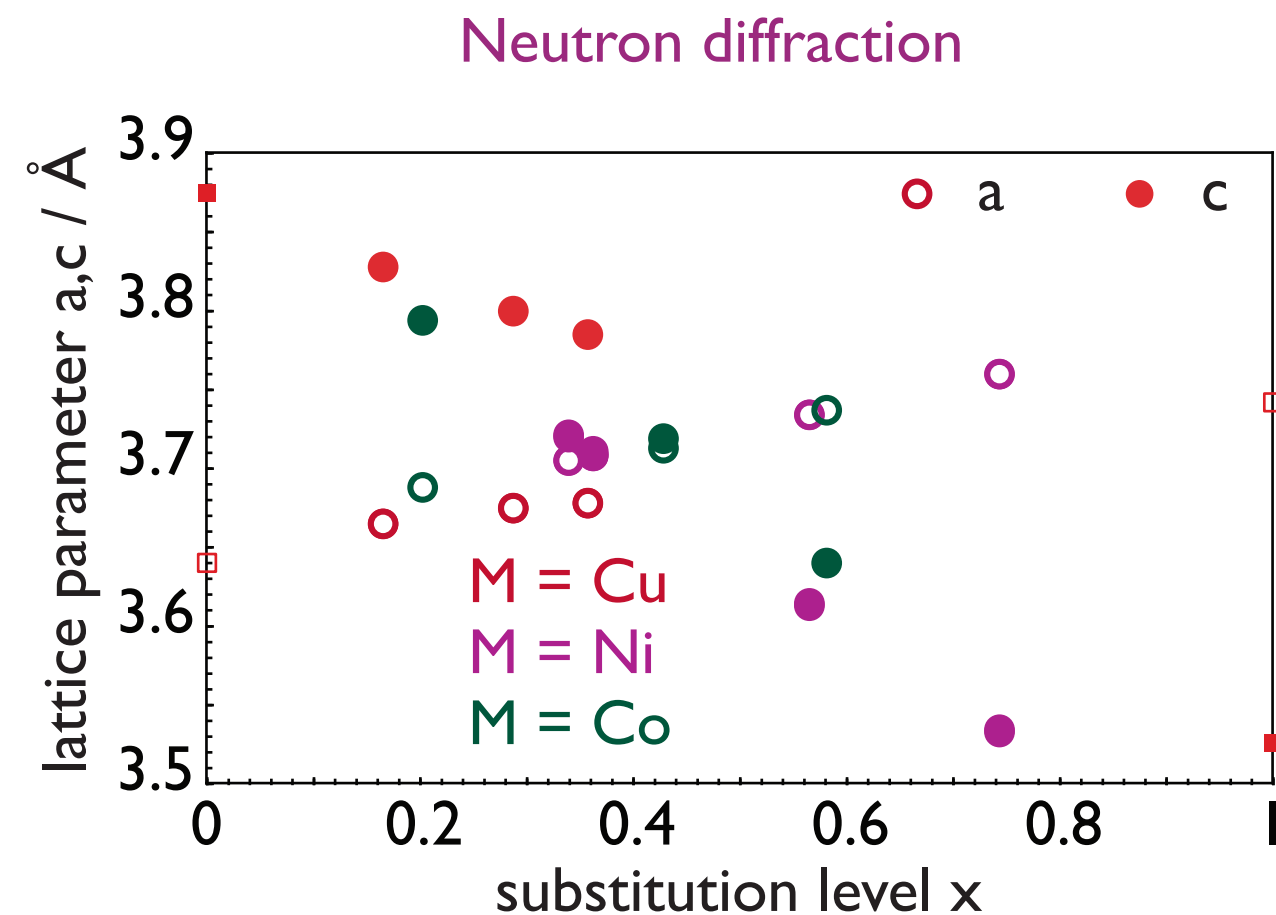
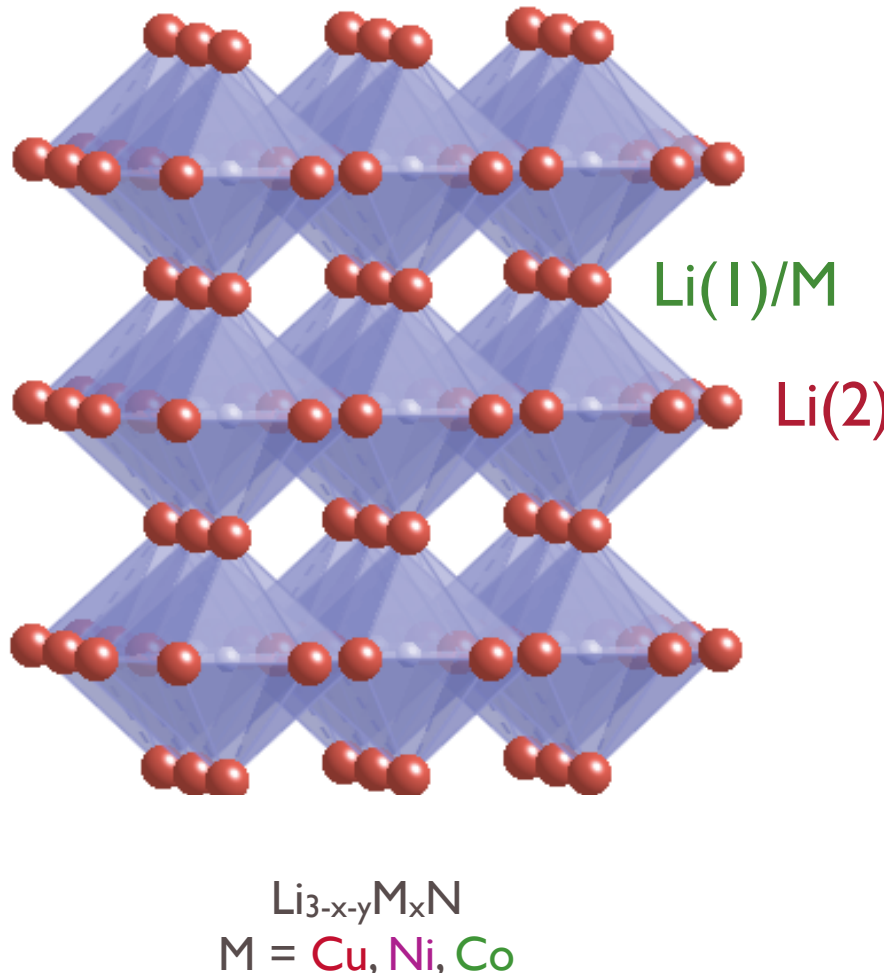
“Solution-like” approach:
Fast MAS, efficient decoupling etc.
“Recoupling” to reintroduce anisotropic interactions



Li^+ transport in metallocnitrides

Layered metallocnitrides:

- ★ ternary transition metal substituted nitrides $\text{Li}_{3-x-y}\text{M}_x\text{N}$: M = Cu, Ni, Co
- ★ Li_3N structure retained, M in Li(I) sites, vacancies in the $[\text{Li}_2\text{N}]$ plane are disordered
- ★ $\text{Li}_{2.6}\text{Co}_{0.4}\text{N}$ has been proposed as an anode for lithium batteries



D. H. Gregory, P. M. O'Meara, A. G. Gordon, J. P. Hodges, S. Short and J. D. Jorgensen, *Chem. Mater.*, **14**, 2063 (2002).

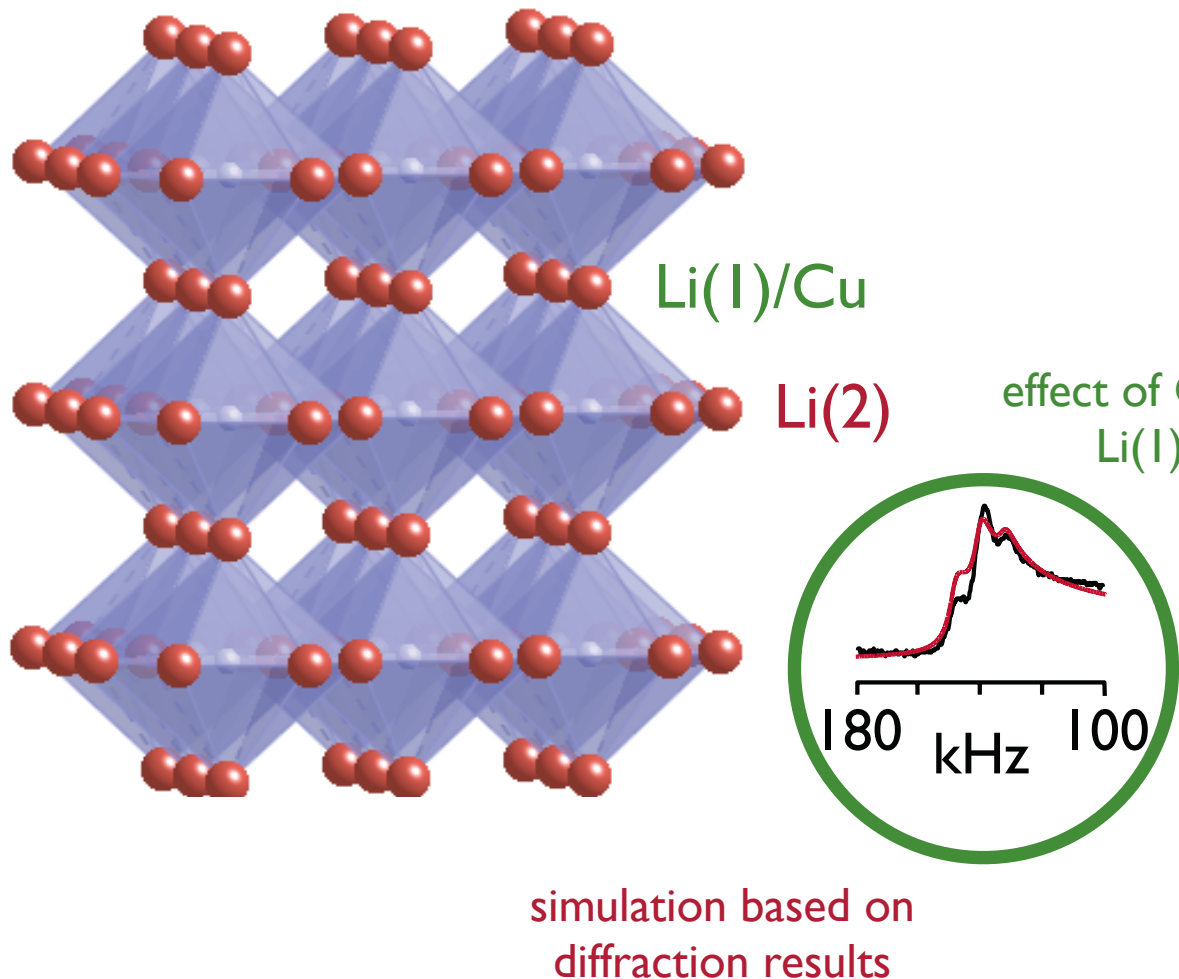
Z. Stoeva, R. Gomez, D. H. Gregory, G. B. Hix and J. J. Titman, *Dalton Trans.*, **19**, 3093 (2004).

J. Cabana, Z. Stoeva, J. J. Titman, D. H. Gregory, and M. R. Palacin, *Chem. Mater.*, **20**, 1676 (2008).

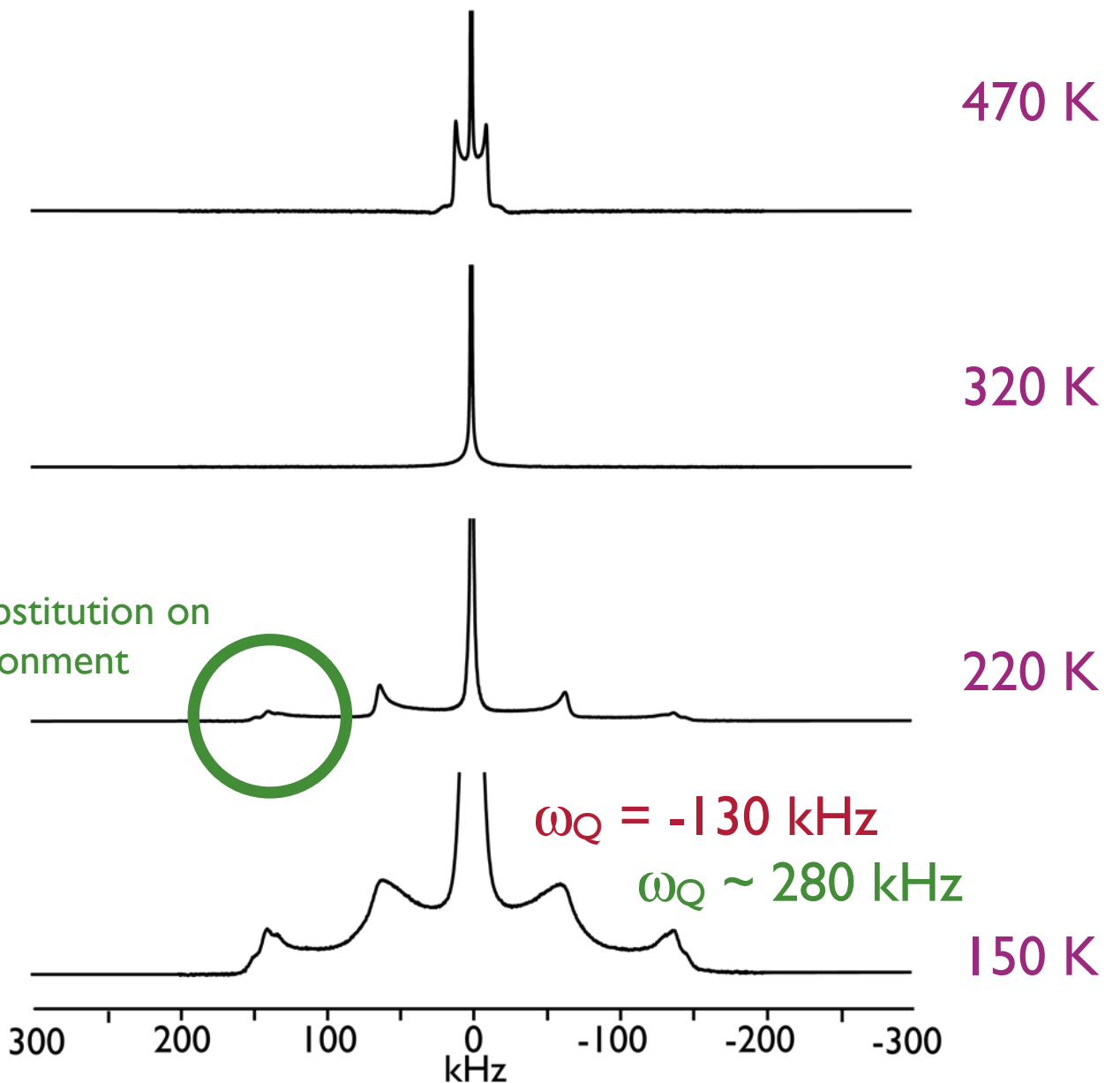
$\text{Li}_{3-x}\text{Cu}_x\text{N}$: diamagnetic

$\text{Li}_{3-x}\text{Cu}_x\text{N}$:

- ★ $x < 0.4$, negligible vacancy concentration
- ★ diamagnetic



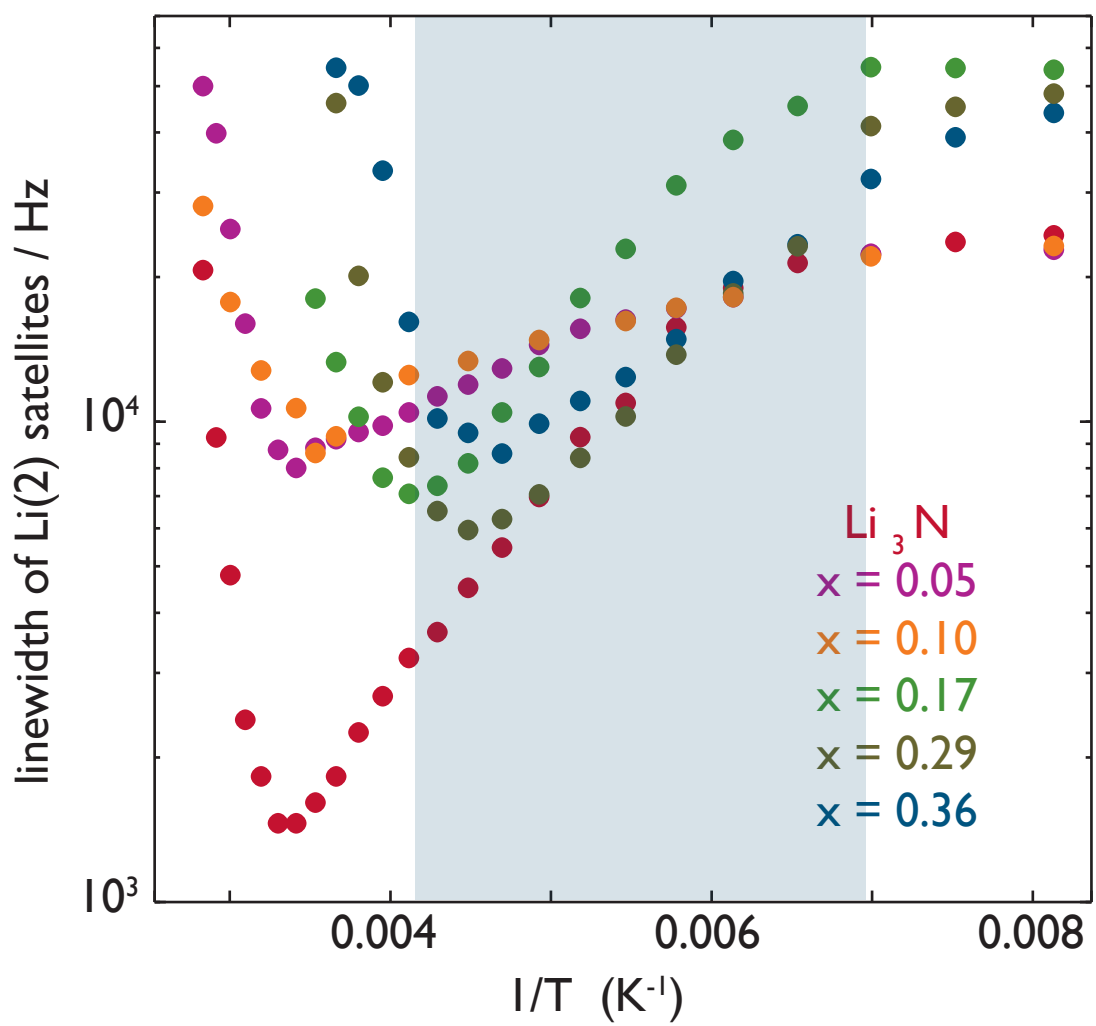
VT wideline lithium-7 spectra
 $x = 0.29$



Consistent with neutron diffraction

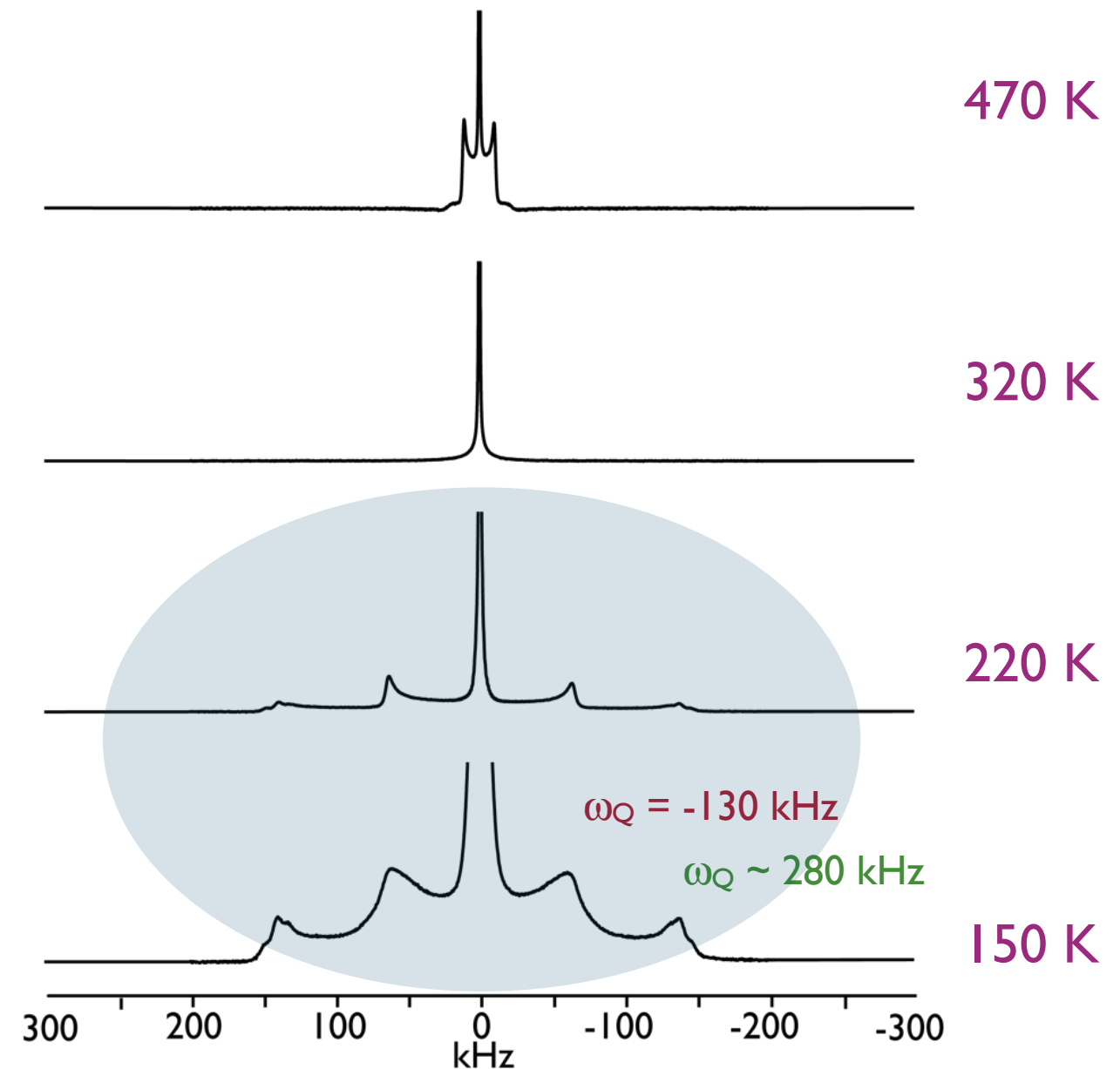
$\text{Li}_{3-x}\text{Cu}_x\text{N}$:VT wideline NMR

Motional narrowing of dipolar broadened satellites, particularly Li(2) due to intra-layer diffusion



Extract diffusion parameters (D, E_a) from narrowing

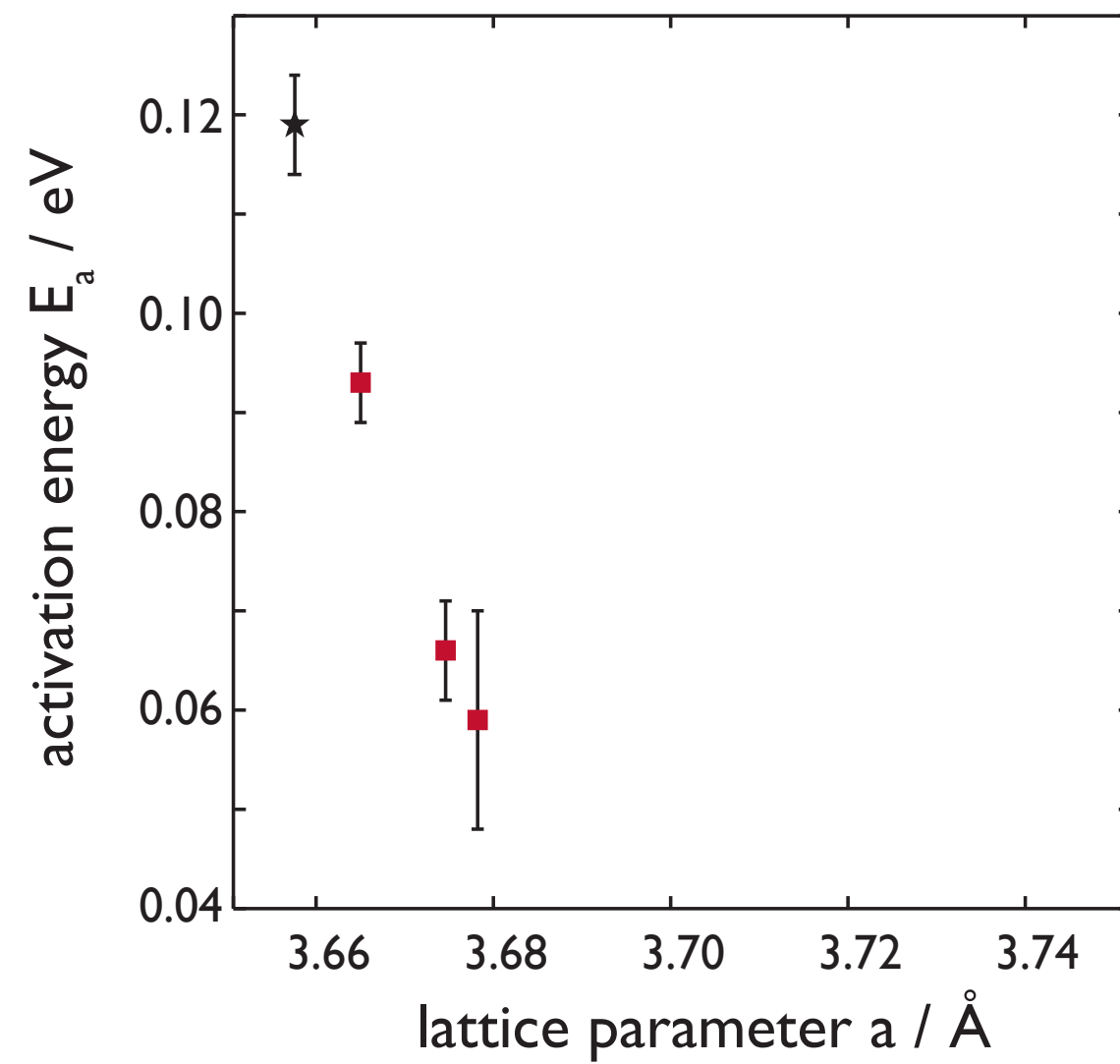
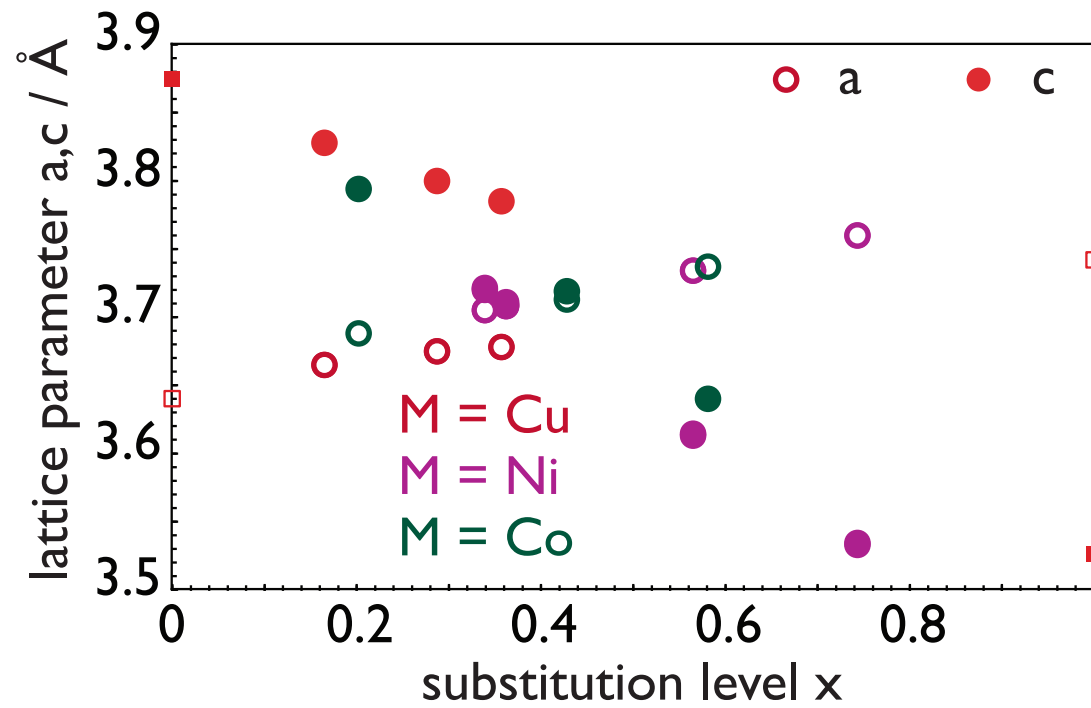
VT wideline lithium-7 spectra
 $x = 0.29$



$\text{Li}_{3-x}\text{Cu}_x\text{N}$: correlation between structure and dynamics

Intra-layer diffusion: As x increases

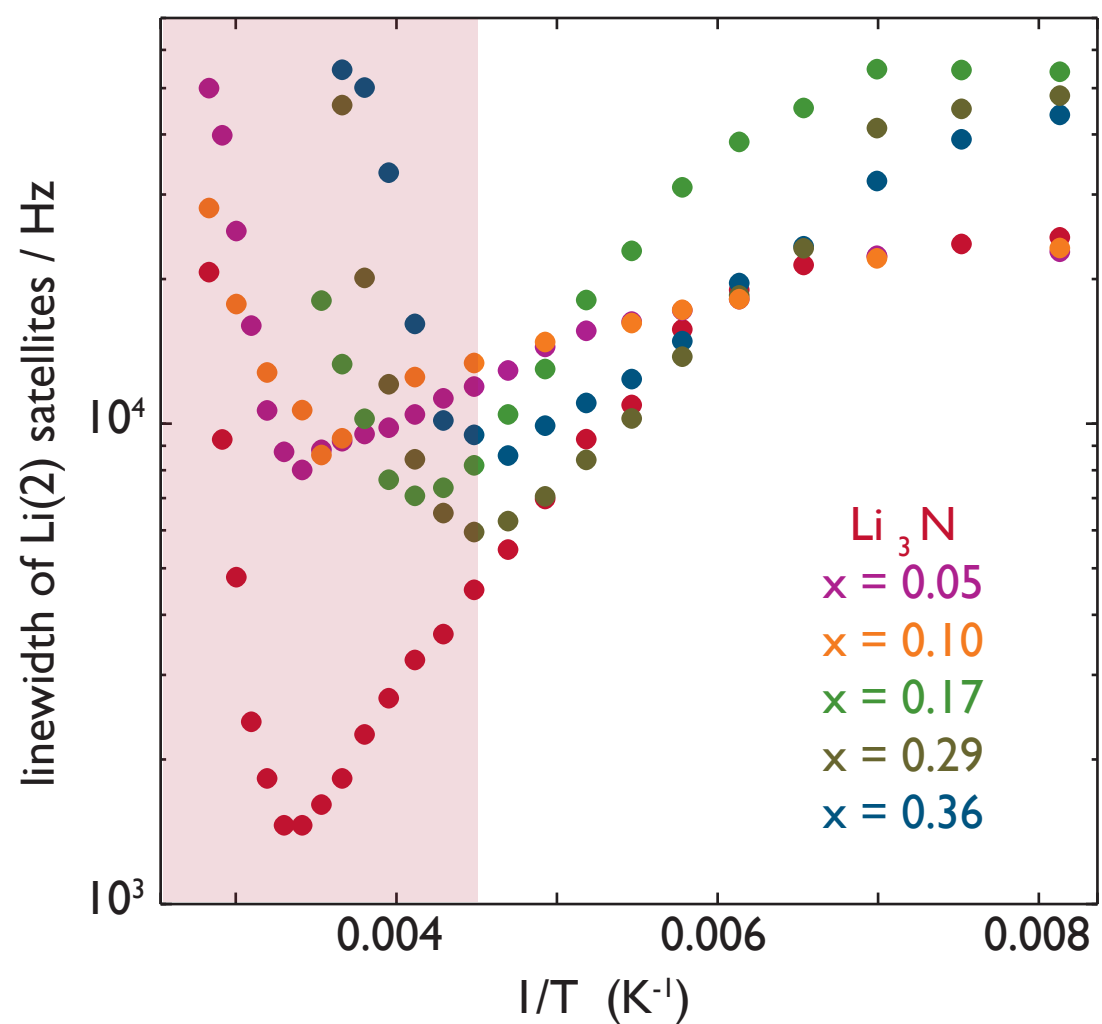
- ★ a lengthens, resulting in a more open framework which is expected to lower E_a



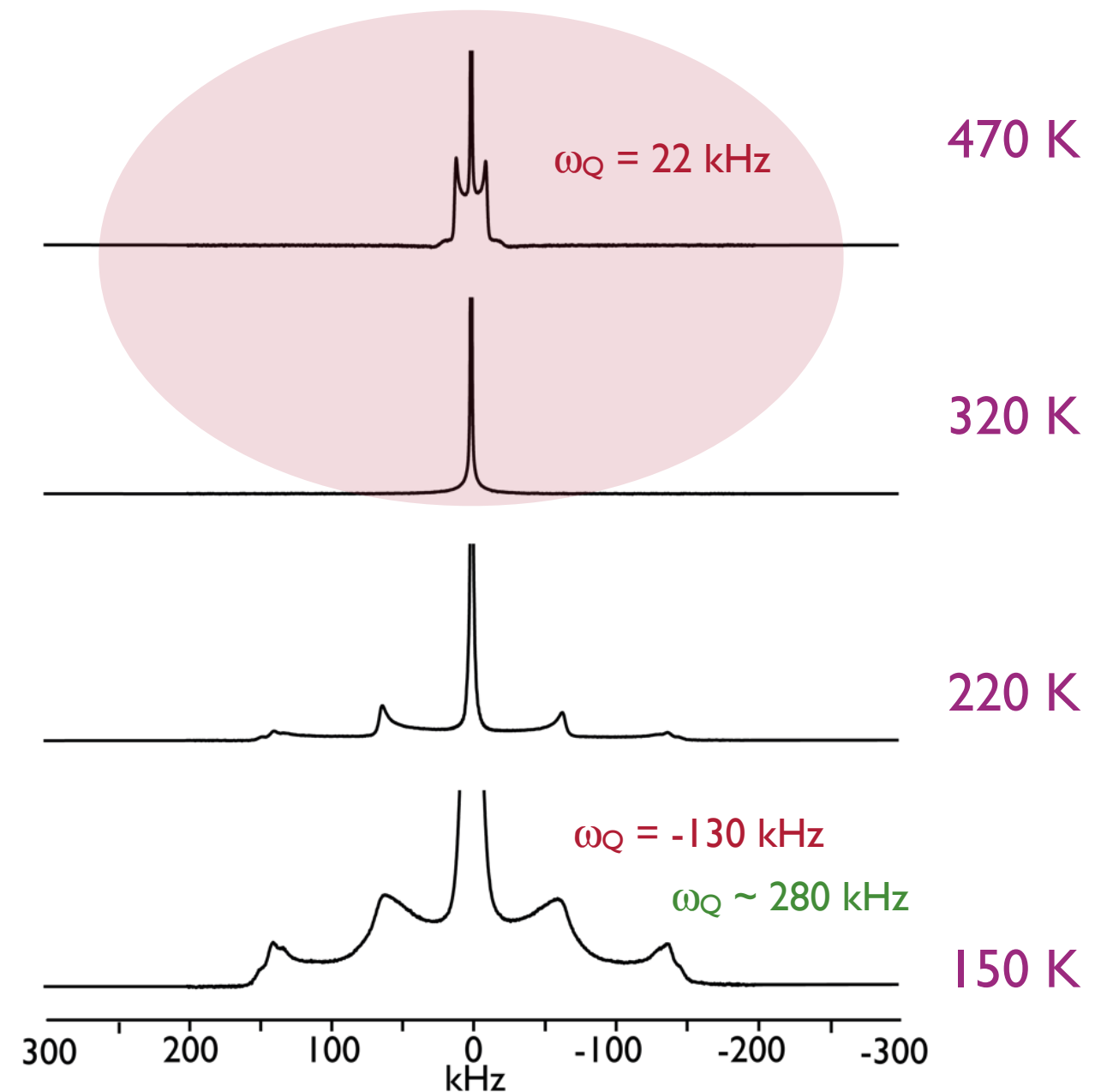
E_a correlated with substitution level

$\text{Li}_{3-x}\text{Cu}_x\text{N}$:VT wideline NMR

Exchange broadening of both satellites,
suggests an exchange mechanism for
inter-layer diffusion



VT wideline lithium-7 spectra
 $x = 0.29$

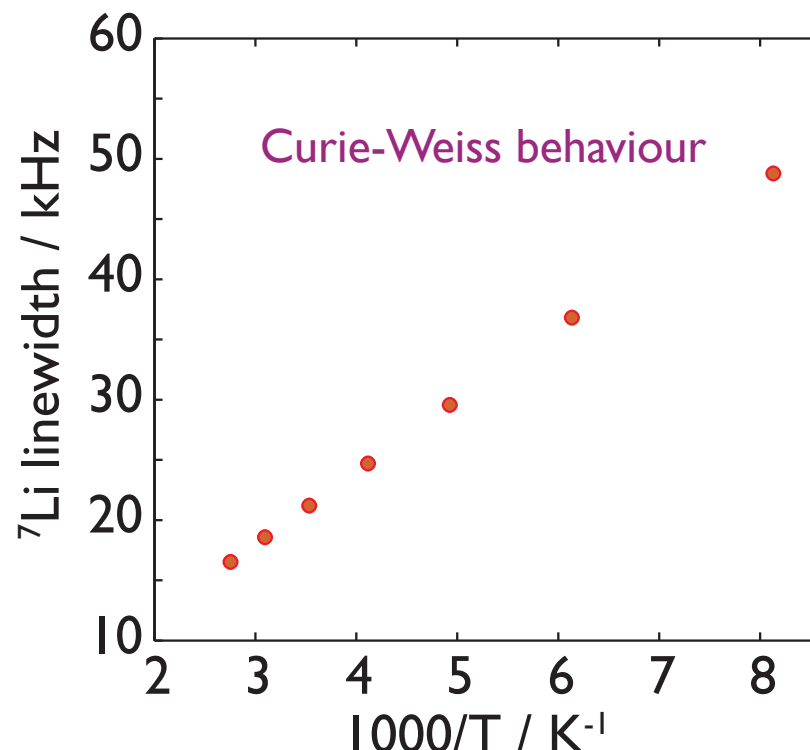
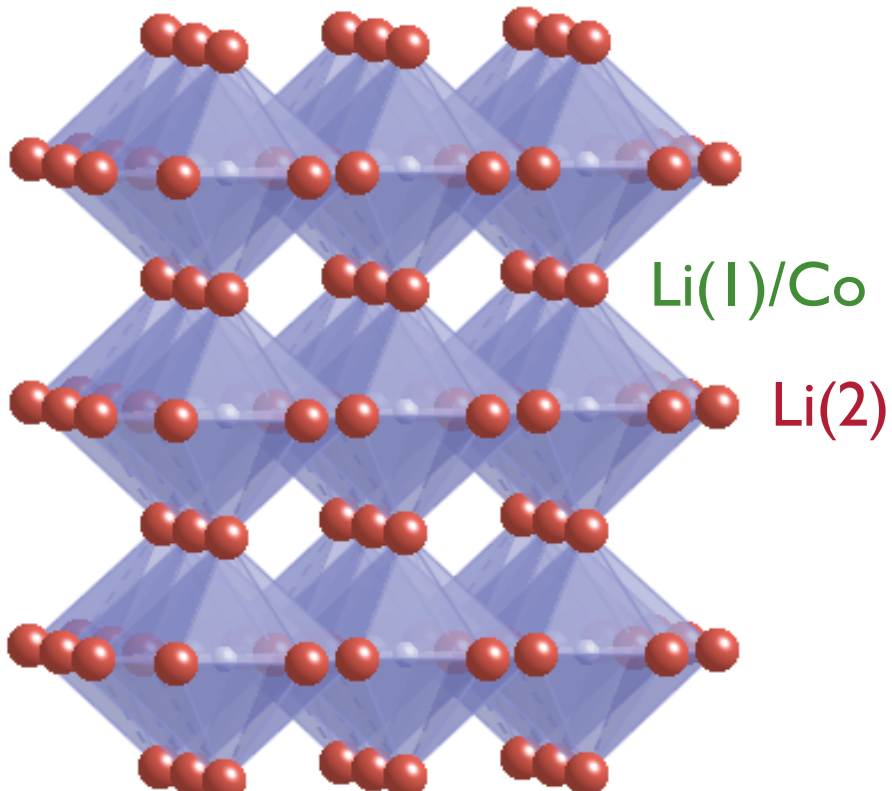


Anisotropic diffusion cf. parent Li_3N

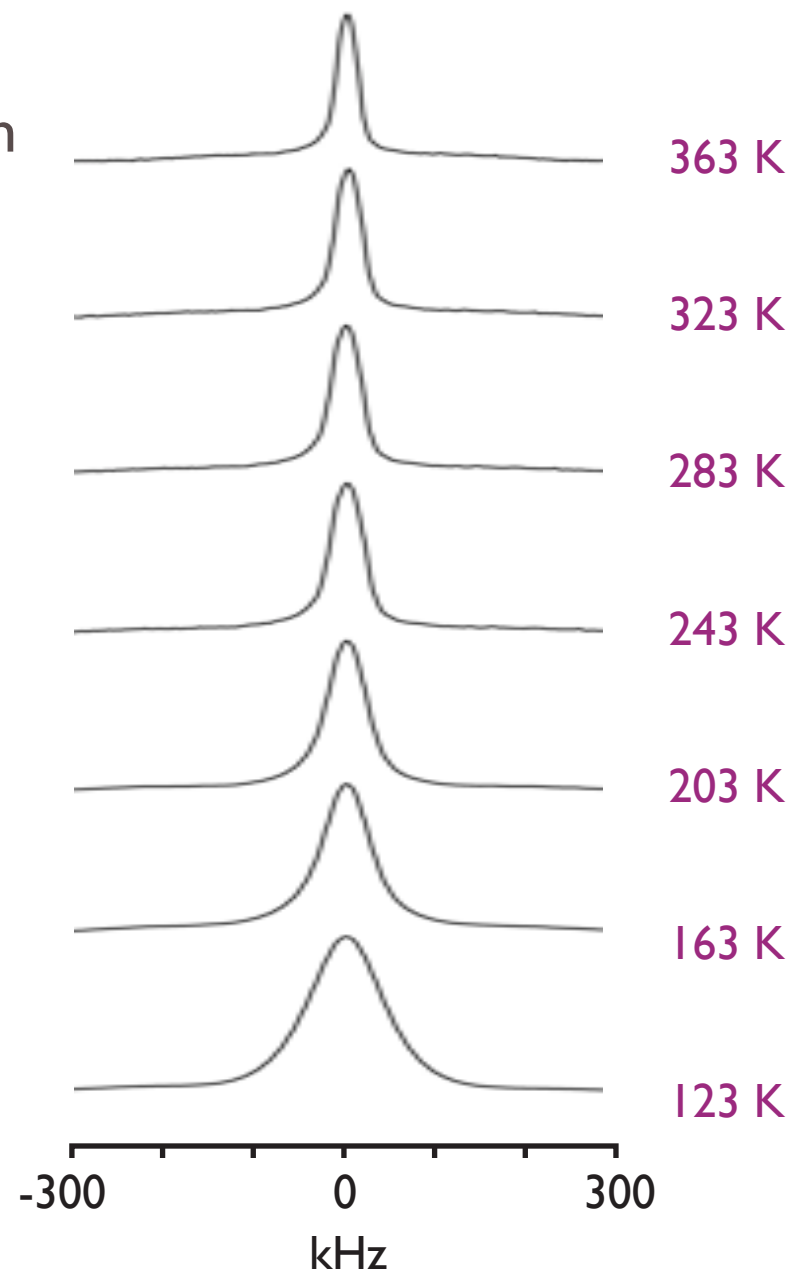
$\text{Li}_{3-x-y}\text{Co}_x\text{N}$: paramagnetic

$\text{Li}_{3-x-y}\text{Co}_x\text{N}$:

- ★ $x < 0.6$, high vacancy concentration
- ★ **strongly paramagnetic**
- ★ interaction with electronic moments dominates NMR relaxation



VT wideline lithium-7 spectra
 $x = 0.43, y = 0.24$

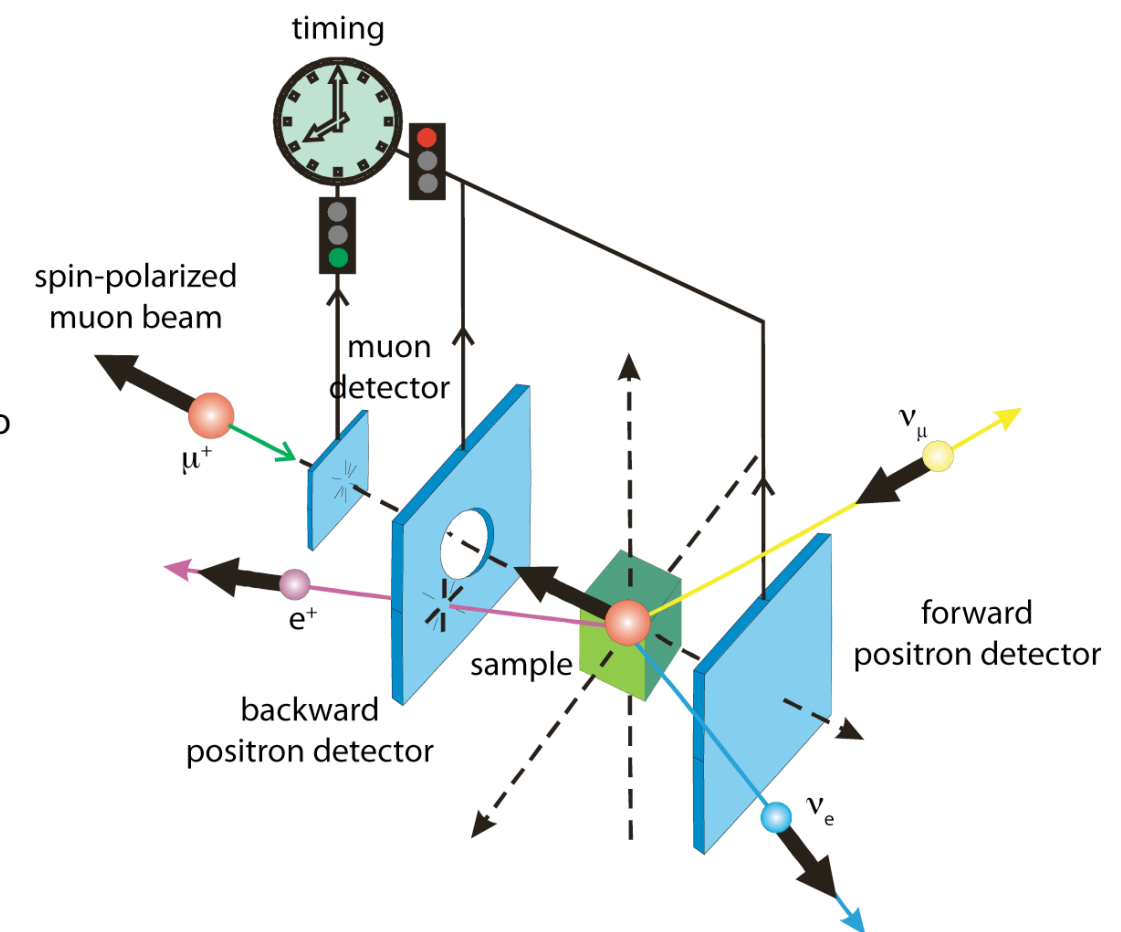
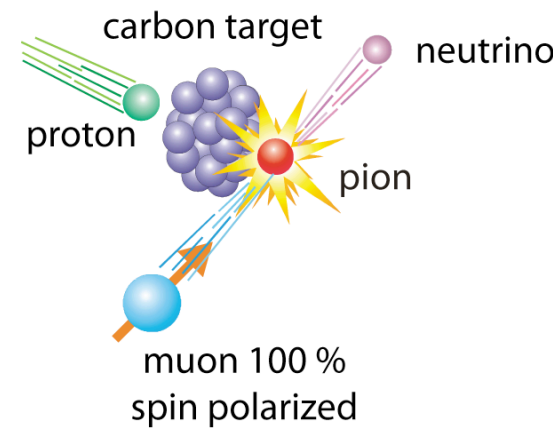
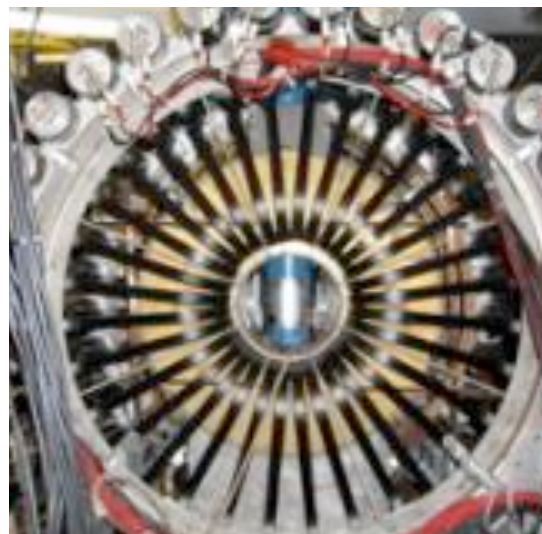


Problem with NMR studies of electrode materials

Solution: muon spin relaxation

Implanted muons probe **local** magnetic fields:

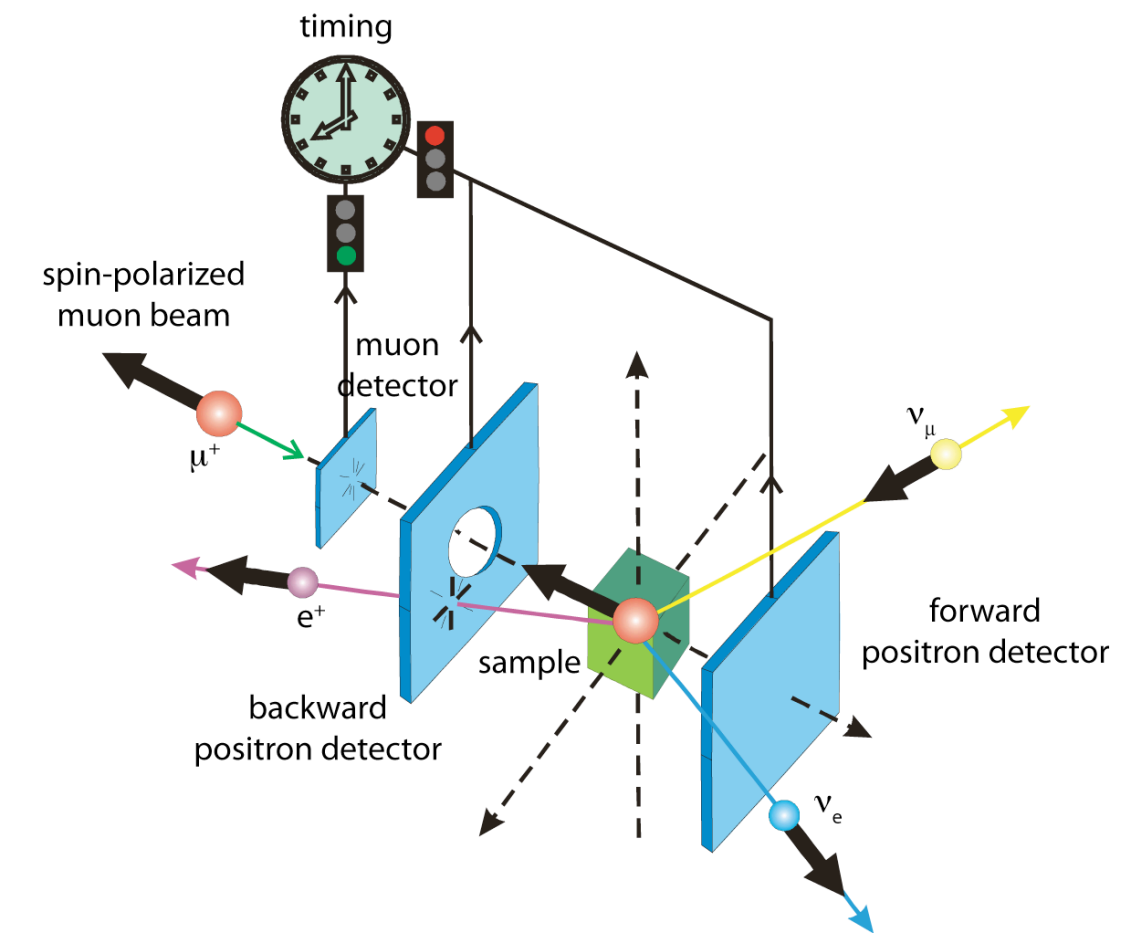
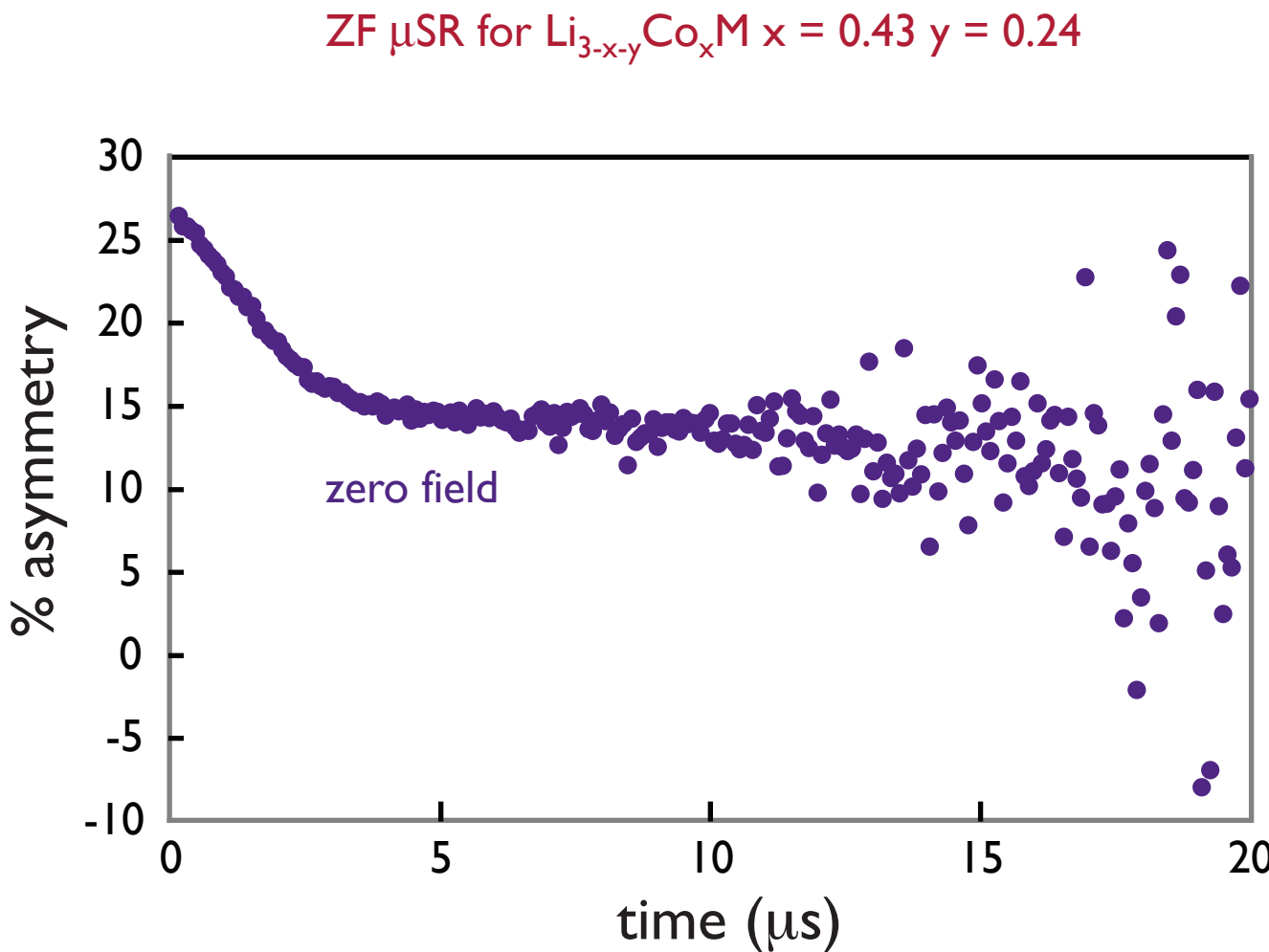
- ★ 1/9 mass of proton; half-life 2 μs
- ★ spin-1/2; magnetic moment 3.18 times that of the proton
- ★ muon beam 100 % spin polarized
- ★ 10^7 muon implantations; anisotropy of emitted positrons at a particular decay time gives average muon spin polarization



$\text{Li}_{3-x-y}\text{Co}_x\text{N}$: ZF- μ SR

Zero-Field μ SR: muon polarization varies according to a dynamic Kubo-Toyabe function

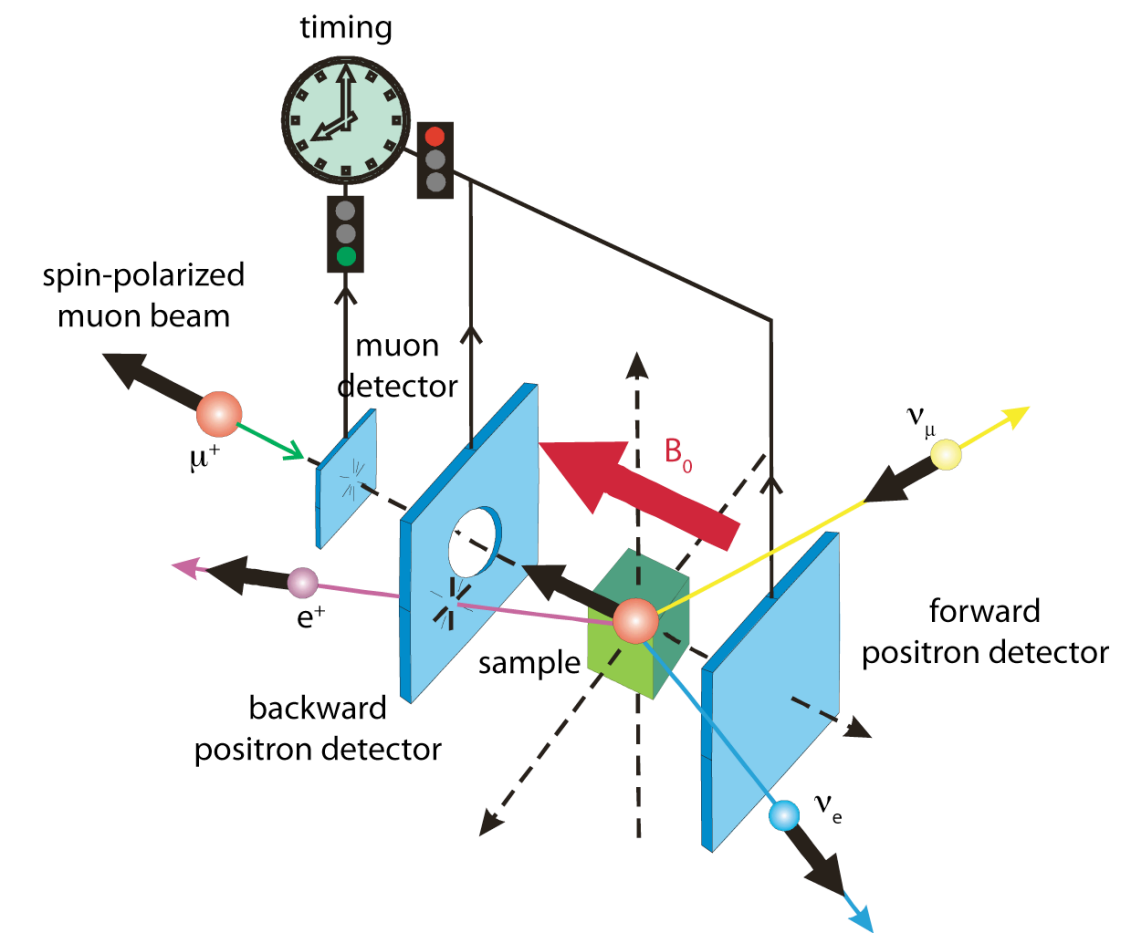
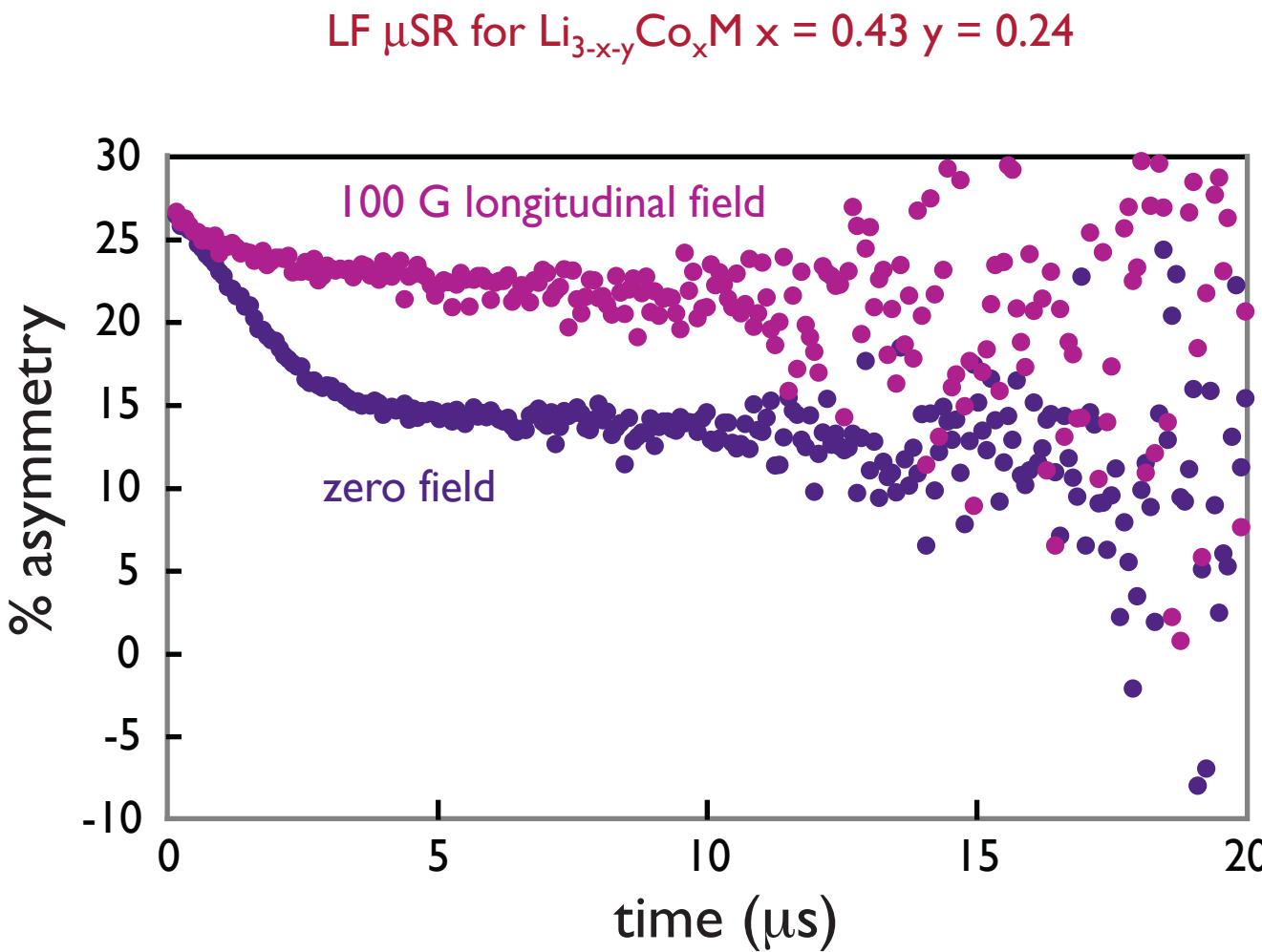
- ★ depolarization rate measures the local (nuclear) field distribution
- ★ muon fluctuation rate takes account of muon hopping
- ★ electronic moments result in a paramagnetic contribution to relaxation (as for NMR)



$\text{Li}_{3-x-y}\text{Co}_x\text{N}$: LF- μ SR

Longitudinal-Field μ SR:

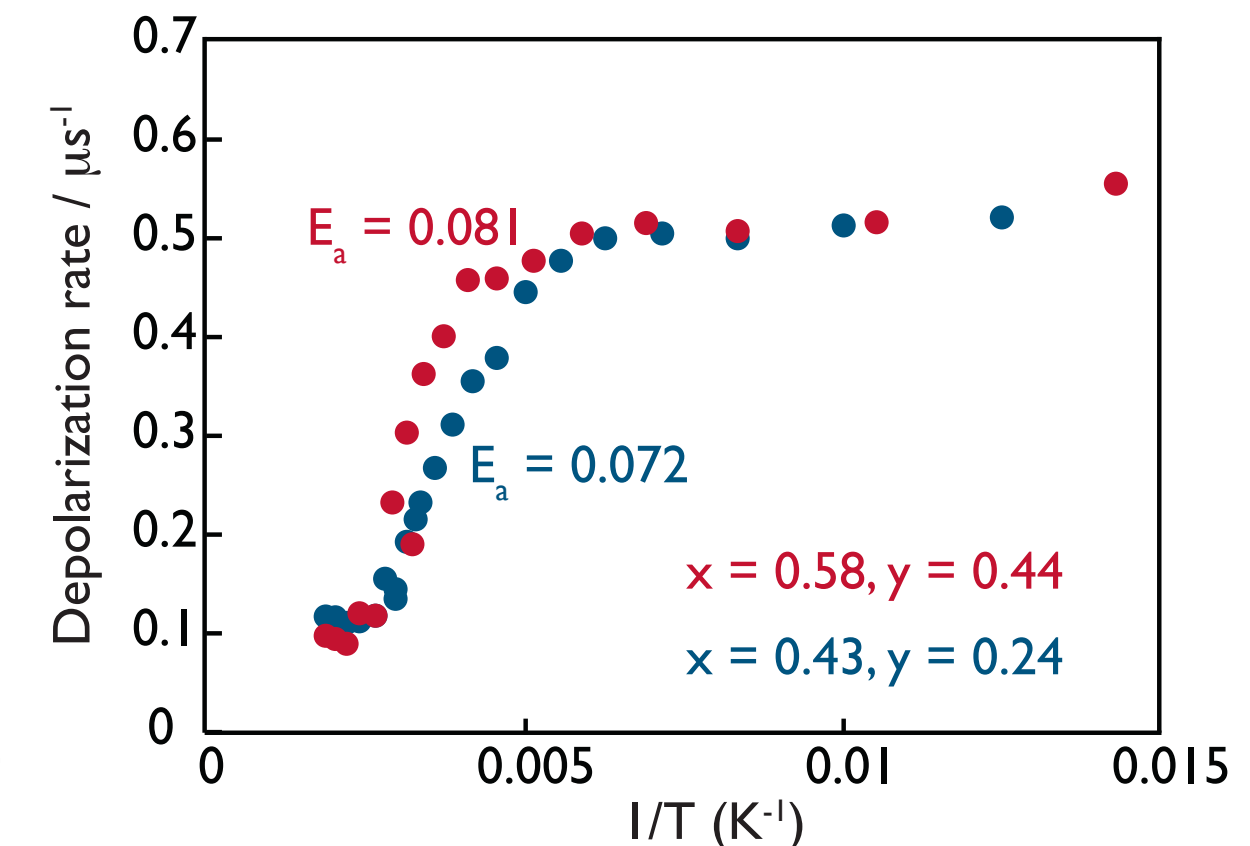
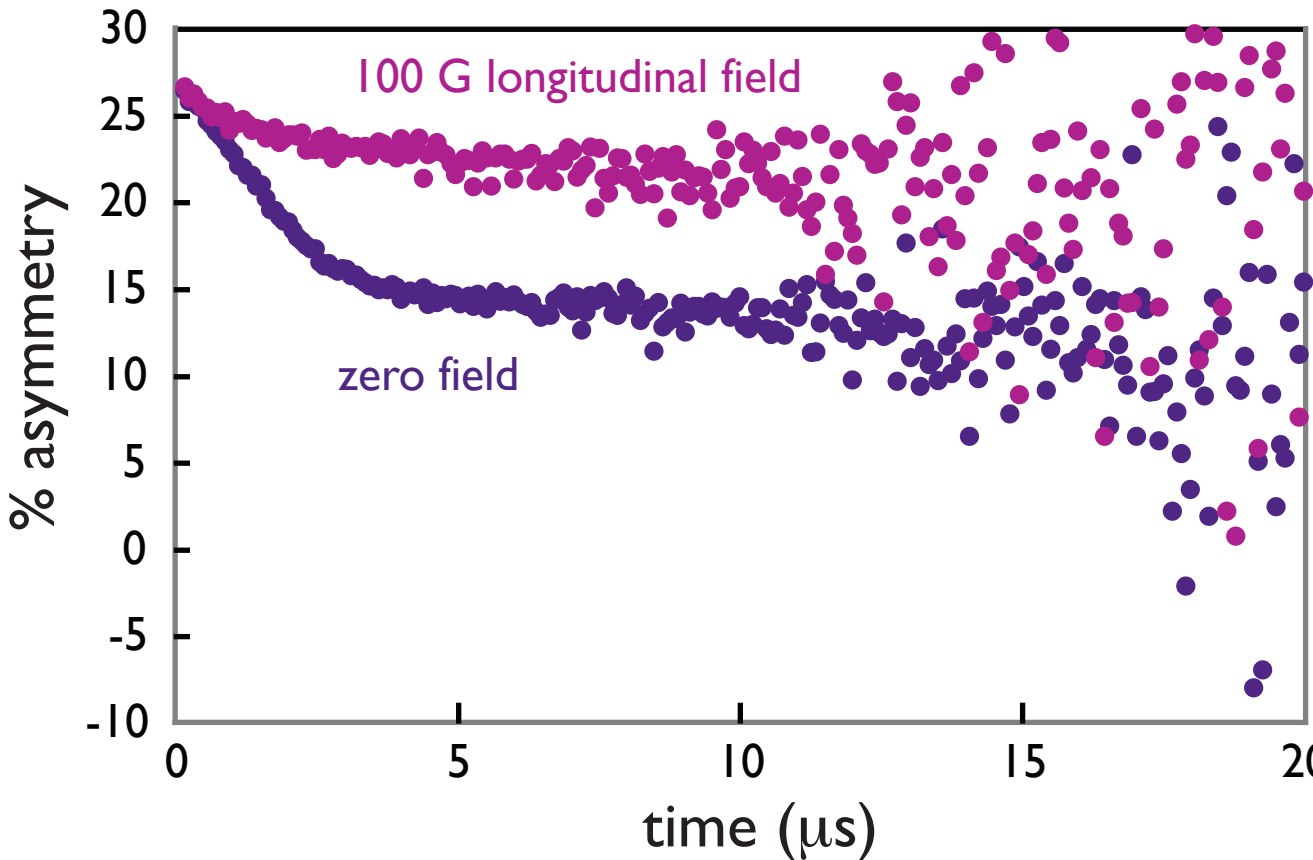
- ★ longitudinal field (100 G) quenches the nuclear local fields
- ★ separates the paramagnetic contribution to muon relaxation



$\text{Li}_{3-x-y}\text{Co}_x\text{N}$: measurement of diffusion parameters

Analysis:

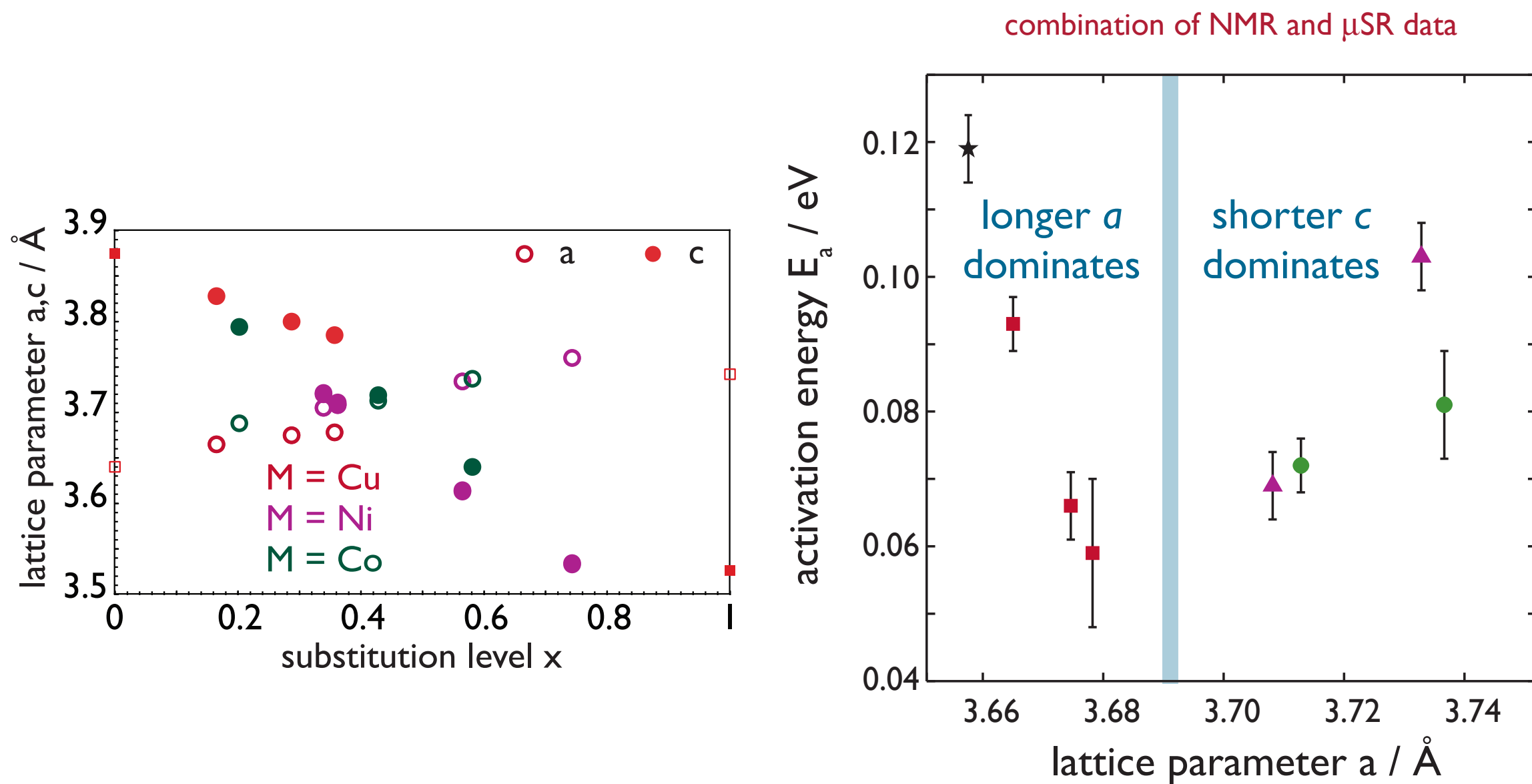
- ★ obtain depolarization rate corrected for a paramagnetic contribution
- ★ local field distribution is motionally narrowed by Li^+ diffusion
- ★ model its temperature dependence to extract diffusion parameters



$\text{Li}_{3-x-y}\text{M}_x\text{N}$: correlation between structure and dynamics

Intra-layer diffusion: As x increases, competition between two effects

- ★ a lengthens, resulting in a more open framework which is expected to lower E_a
- ★ c shortens, resulting in a less polar, more covalent framework which is expected to raise E_a



Suggests an optimum substitution level

$\text{Li}_{3-x-y}\text{M}_x\text{N}$: conclusions

Li^+ diffusion:

... is correlated with structure in $\text{Li}_{3-x-y}\text{M}_x\text{N}$

In particular **intra-layer \mathbf{E}_a**

... can be optimized by tuning the substitution level x

μSR allows information about dynamics to be obtained even for paramagnetic materials

Acknowledgments



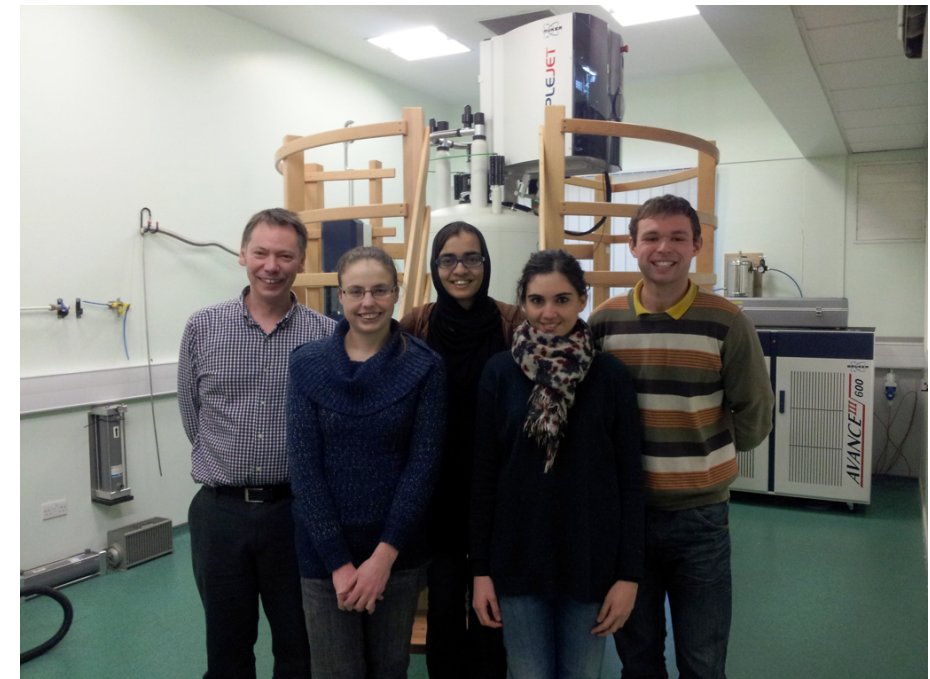
The University of
Nottingham



EPSRC
Engineering and Physical Sciences
Research Council

HIGHER EDUCATION
FUNDING COUNCIL
hefce FOR ENGLAND

Axel Heindrichs, Charles Crockford,
Giuseppe Grasso, Gyan Agarwal, John
Godward, Ruben Gomez, Limin Shao,
Zlatka Stoeva, Andrew Jurd, **Andrew
Powell**, Yanqi Wu, **Daniel Lee**, David
Bennett, Christopher Stapleton,
Gregory Martin, **Habeeba Miah**,
Lyndsey Knight, Francesca Martini



Martin Schröder (Nottingham): metal organic frameworks; **Duncan Gregory** (Glasgow): lithium battery materials; **Steve Armes** (Sheffield): colloidal nano-composites; **Jonathan Yates** (Oxford): CASTEP calculations; **Dinu Iuga**: (UK 850 MHz Solid-state NMR Facility): high-field ultrafast MAS measurements; **James Lord**, (ISIS Muon Facility): muon spin resonance

UK 850 MHz Solid-state NMR Facility

EPSRC

Engineering and Physical Sciences
Research Council

 **BBSRC**

 **Advantage
West Midlands**
www.advantagewm.co.uk

investing
in **your** future
European Regional Development Fund
European Union

